JIMMA UNIVERSITY
SCHOOL OF GRADUATE STUDIES
JIMMA INSTITUTE OF TECHNOLOGY
SCHOOL OF CIVIL AND EN5VIRONMENTAL ENGINEERING

PREDICTING SEDIMENT YIELD OF DIDESSA RIVER BASIN AND SEDIMENTATION OF ARJO DIDESSA RESERVOIR

A Thesis Submitted To Jimma Institute of Technology, School Of Post Graduate Studies In Partial Fulfilment of the Requirement for the Degree of Master of Science in Hydraulic Engineering

By

Fayera Gudu Tufa

November, 2015

Jimma, Ethiopia

JIMMA UNIVERSITY
SCHOOL OF GRADUATE STUDIES
JIMMA INSTITUTE OF TECHNOLOGY
SCHOOL OF CIVIL AND ENVIRONMENTAL ENGINEERING

PREDICTING SEDIMENT YIELD OF DIDESSA RIVER BASIN AND SEDIMENTATION OF ARJO DIDESSA RESERVOIR

A Thesis Submitted to Jimma Institute of Technology, School of Post Graduate Studies in Partial Fulfilment of the Requirement for the Degree of Master of Science in Hydraulic Engineering

By

Fayera Gudu Tufa

Advisor: Dr.-Ing., Tamene Adugna (PhD)

Coadvisor: Mr. Sifan Abera (Msc.)

November, 2015

Jimma, Ethiopia

SCHOOL OF POST GRATUATE STUDIES

JIMMA UNIVERSITY

As members of the Examining Board of the Final MSc Open Defence, we certify that we have read and evaluated the thesis prepared by Fayera Gudu Tufa entitled: **Predicting Sediment Yield of Didessa River Basin and Sedimentation of Arjo Didessa Reservoir** and recommend that it be accepted as fulfilling the thesis requirement for the degree of: Master of Science in ***Hydraulic Engineering.***

Name	Signature	Date
Name of chairman	Signature	Date
…………………........................	....	....
Name of Main Advisor	Signature	Date
…………………........................	....	....
Name of Co-advisor	Signature	Date
………………….......................	....	....
Name of Internal Examiner	Signature	Date
………………….......................	....	....
Name of External Examiner	Signature	Date
………………….......................	....	....

Declaration

I declare that this research is my work and all sources of materials and data used for this thesis have been duly acknowledged. This thesis has been submitted in partial fulfilment of the requirement for master of degree at Jimma University and deposited at university library to be made available to all users.

Fayera Gudu Tufa Signature...................... Date......................

Certification

I hereby certify that I have read this thesis prepared under my direction and recommend that it be accepted as fulfilling the thesis requirement.

Name of Advisor	Signature	Date
Dr.-Ing., Tamene Adugna	....	....

Name of Co-advisor	Signature	Date
Mr. Sifan Abera	....	....

DEDICATION

I dedicate this thesis manuscript to all my family for their affection, love and dedicated partnership in the success of my life.

ACKNOWLEDGEMENT

Above all and everything I thank Almighty God for giving me life and wisdom to achieve my dreams.

Primarily, I would like to extend my heartfelt acknowledgement to Jimma Institute Technology for allowing me to take part in graduate study of Hydraulic Engineering in Jimma University. Also, Special thanks to Ethiopian road Authority for covering my study fee to carry out my MSc. Degree in Hydraulic Engineering.

I am grateful to my advisor Dr.-Ing., Tamene Adugna (PhD) for the devotion of his precious time to guide me in every steps of this thesis work and provide me important and updated materials and tools. I am also grateful to my co-advisor Mr. Sifan Abera (MSc., PhD fellow) for his genuine help, cooperation and guidance throughout this work.

I am thankful to the Ethiopian ministry of water resources and National meteorology service agency for their willingness to provide me the important priceless data elements. I am also grateful to Oromia water works design and supervision Enterprise for their willingness to provide me detail data for Arjo Didessa reservoir.

My gratitude also goes Department of water resources and Environmental Engineering, particularly for staff members for their considerable support and comments.

Finally, I would like to extend my deepest gratitude to my family, without their encouragement, support and care this would not have happened.

TABLE OF CONTENTS

LIST OF TABLES

LIST OF FIGURES

EXECUTIVE SUMMARY

Predicting sediment yield is essential for design of dams, pollutant control and development of integrated watershed management practices. Poor land use practices and improper management systems have played a significant role in causing high soil erosion rates, sediment transport, reservoir sedimentation and loss of agricultural nutrients.

Didessa river basin which is located in the southernmost part of the Blue Nile Basin, contributing roughly a quarter of the total flow of the Blue Nile as measured at Sudan border. It is the largest tributary of the Blue Nile in terms of its volume of water and the drainage area is nearly 27711.9km^2*. The basin is geographically located between 36*^{0} *02*$'$ *and 36*^{0} *46' longitude, and 7*^{0} *43*$'$ *and 8*^{0} *13 latitude. The Didessa river basin is characterized by high rainfall occurring during summer and moderate land use change from forest to agricultural land due to rapid population growth. The lower part of the catchment is characterized by Poor land cover coupled with hilly topography led to quick concentration of runoff and sediment into outlet.*

The general objective of this study was to predict sediment yield of Didessa river basin and sedimentation of Arjo Didessa Reservoir using physically based SWAT models. The SWAT model utilize GIS and DEM to delineate watershed and extract the stream networks. This study applied SWAT model to assess sediment yield at Arjo Didessa reservoir and Didessa river basin outlet. The simulated stream flow was calibrated for six years (1995 to 2001) and validated for five years (2001 to 2006) at Toba gauging station using SWAT-CUP to evaluate the performance of the model. In addition, Suspended sediment concentration was generated by rating curve from observed sediment sample and compared with simulated value to check the capability of SWAT model to simulate sediment yield and appreciable agreement was obtained. The trap efficiency and sedimentation rate of Arjo Didessa reservoir were also determined.

The model was successfully calibrated and validated. The model performance for calibration and validation periods have been evaluated by using statistical parameters, Coefficient of determinant (R^2*) and Nash-Sutcliffe (*E_{NS}*). For calibration* R^2 *and* E_{NS} *were found to be 0.79 and 0.76 respectively, and 0.66 and 0.65 during validation. The sediment yield at Arjo Didessa reservoir and sedimentation rate found to be 0.99Mton/year and 0.86Mm*^{3}*/year respectively. The reservoir trap efficiency found to be 98%. Sediment yield of the basin as measured at the outlet of the whole basin was found 8.29Mton/year.*

The erosion prone area which needs immediate watershed management in Didessa river basin were also identified. The middle part of the basin around Jimma Arjo, Limmu kosa, and downstream part of the area around Limmu, Gida and part of west Wollega have been identified as soil erosion prone area.

Key words: *Didessa river basin, sediment yields, Sedimentation rate, SWAT model, SWAT-CUP, Trap efficiency*

ACRONOMY

AGNPS	Agricultural Non-point Source Pollution Model
ANSWERS	Areal Nonpoint Source Watershed Environment Response Systems
ARS	Agricultural Research Service
CREAMS	Chemicals, Runoff and Erosion from Agricultural Management Systems
CV	Curve number
DEM	Digital Elevation Model
ENMSA	Ethiopian National Meteorological Service Agency
E_{NS}	Nash-Sutcliffe Efficiency
EPIC	Erosion-Productivity Impact Calculator
ESRI	Environmental Sciences Research Institute
FAO	Food and Agricultural Organization
GERD	Grand Ethiopian Renaissance Dam
GIS	Geographic Information System
GLEAMS	Groundwater Loading Effects of Agricultural Management System
GLUE	Generalized Likelihood Uncertainty Estimation
GPS	Global Position System
HRU	Hydrologic Response Unit
ICOLD	International Committee of Large Dam
Km	Kilometre
Km^2	Square Kilometre
m	Meter
m.a.s.l	Mean at sea level
MCMC	Markov chain Monte Carlo
MDDL	Minimum Draw down Level
Mha	Million Hectare
MoWIE	Ministry of Water, Irrigation and Energy
Mton	Million Tonne
MUSLE	Modified Universal Soil Loss Equation
MW	Mega Watt

NMSA	National Metrological Service Agency
PBIAS	Percent Bias
RCH	Reach
RC	Reinforced Concrete
RMSE	Using Root Mean Square Error
RS	Remote Sensing
RSR	Observations Standard Deviation Ratio
SRTM	Shuttle Radar Topography Mission
SUFI2	Sequential Uncertainty Fitting Version 2
SWAT	Soil Water Assessment Tools
SWAT-CUP	SWAT calibration and Uncertainty Program
SWRRB	simulator for Water Resources in Rural Basins
SYLD	Sediment Yield
TE	Trap Efficiency
TSS	Total Suspended Sediment
USDA-SCS	US Department of Agriculture – Soil Conservation Service
WBISPP	Woody Biomass Inventory and Strategic Planning Project

1. INTRODUCTION

1.1 Background

Soil and water are basic principal natural resources of a country. Heavy population pressure, over exploitation of the land, torrential rain, have created natural imbalance. When natural harmony is disturbed, these resources become vulnerable to erosion (Ndorimana *et al.*, 2005).

Erosion of the land surface takes place in the form of sheet erosion, rill and inter-rill erosion, and gully erosion (Awulachew *et al.*, 2008). The process of erosion and transportation of sediment are complex. The detachment of particles in the erosion process occurs through the kinetic energy of raindrop impact, or by the forces generated by flowing water. Once a particles are detached, it must be entrained before it can be transported away. Both entrainment and transport depends on the shape, size and weight of the particle and the force exerted on the particle by the water. When these forces are diminished to the extent that the transport rate is reduced or transport is no longer possible, deposition occurs (Ndorimana *et al.*, 2005).

Deposition occurs when the forces are diminished enough leading to a reduction or cessation of transport. Therefore, when a river flow enters a reservoir, its velocity and transport capacity are reduced and its sediment load is eventually deposited. The amount and rate of deposition in a reservoir are mainly determined by detention storage time, shape of the reservoir and operating condition of the reservoir. The depositional pattern usually starts with the courser materials depositing towards the reservoir head water, while the finer sediment is transported further into the reservoir. The aggradations continues more and more until a delta is formed (Ahmed, 2008).

Reservoirs located in the Nile basin suffer from sediment deposition which has resulted in tremendous reduction in their capacities, for example Roseires and Khashm El Girba reservoirs in Sudan, located respectively at the Blue Nile and river Atbara, their capacities have been reduced dramatically. Other examples may include sediment deposition in high Aswan dam in Egypt, and dams constructed in Ethiopia. Soil erosion in the basin has endangered reservoir projects and caused doubt about the viability of existing and future schemes (Ndorimana *et al.*, 2005).

The deposition of sediment in drainage ditches, irrigation canals, and in navigation and natural stream channels creates serious problems in loss of services and cleanout costs. The deposition of sediment in our natural stream channels has greatly aggravated floodwater damages. The deposition of sediment in channels decreases the channel capacity and the flood-carrying capacity. This results in higher and more frequent overflows.

Throughout Ethiopia, soil loss is a critical problem. Soil erosion in the Ethiopian high lands is a natural phenomenon due to erosive rain fall, steep slope and undulating topography but is enhanced under agricultural systems that reduce protective soil cover (Guzman *et al*., 2013). Sheet and rill erosion, is estimated to be very high. The intensified use of the already stressed resources due to high population growth in Ethiopia makes soil erosion the most series problem affecting the quality of soil, land and water resources upon which humans depend for their subsistence (Shiferaw and Holden, 1999).

Ethiopia loses about 1.3 billion metric tons of fertile soil every year and the degradation of land through soil erosion is increasing at a high rate (Hurni, 1988; Setegn et al., 2010). There are four area of high sheet erosion in the Blue Nile Basin. These are East and West Gojam, Lake Tana basin, Upper Jema sub-basin in south wello and the fourth area is located south of Abay Gorge in East Wollega. Two subsidiary areas with a high erosion hazard are the upper Didessa valley (which is study area) and along the escarpment hills to the west of Lake Tana in the upper Dinder and Beles Valleys (Awulachew *et al*., 2008).

Predicting the quantity and rate of sediment enter into the outlet located at the downstream of the basin or reservoir, which support decision makers in developing watershed management plans for better soil and water conservation measures is needed. However, reliable measurement of various hydrological parameters like sediment yield, which is very important in operation and management of hydropower projects, irrigation projects and reservoirs is difficult task in remote and inaccessible areas.

The use of simulation models can partially solve the problem of hydrologic evaluation of watersheds in conditions with limited and unavailable data of discharge and sediment yield (Tyagi *et al*., 2014).

A suite of physically based, spatially distributed hydrological models are now available. The USDA-Agricultural Research Service (ARS) developed CREAMS (Chemicals, Runoff, and Erosion from Agricultural Management Systems) (Knisel, 1980) model to simulate the long-term impact of land management on water leaving the edge of a field. Several other distributed models for hydrologic and pollutants transport modelling include ANSWERS (Areal Nonpoint Source Watershed Environmental Response Simulation) (Beasley and Huggins, 1982), GLEAMS, EPIC (Erosion Productivity Impact Calculator) (Williams, 1995), EUROSEM (European Soil Erosion Model) (Morgan et al., 1998), AGNPS (Agricultural Non-point Source Pollution Model) (Young et al., 1989) and SWRRB (Williams et al., 1985) are available. These models were all developed for specific problems and have limitations for modelling watersheds with hundreds or thousands of sub-watersheds (Tyagi *et al*, 2014).

The soil and water assessment tool (SWAT) (Arnold *et al.*, 1998), a physically based, spatially distributed model overcomes these limitations and is being increasingly used to assess the hydrological behaviour of large and complex watersheds. Rapid parameterization of hydrologic models can be derived using remote sensing (RS) and geographic information systems (GIS) as remotely sensed data provides valuable and up-to-date spatial information on natural resources and physical terrain parameters.

SWAT is one of the most widely used watershed-scale water quality models in the world. The SWAT model has proven to be a very flexible tool for investigating a broad range of hydrologic and water quality problems at different watershed scales and environmental conditions, and has proven very adaptable for applications requiring improved hydrologic and other enhanced simulation needs (Neitsch *et al*., 2005).

Many researchers have been used SWAT model to predict soil erosion and sediment yield in different sub-basins of Blue Nile basin. For example, Setegn et al. (2010) applied SWAT model to Anjeni-gauged watershed (113.4ha) to predict monthly sediment yield. The model was successfully calibrated and validated. Ayana *et al*. (2012) applied soil and water assessment tool (SWAT) model to Finchaa watershed (3,251 km^2) to simulate the sediment yield from the basin and the result was quite acceptable.

This study focused on prediction of sediment yield of Didessa river basin and sedimentation of Arjo Didessa reservoir using SWAT model. The upland sediment from each sub basin of the watershed was determined and routed.

1.2 Statement of the problem

The Nile basin watersheds are seriously suffering accelerated soil erosion. Valuable soil nutrients are lost from the land, where they are needed, deposited in the water system and ultimately in the reservoirs. Most of the sediment in the Nile flows from the Ethiopian highlands through the Blue Nile (Abbay in Ethiopia) and Atbara River. Nearly all of the sediment about 90% comes from the Blue Nile during the flood season (July - October) (Ahmed, 2008).

Soil erosion is the source of sediment in Blue Nile and a major problem in Ethiopia. Deforestation, overgrazing, and poor land management accelerated the rate of erosion. Many farmers in Ethiopian highlands cultivate sloped or hilly land, causing topsoil to be washed away during the torrential rains of the rainy season. The rains also leach the highland soils of much fertility. In most parts of Ethiopia the high intensity rainfall occurs when the cultivated land has low cover, which can reduce the impact of the high intensity raindrop and the high runoff which can be slowed by soil cover.

With the fast growing population and the density of livestock in the basin, there is pressure on the land resources, resulting in even forest clearing and overgrazing. Increasingly mountainous and steeper slopes are cultivated, in many cases without protective measures against land erosion and degradation (Haile, 2010).

As a result, soil particles on the surface of a watershed can be eroded and transported through the process of sheet, rill and gully erosion. The loss of top soil cause environmental problems and reduce agricultural productivity of the watershed. Once eroded, sediment particles are transported through a channel system and eventually deposited in reservoirs, lakes or at sea. Sediment deposition in reservoirs and irrigation systems leads to serious problems. It reduce the reservoirs storage capacities and hence leading to hydropower generation problems.

Those sediments reaching the dam and passing through spillway and ducts, cause abrasions on the structures, gates, piping, turbines and other pieces. Sedimentation in irrigation systems leads to water shortage and irrigation management difficulties.

Didessa watershed has a largest share in Blue Nile watershed; however, most studies related to the Blue Nile River have focused on the northern part of the Blue Nile basin.

Different articles which studied about sediment yield in upper Blue Nile have been published in last decade.

For example, Desale and Binyam (2015) studied The Effect of Upstream Land Use Practices on Soil Erosion and Sedimentation in the Upper Blue Nile Basin, Ethiopia. Haregeweyn *et al*. (2006) studied Characteristics and Sediment Deposition Problems Reservoirs in Tigray (Northern Ethiopia) to survey and evaluate sediment characteristics and problems for 54 reservoirs in Tigray region of Ethiopia. Setegn (2008) studied Hydrological and sediment yield modelling in Lake Tana basin, Blue Nile Ethiopia. In addition there are a number of articles on study of sediment yield in Blue Nile river basin in general. These articles were discussed in literature review.

However, there is no article/literature on study of sediment yield in Didessa river basin specifically. This makes the Didessa sub-basin one of less studied areas. But, government is planning to develop irrigation and hydropower schemes in Didessa river basin. For example, Arjo Didessa dam which can store 1924.6Mm^3 to irrigate more than 80,000ha area is under construction. These structures capture stream flow from Didessa River. Together with this stream flow, suspended and bedload sediment will enter the reservoir and part of it will deposit. Sedimentation within reservoirs is a problem as it decrease the storage capacity and hence makes the structures less efficient.

Therefore, study of prediction of sediment yield of Didessa river basin is most important for design of diversion and storage structures and the study of Arjo Didessa reservoir sedimentation is important to estimate the span life of the reservoir. This clandestine pledge me to study the prediction of sediment yield in Didessa river basin and sedimentation Arjo Didessa reservoir.

1.3 Objectives of the Study

1.3.1 General Objective

The main objective of this study is to quantify the amount of sediment yield from the Didessa river basin and sedimentation of Arjo Didessa reservoir by using SWAT model.

1.3.2 Specific Objectives

1. Calibrate, Validate and undertake sensitivity analysis of a semi-distributed hydrological model for stream flow
2. To determine the upland soil erosion from watershed Didessa river basin
3. To identify soil erosion vulnerable area in the Didessa river basin
4. To quantify the amount of sediment yield inflow in to the Arjo Didessa dam reservoir and out flow from the basin to join Blue Nile River.
5. To predict Arjo Didessa reservoir trap efficiency and reservoir sedimentation rate.

1.4 Research Questions

1. Which sub basin of Didessa watershed contribute more sediment to Arjo Didessa dam reservoir.
2. How much is the soil erosion in the Didessa watershed, and how this is routed up to the outlet or reservoir?
3. How much is the sediment routed from outlet, trapped in reservoir?
4. How can these be modelled in an integrated way, i.e., both soil erosion, and sediment transport?

1.5 Significance of the study

Any types of Dam design includes dead storage part of the reservoir where mainly deposited sediment that comes from the watershed. Dead storage is the volume that is below the invert of the lowest-level outlet and which cannot be drained by gravity. When sediment can be deposited in place of inactive storage that reduce the amount of water that passes through the outlet or may close the outlet gate. Then take action and quantifying the amount of sediment that inflow from watershed is main part of the dead storage design and also for operation of the reservoir of the dam. This study is useful for designer and policy maker to take appropriate measures or decisions on the watershed process and will be taken some mitigation actions.

2. LITERATURE REVIEW

2.1 Worldwide Aspects of Soil Erosion

Soil erosion is a physical process of degradation caused by losing particles from soil surface due to raindrop impact and runoff events (de Vente and Poesen, 2005). (Morris, G and Fans, J, 1998) Defined soil erosion as the process whereby earth or rock material is loosened or dissolved and removed from any part of the earth's surface.

Erosion may be classified according to the erosion site (sheet, rill, interrill, gully, and channel) or the erosive process (raindrop, channel, mass wasting). Interrill erosion or sheet erosion is the detachment and transport of soil particles due to rain splash and shallow pre channel flow. Rill erosion is the detachment and transport of soil particles by concentrated flow in small channels or rills not more than a few centimetres deep that are eliminated by normal cultivation techniques. Gully erosion and channel erosion may refer to either the gradual or the massive erosion of the beds and banks of gullies and stream channels. Mass wasting refers to erosion associated with slope failures, including landslides and similar slope movements. Whereas gross erosion is the sum of all types of erosion rill, gully, channel erosion and mass wasting. The relative importance of each type of erosion varies from area to area. Sheet and rill erosion occurs particularly in grazing and cultivated area of mild slope where runoff is not concentrated in well-defined channel. (Morris, G and Fans, J, 1998).

Most sediments enter reservoirs as a consequence of rainfall erosion and subsequent transport by streams. Successful reduction of sediment yield requires accurate conceptual and quantitative models of the erosion and transport processes responsible for sediment delivery to the impoundment. Watershed management programs frequently fail to reduce sediment yield, despite large expenditures, because the physical nature of the problem is not properly diagnosed, or the economic and cultural conditions leading to accelerated erosion are not addressed and erosion control practices are abandoned as soon as subsidies are removed (Morris, G and Fans, J, 1998).

The processes of erosion, entrainment, transportation and deposition of sediments in a river catchment are complex.

The detachment of particles in the erosion process occurs through the kinetic energy of raindrop, or by the forces generated by flowing water. Once a particle has been detached, it must be entrained before it can be transported away. Both entrainment and transport depend on the shape, size and weight of the particle and the forces exerted on the particle by the flow. When these forces are diminished to the extent that the transport rate is reduced or transport is no longer possible, deposition occurs (Ndorimana *et al.*, 2005).

Today, soil erosion is almost universally recognized as a serious threat to man's well-being. Estimated worldwide costs of soil erosion to be about hundred billion dollars per year, more than 70 dollars per person per year. Water erosion had accounted for about 55% of the almost 2billion hectare of degraded soils in the world (Pimentel *et. al*. 1994; Amare, 2005).

Land degradation is a major concern to many nations and to the international community. Soil erosion affects both developed and developing nations. There is no region of the glob where soil erosion due to water is not a threat to the long term sustainability of mankind. For developing nations, soil erosion is among the most chronic environmental and economic burdens. And many of these nations are in the tropics and in the drier zones. Soil erosion is getting worse in sub-Saharan Africa; it has increased 20 fold in the last three decades as more and more people are forced to move out of the good bottomlands to fragile hillside (Taffa, 1999; Amare, 2005). (Julien and Shah, 2005; Wolancho, 2012) stated that countries in Africa are experiencing deforestation, mainly from agricultural expansion and land degradation which are leading causes of soil erosion and sedimentation.

Soil erosion is a major watershed problem in many developing countries (Moquanint and Awulachew, 2008). Tamene *et al*., 2006) stated that reservoir sediment deposition is a reflection of watershed erosion and deposition process which are controlled by terrain form, soil type, surface cover, drainage networks and rain fall related environmental attributes.

2.2 Soil Erosion in Ethiopia

Soil erosion is a major problem in Ethiopia. Deforestation, overgrazing and poor land management accelerated the rate of erosion. Many farmers in Ethiopian high lands cultivated sloped or hilly land, causing top soil to be washed away during the torrential rains of the rainy season. In most part of Ethiopia the high intensity rainfall occurs when the cultivated land has low cover, which can reduce the impact of the high intensity raindrop. High intensity storms cause significant erosion and associated sedimentation, increasing the cost of operation and maintenance and shortening lifespan of water resources infrastructures (Haile, 2010).

Poor land use practices, improper management systems and lack of appropriate soil conservation measures have played a major role for causing land degradation problems in the country (Setegn *et al*., 2009).

Soil degradation is the most immediate environmental problem facing Ethiopia. The loss of soil, and the deterioration in fertility, moisture storage capacity and structure of the remaining soils, all reduce the country's agricultural productivity. Soil erosion is greatest on cultivated land where the average annual loss is 42 tons per hectare, compared to 5 tons per hectare from pastures. As a result, almost half of the loss of soil comes from areas under cultivation even though they cover only 13 percent of the country (http://www.idp-uk.org). Ethiopia loses about 1.3 billion metric tons of fertile soil every year and the degradation of land through soil erosion is increasing at a high rate (Hurni 1989; Setegn *et al*., 2009).

Overgrazing, deforestation and poor agricultural practices, such as cultivation of slopes (up to 16%) not suited to agriculture, have contributed to soil erosion so severe, particularly in Tigray and parts of Amhara region, that as much as 200,000 hectares of arable land have been washed away each year. Not surprisingly the highest average rates of soil loss are from former cultivated lands currently unproductive due to degradation and with very little vegetative cover to protect them (http://www.idp-uk.org).

Also, the rugged topography of the highlands suffers brief but extremely heavy rainfalls that characterize many areas and centuries-old farming practices, that do not include conservation measures, have accelerated soil erosion in much of Ethiopia's highland areas. In the dry lowlands, persistent winds also contribute to soil erosion.

The severity of the soil degradation problem is greatest in the north of the country and the Eastern Highlands, with the Amhara and Tigray highlands the most severely affected areas. It is no coincidence that the regions with greatest damage due to soil degradation are also the ones most affected by famine (http://www.idp-uk.org).

2.3 Soil Erosion in Blue Nile Basin

The Blue Nile River, which originates from the steep mountains of the Ethiopian Plateau, is the major source of sediment loads in the Nile basin. Soil erosion from the upstream of the basin and the subsequent sedimentation in the downstream area is an immense problem threatening the existing and future water resources development in the Nile basin.

The benefits gained by the construction of micro-dams in the Upper Nile are threatened by the rapid loss of storage volume due to excessive sedimentation (El-Swaify and Hurni, 1996; Tamene *et al*., 2006). In the downstream part of the basin (e.g., in Sudan and Egypt) excessive sediment load led to massive operation cost of irrigation canals desilting, and sediment dredging in front of hydropower turbines (Betrie *et al*., 2011)

The total soil eroded within the landscape in the Abay Basin is estimated to be 302.8 million tonnes per annum and from which cultivated land is estimated to be 101.8 million tonnes per annum. Thus, about 66% of soil being eroded is from non-cultivated land (mainly from communal grazing and settlement areas). The area of cropland subject to unsustainable losses (where loss exceeds soil formation or 12.5 tonnes/ha/yr) are 968,900, 104,000 and 956,900 ha in the Amhara, Benishangul Gumuz and Oromiya areas of the Basin, respectively. Thus, a total of about 2.03 million hectares of cultivated land have unsustainable soil loss rates (Awulachew *et al*., 2008).

2.4 Previous Studies in Didessa River Basin

Didessa watershed has a largest share in Blue Nile watershed; however, most studies related to the Blue Nile River have focused on the northern part of the Blue Nile basin and Didessa sub-basin is less studied areas. Didessa River is one of the major upstream tributary of Blue Nile basin which has the problems mentioned above. More researchers have been studied on northern part of the Blue Nile basin and roughly on Didessa River.

Didessa river basin generates a large proportion of the runoff between February and July owing to the higher rainfall over the south-west of the basin (Conway, 2000; Haile, 2010) report showed that the. According to (Admasu, 2011) some part of the living in environment, especially on the northern side of Didessa basin has been suffering from climax deforestation and land degradation. Adgolign (2015) assessed spatio-temporal occurrence of surface water resources in the basin. He predicted monthly and annual stream flow and hydrologic components in Didessa basin. Tesfaye and Wondimu (2014) studied Morphometric Analysis of Didessa River Basin to evaluate the effect of morphometric parameters on the hydrology and morphology of the basin. During the study there were no literature assessed, concerning Didessa river basin sediment.

Therefore, the study of sediment yield prediction and Arjo Didessa reservoir sedimentation is very important for policy makers and water development project designers in order to identify the effective watershed management practice and implement. This paper is going study Didessa river basin sediment yield, trap efficiency of Arjo Didessa reservoir, reservoir sedimentation rate and identification of soil erosion prone area in the basin to fill the gaps which were not studied by different researchers (Admasu (2011), Tesfaye and Wondimu (2014), and Adigolign (2015)) in the area.

2.5 Sediment Yield and Sedimentation

Sediment yield refers to the amount of eroded sediment discharged by a stream at any given point over a period of time, which is also the amount which will enter a reservoir located at the downstream limit of its tributary watershed (Vanoni, 2006; Tadesse, 2013). The most common unit for sediment yield is tonnes/year. The specific sediment yield is the yield per unit of land area which is most commonly given in tonnes/km^2/year.

Long-term sediment yield estimates have been used for sizing storage reservoirs and estimating reservoir life (Morris and Fan, 1998). Therefore accurate estimation of sediment yield is very important in order to plan a reservoir and efficiently manage its sediment so that the reservoir can meet its requirements.

The erosions or sediments settled due to the influence of the reservoir, expand to upstream and downstream, and are not equally distributed even within the lake.

The upstream deposition is called backwater deposit, named after the hydraulic phenomenon, being also ascending since the deposits in that area increase. The depositions within the reservoir are called delta, overbank and bottom-set deposit. Coarse make up the delta, while the inland deposits are made up by finer sediments (Mahmood, 1987). Floods produce another kind of deposition, occurring along both stream and reservoir, being made up by thin and coarse, named flood plain deposit.

Storage loss is one of many sedimentation problems that can affect reservoirs. Operation of storage reservoirs is severely impacted by the time half the volume has been sediment, but severe sediment-related problems can appear when only a small percentage of the storage capacity has been lost; as reservoirs age and sediments continue to accumulate, sediment-related problems will increase in severity and more sites will be affected.

At any dam or reservoir where sustainable long-term use is to be achieved, it will be necessary to manage sediments as well as water. This is not a trivial challenge. Many type of sediment-related problems can occur both upstream and downstream of dams, and sediment entrainment can also interfere with the beneficial use of diverted water. Sediment can enter and obstruct intakes and greatly accelerate abrasion of hydraulic machinery, thereby decreasing its efficiency and increasing maintenance costs (Mahmood, 1987*)*.

Conversion of sedimenting reservoirs into sustainable resources which generate long term benefits requires fundamental changes in the way they are designed and operated. It requires that the concept of a reservoir life limited by sedimentation be replaced by a concept of managing both water and sediment to sustain reservoir function.

The largest source of sediment in the Nile Basin is located in the Ethiopian Highlands where 85% of the Nile water comes from. The soil that is eroded from the Ethiopian highlands creates serious problems in the operation and maintenance and sustainability of irrigation canals and large reservoirs constructed along the Nile (e. g Roseries, Sennar, Girba and Aswan High Dam) (Awulachew *et al*., 2008).

For example, Sennar Dam was constructed in 1925, it was the second dam built on the Nile system, after the Old Aswan Dam in Egypt (1902). The original capacity of the Sennar Reservoir was 930 Mm^3.

Because of its good design and the proper implementation of operational rules as well as relatively low sediment input because of less upstream degradation, there was relatively little sedimentation in the reservoir during the first 56 years (1925-1981). Throughout that period the rate of sedimentation never exceeded 0.5% per year (4.6 Mm^3). Consequently, there was only a 28% reduction in the reservoir capacity over the first 56 years. However, between 1981 and 1986 the rate of sedimentation increased dramatically to a rate of 80 Mm^3 per year (reduction of 400 Mm^3 (43%) in only 5 years). In total, over a period of 61 years the Sennar Dam lost 660 Mm^3 (71% of its original capacity). Currently, the Sennar Reservoir is no longer used to store significant volumes of water (Awulachew *et al.*, 2008).

Betrie *et al*. (2011) predicted average sediment yield at the outlet of the Upper Blue Nile using SWAT model and the result was 117Mton/year for existing conditions. The result was comparable with 140Mton/year which was estimate by Ndorimana *et al.* (2005) that includes bed load as well. The bed load approximately accounts for 20–25% of the total load.

Currently Ethiopian government is constructing huge dam on Abbay River at 30km from Ethio-Sudan border with total reservoir capacity of 70 billion m^3. The reservoir is subjected to the sediment generating from Blue Nile watershed. (Tadesse, 2013) reported that the annual sediment load inter into the reservoir is 245 million tonnes, trap efficiency of 100% and average deposit density 1.12 t/m^3. The reservoir storage capacity will be lost at an average rate of 0.3% per year.

The annual sediment load at Arjo Didessa reservoir including the bed load had been estimated during the feasibility Study and found to be 0.7756 Mm^3/year. The 50-Year and 100-Year sediment volumes are estimated to be 38.78 Mm^3 and 77.56 Mm^3 respectively (OWWDSE, 2009).

2.6 Hydrological Models

Modelling is defined as the process of organizing, synthesizing, and integrating component parts into a realistic representation of the prototype. The following are some of the benefits of modelling: Models help sharpen the definition of hypotheses, define and categorize the state of knowledge, provide an analytical mechanism for studying the system of interest, and can be used to simulate experiments instead of conducting the experiments on the watershed itself (USDA, 1972).

Great numbers of soil erosion and sediment transport models have been developed based on laboratory, field, analytical and numerical methods such as finite difference and finite element.

Models can be classified in to different categories *(*Beven, 1992*)*. 1. Empirical and physical models; Empirical developed from regression of observed data where as physical based models are developed based on the physics such as conservation of mass and momentum. 2. Deterministic and stochastic model; Deterministic model provides same result for two equal sets of input data while stochastic model result in different output (Refsgaard, 1996). 3; Lumped and distributed models. Lumped model consider a system as black box and everything is spatially averaged as a single system. However, distributed models consider the heterogeneities by dividing the system in to smaller groups.

2.6.1 Model Selection

Now days, various physically based spatially distributed hydrological models are available. Some of these models are CREAMS model, GLEAMS, EPIC, OPUS, AGNPS and SWRRB. These models were all developed for specific problems and have limitations for modelling watersheds with hundreds or thousands of sub-watersheds. SWAT, a physically based spatially distributed hydrological model overcomes these limitations and is being increasingly used to assess the hydrological behaviour of large and complex watersheds. The other advantage of using SWAT model is that it is GIS interface model. Rapid parameterization of hydrologic models can be derived using remote sensing and GIS as remotely sensed data provides valuable and up-to-date spatial information on natural resource and physical terrain parameters (Tyagi *et al*, 2014).

SWAT model is computationally efficient. Simulation of very large basins or a variety of management strategies can be performed without excessive investment of time or money, and enables users to study long term impacts. In addition, SWAT uses MUSLE to simulate sediment erosion from HRU which replaces the traditional USLE equation. MUSLE use runoff factor than rain fall factor to estimate sediment yield (Williams, 1977). Therefore, SWAT model was selected for this study.

2.6.2 SWAT Model Application

Tyagi *et al.* (2014) used SWAT model to asses discharge and sediment transport from two different forest cover types namely Arnigad and Bansigad watersheds located in lower Himalaya, India. The study was carried out to examine the applicability of soil and water assessment tool (SWAT) in estimating daily discharge and sediment delivery from mountainous forested watersheds to assess the impact of forest cover types on stream discharge pattern and sediment load.

SWAT model was successfully calibrated and validated for daily discharge and sediment concentration using the observed data. The performance of the model was evaluated using the statistical measures of coefficient of determination (R^2) and Nash-Sutcliffe Efficiency (E_{NS}). The result showed a very good agreement between observed and simulated daily values, With R^2 value of 0.91 and E_{NS} of 0.85 in discharge simulation and R^2 value of 0.89 and E_{NS} of 0.83 in sediment simulation in Arnigad watershed. The model also exhibited high performance on Bansigad watershed with an R^2 value of 0.91, and an ENS of 0.9 in discharge simulation; and an R^2 value of 0.86, and an ENS of 0.82 in sediment simulation.

Huang (2015) applied water and soil assessment tool (SWAT) model to assess the impacts of land use change on soil and water losses from Yang Ming Shan National Park Watershed in northern Taiwan. The study utilized two land-use data periods, one in 1996 and another in 2007, along with the SWAT model to simulate soil and water losses in Yang Ming Shan National Park. Based on the baseline scenario, the SWAT model was also successful in simulating the future scenario. Study results for scenario 2007, as compared to 1996 baseline period indicate that land use change shows forest land decreases about 6.9%, agricultural land increases about 9.5%, and causes sediment yield increase of 0.25 t/ha.

Mequanint and Awulachew (2008) used SWAT (Soil and Water Assessment Tool) in Gumera watershed of the Abbay Basin, Ethiopia, to predict sediment yield, runoff, identify spatial distribution of sediment, and to test the potential of watershed management interventions in reducing sediment load from 'hot spot' areas. The model was calibrated and validated against measured flow and sediment data. Both, calibration and validation results, showed a good match between measured and simulated flow and suspended sediment.

Adgolign (2015) applied SWAT model to Didessa Sub-basin of the Abbay (Upper Blue Nile) Basin, West Ethiopia to assess spatio-temporal occurrence of surface water resources in the basin. He predicted monthly and annual stream flow and hydrologic components in Didessa Sub-basin and the obtained result showed hydrologic model with very good values of model performance evaluation parameters.

Setegn (2008) applied Soil and Water Assessment Tool (SWAT) model to the northern High lands of Ethiopia for modelling of Hydrology and Sediment Yield in Lake Tana Basin, Blue Nile, Ethiopia. The study was to test the performance and feasibility of SWAT model to examine the influence of topography, land use, soil and climatic condition on streamflow, soil erosion and sediment yield. The model was successfully calibrated and validated on four tributaries of Lake Tana as well as Anjeni watershed using SUFI-2, GLUE and ParaSol algo-rithms. There was a good agreement between the measured and simulated flows and sediment yields with higher values of coefficients of determination and Nash Sutcliffe efficiency.

Ayana *et al.* (2012) applied (SWAT) model to simulate the sediment yield from the Finchaa watershed (area 3,251 km^2), located in Western Oromia Regional State, Ethiopia to examine the applicability of the SWAT model in a watershed with a high sediment runoff modulus. The result showed that the SWAT model is capable for predicting sediment yields and hence can be used as a tool for water resources planning and management in the study watershed.

2.6.3 SWAT-CUP

When a SWAT simulation is taken place there will be discrepancy between measured data and simulated results. So, to minimize this discrepancy, it is necessary to determine the parameters which are affecting the results and the extent of variation. SWAT-CUP is a computer program for calibration of SWAT models. It is a public domain program, and as such may be used and copied freely. The program links SUFI2, PSO, GLUE, Parasol, and MCMC procedures to SWAT. It enables sensitivity analysis, calibration, validation, and uncertainty analysis of SWAT models. SWATCUP2012 has been tested for all procedures prior to release (Abbaspour, 2014). SWAT-CUP has been used by different researchers in different area for SWAT model calibration. Currently, there is a wide application of SWAT-CUP in calibration and uncertainty.

Setegn *et al*. (2009) used Sequential Uncertainty Fitting (SUFI-2) to calibrate and validate the SWAT model for flow in Lake Tana Basin on a daily basis and for flow and sediment yield in Anjeni gauged watershed on a monthly basis.

The monthly calibration and validation of the SWAT model for flow and sediment yield in Anjeni watershed have shown that the model can predict the flow and sediment yield. The statistical comparison between the measured monthly sediment yield and best simulation result from SUFI-2 algorithms showed a good agreement. The result was verified by NSE = 0.81, PBIAS = 28%, RSR = 0.23 and R^2 = 0.85 for calibration and NSE = 0.79, PBIAS = 30%, RSR = 0.29 and R^2 = 0.80 for validation periods. The results showed good result both for calibration and validation periods.

Gebremicael, *et al*., (2013) used SWAT-CUP, SUFI-2 to calibrate SWAT model of the Upper Blue Nile in analysing the trend of runoff and sediment changes and obtained best fitting model evaluation parameters.

Singh, *et al*., (2013) applied SWAT-CUP, SUFI-2 to evaluate the performance of SWAT model for the stream flow measurement of the Tungabura catchment in India, and they reported that the obtained results showed correlation between measured and simulated discharge at the 95% level of confidence.

Adgolign (2015) used SUFI-2 to calibrate SWAT model of Didessa river basin for stream flow calibration and obtain very good correlation between observed and simulated discharge.

3. METHODOLOGY AND MATERIALS

3.1 Study Area

The Blue Nile and its tributaries all rise on the Ethiopian plateau at an elevation of 2000 to 3000m. The Blue Nile starts at Lake Tana in the north western Ethiopian high lands. After leaving Lake Tana it passes through deep Ethiopian gorges and valleys for about 1609Km before entering Sudan. The Blue Nile basin encompasses 14 main sub basins with a total area of 176650km^2. Its catchment accounts for about 20% of Ethiopian land surface.

Out of 14 sub basins; the Didessa river basin, which is the study area, is located in the southernmost part of the Blue Nile basin. Didessa river basin drainage area is nearly 27711.9km^2. The drainage area touches the four administrative zones of Oromia regional state of Ethiopia: Jimma zone in the most upper and middle part, Illibabur zone in the middle part and East and West Wollega in the lower part. The Didessa sub basin is geographically located between 36^{0}02’ and 36^0 46’ East longitude, and between 7^0 43’ and 8^0 13’ north latitude.

The altitude in Didessa river basin ranges between 633 m.a.s.l at the Didessa-Abbay confluence and 3144 m.a.s.l at the source of Anger River, one of the major tributaries of Didessa river, in Abe Dongoro District of Horro Guduru Wolloga Administrative Zone, Northeast of the basin. The highlands in the north eastern and southern parts of the basin are higher in altitude than 2100 m.a.s.l. The low lands, with altitudes less than 1100 m.a.s.l are located at the eastern remote areas of Anger sub-basin and the northern end of the sub basin, following the Valley of Didessa River.

The southern part of the sub-basin is highly forested compared to the middle and northern catchments. This part of catchment was suffered (especially in1980s and 1990s) due to expansion of agriculture, about 17% of the forest land has been converted to cultivated land. The middle part of the sub-basin is also covered with high forest of Sigmo and Limu Seka. According to WBISPP report, 18% of Sigmo forest has been converted to cultivated land in the last 30 years. The northern part of the Didessa river basin which is mainly located on Illubabur and East Wollega zones of Oromia regional state are intensively cultivated and have been going through a high rate of deforestation for the last half a century (WBISPP, 2001, Admasu, 2011).

The mean annual rain fall ranges between 1492.75mm in the southern to 2044mm in the northern catchments. The majority of the area is characterized by a humid tropical climate with heavy rain fall and most of the total annual rain fall is received during one rainy season called summer. The maximum and minimum temperature varies between 18.88 – 35.33^{0}C and 6.58 – 16.91^{0}C, respectively (See Appendix A).

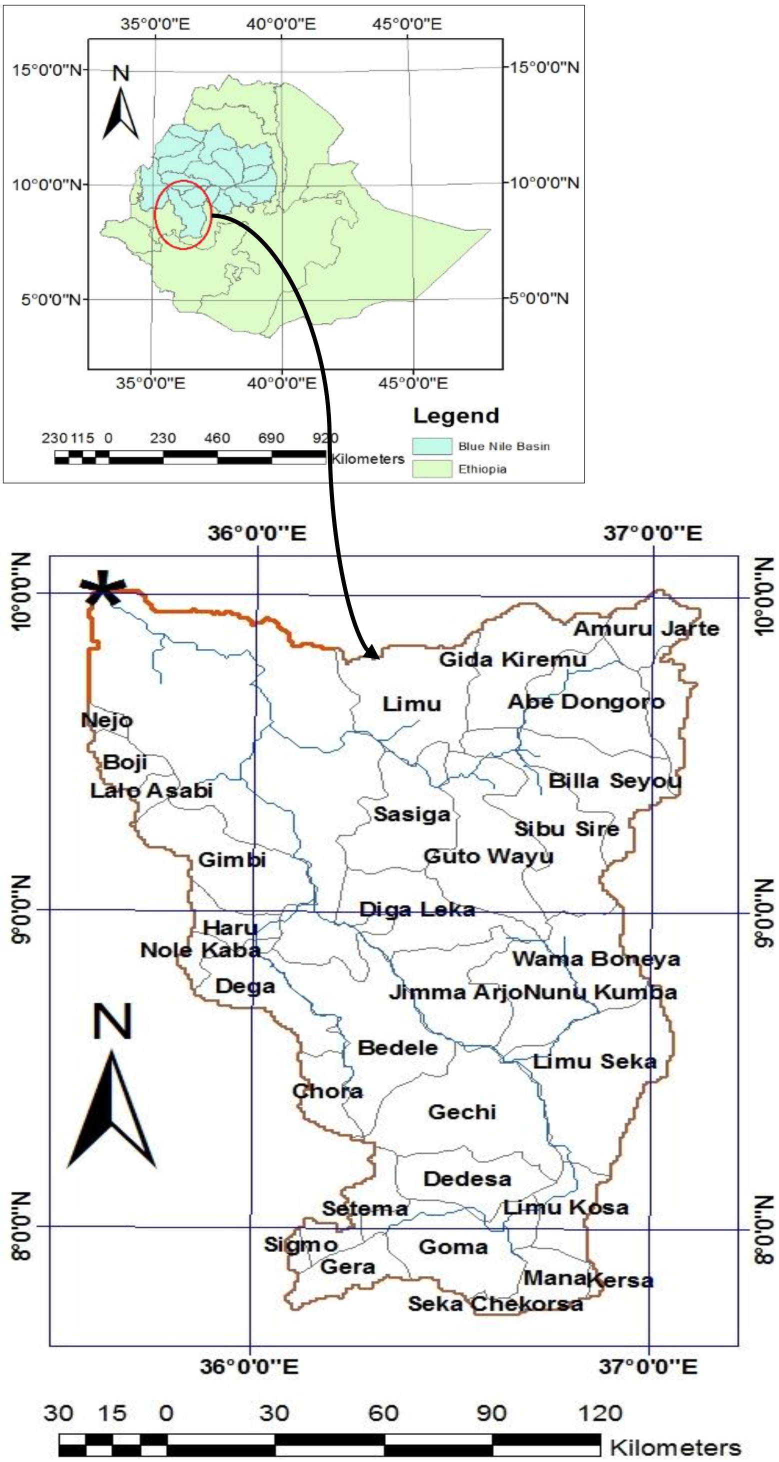

Figure 3. 1 Location of study area

3.1.1 Arjo Didessa Irrigation Project

The project area is located within Didessa River basin which is in turn located in Abay River basin. It is within the Western Oromia National Regional State; particularly at tri junction of East Wollega, Ilubabor and Jima zones. The basin of the irrigation project is bordered by Omo-Gibe River basin on eastern side and Baro Akobo River basin on South West side. The total area of the catchment at the proposed dam is about 8,250.13 km^2.

The project area can be reached from Addis Ababa through two alternative high ways that take either to Bedele or Nekemt. The all- weather gravel road that takes from Nekemt to Bedele passes through the project area. Hence, in general the project area is about 480km from Addis Ababa through Jima and Bedele.

The basin drains a part of Jima high lands including Goma (Agaro), Setema, Sigimo, Limu Saka, and part of Ilubabor including Borecha, Didessa, Gachi and Bedelle Woredas above the proposed dam. Arjo, Nunu Kumba, Sibu Sire and Wama Bonaya woredas are also within the catchment. The command area is drained by river Didessa and other tributaries such as Wama River. The general slope of the basin/or catchment is toward NE, E and NW directions. The area has generally a rugged topography with the highest and lowest elevation is about 2890 and 1030 m amsl respectively located at Sigimo-Gera area and Didessa river valley (OWWDSE, 2009).

Table 3. 1 Monthly total and Minimum flow of Didessa near Arjo (OWWDSE, 2009)

Months	Parameters					
	Total monthly flow		Minimum monthly flow		Difference	
	m^3/sec	m^3/month	m^3/sec	m^3/month	m^3/sec	m^3/month
Jan	17.64	47238048	4.473	11980483	13.16	35257565
Feb	12.4	29994209	2.25	5443200	10.15	24551009
Mar	10.44	27973924	0.966	2587334	9.48	25386589
Apr	15.64	40527302	4.557	11811744	11.08	28715558
May	29.14	78052326	10.364	27758938	18.78	50293388
Jun	98.47	255236832	45.433	117762336	53.04	137474496
Jul	263.37	705408958	137.36	367918416	126	337490542
Aug	423.39	1134009026	220.65	590994317	202.74	543014709
Sept	343.82	891191981	217.78	564477984	126.05	326713997
Oct	218.67	585697513	58.377	156356957	160.3	429340556
Nov	68.32	177074554	26.258	68060736	42.06	109013818
Dec	35.65	95485139	13.792	36940493	21.86	58544646
Qtot		4,067,889,811		1,962,092,938		2,105,796,874

Main Dam

The earth and rock fill dam has been planned and designed to be located on river Didessa at about 1.5 km above its confluence with Wama River. The salient features of the dam for the irrigation Project were as follows:

Dam crest level	1359.00 m
Bed level	1312.00m
Dam height	47.00m
Dam bottom position length	561.69m
Dam crest Length	502 m
Dam crest width	10.00m
Dam bottom width	302.15m
Maximum water level	1357.00m
Full reservoir level	1354.00m

The Reservoir

Total catchment area of the dam	$5632km^2$
Surface area at maximum water level	$115.05km^2$
Maximum water capacity	2256.30 Mm^3
Full Reservoir capacity	1924.60 Mm^3
Minimum drawdown Capacity	874.70 Mm^3
Live Storage	1049.90 Mm^3

Ungated Ogee Type Spillway

Location	on right bank
Spillway crest elevation	1354.00m
Spillway crest length	125.00m
Weir height	17.00m
Design flood (PMF)	$300m^3/s$
Spillway outflow routed discharge	$1438m^3/s$
Spillway flood discharge head	3.00m

River diversion conduit

Total length of diversion conduit	645.78m
Total flood out flow capacity	$215.00m^3/s$

Dam site and flow condition at the dam photo was taken during field survey as shown on figure 3.2.

Figure 3. 2 Arjo Didessa Dam Site and River Flow at dam site

Flow parameters like monthly flow out from reservoir, monthly flow in to reservoir and consumptive use of water are needed for SWAT model to simulate trap efficiency of the reservoir. These data were obtained from OWWDSE and described in table 3.1 and 3.2. Reservoir parameters like reservoir surface area at full capacity, capacity of reservoir are also needed and obtained from the same source for this study.

Table 3. 2 Monthly inflow, residual and out flow from reservoir (OWWDSE, 2009)

Months	Mean Monthly Inflow(Mm^3)	Capacity of the Div. Cond.(Mm^3)	Residual Storage(Mm^3)	Respective Max. WL(masl)
Jan	54.10	557.28	0.00	1312.00
Feb	39.76	557.28	0.00	1312.00
Mar	46.27	557.28	0.00	1312.00
Apr	54.90	557.28	0.00	1312.00
May	115.29	557.28	0.00	1312.00
Jun	321.72	557.28	0.00	1312.00
Jul	749.63	557.28	192.35	1328.00
Aug	1097.04	557.28	539.76	1336.63
Sep	1038.61	557.28	481.33	1335.47
Oct	787.84	557.28	230.56	1329.02
Nov	352.56	557.28	0.00	1312.00
Dec	120.11	557.28	0.00	1312.00

3.2 Material used

Materials and tools used for this study include ArcGIS10.1, ArcSWAT2012, PCPSTAT, dew02, SWAT-CUP, XLSTAT2015 and digital camera

I. ArcGIS10.1

Geographic information system is an information system focusing on the collection, modelling, management, display, and interpretation of geographic data. ArcGIS10.1 extension is a graphical user interface for the SWAT (Soil and Water Assessment Tool) model (Arnold et al., 1998). ArcGIS10.1 was first installed on the system to display SWAT2012 toolbars

II. ArcSWAT2012

ArcSWAT2012 was installed by default in the folder C:\SWAT\ArcSWAT\ and has been used to simulate hydrological parameters including sediment yield in Didessa watershed. The SWAT2012/ArcSWAT Interface requires:

Hardware:

1. Personal computer using a recent processor (2008 or more recent), which runs at 2 gigahertz or faster
2. 2 GB RAM minimum
3. 1 Gigabyte free memory on the hard drive for minimal installation and up to 2 gigabyte for a full installation (including sample datasets and US STATSGO data)

Software (ArcSWAT for ArcGIS 10.0 or 10.1 versions):

1. Microsoft Windows operating system (e.g., XP, Windows 7, Server 2008) with most recent kernel patch
2. Microsoft .Net Framework 3.5
3. Adobe Acrobat Reader version 8 or higher
4. ArcGIS: ArcView 10.0 with Service Pack 5 (Build 4400) OR ArcView (Basic) 10.1 with most recent Service Pack
5. ArcGIS Spatial Analyst extension (ArcGIS 10.0 or 10.1 version)

III. Digital camera

Personal digital camera was used to capture required images during data collection and field observation.

IV. PCP STAT

The program pcpSTAT.exe calculates statistical parameters of daily precipitation data used by the weather generator of the SWAT model (userwgn.dbf).

Table 3. 3 Statistical parameters of Precipitation used by weather generator

No	Parameters	Definition
1	PCPMM(Mon)	Mean total monthly precipitation
2	PCPSTD(mon)	Standard deviation for daily precipitation in month
3	PCPSKW(Mon)	Skew coefficient for daily precipitation in month
4	PR_W1(Mon)	Probability of a wet day followed by a dry day
5	PR_W2(Mon)	Probability of a wet day followed by a wet day
6	PCPD(Mon)	Average number of days of precipitation in month

V. dew02

The programs dew.exe and dew02.exe are designed to calculate the average daily dew point temperature per month using daily air temperature and humidity data. Dew2.exe is used when average daily temperature data is available and dew02.exe is used minimum and maximum daily temperature data is available (Stefan, 2013). In dew02.exe program the input file storing the maximum and minimum daily temperature (℃) and the average daily humidity (%) data in ASCII text file with three columns. The first store maximum temperature, the second minimum temperature and the third daily humidity data.

Table 3. 4 Statistical parameters of temperature used by weather generator

No	Parameter	Description
1	Tmp_max	Average daily maximum temperature
2	Tmp_min	Average daily minimum temperature
3	hmd	Average daily humidity in month
4	dewpt	Average daily dew point temperature

VI. XLSTAT2015

XLSTAT2015 Used to calculate missing data by linear regression.

VII. SWAT-CUP

SWAT-CUP is a public domain program, and as such may be used and copied freely. The program links SUFI2, PSO, GLUE, Para Sol, and MCMC procedures to SWAT. It enables sensitivity analysis, calibration, validation, and uncertainty analysis of SWAT models. SWATCUP2012 has been tested for all procedures prior to release. However, no warranty is given that the program is completely error-free (Abbaspour, 2014).

3.3 SWAT Model Description

SWAT is the acronym for Soil and Water Assessment Tool, a river basin, or watershed, scale model developed by Dr. Jeff Arnold for the USDA (ARS). SWAT was developed to predict the impact of land management practices on water, sediment and agricultural chemical yields in large complex watersheds with varying soils, land use and management conditions over long periods of time (Neitsch *et al*., 2011).

SWAT incorporates features of several ARS models and is a direct outgrowth of the SWRRB model. Specific models that contributed significantly to the development of SWAT were CREAMS and EPIC (Tyagi *et al.*, 2014).

It is a conceptual model that functions on a continuous time step. Model components include weather, hydrology, erosion/sedimentation, plant growth, nutrients, pesticides, agricultural management, channel routing, and pond/reservoir routing. The SWAT model predicts the influence of land management practices on constituent yields from a watershed.

The SWAT watershed model also contains algorithms for simulating erosion from the watershed. Erosion is estimated using MUSLE. MUSLE estimates sediment yield from the surface runoff volume, the peak runoff rate, the area of the HRU, USLE soil edibility factor, the USLE cover and management factor, the USLE support practice factor, USLE topographic factor, and a coarse fragment factor (Neitsch *et al*., 2011).

SWAT has been employed to model watersheds of different scales predict sediment yield, runoff, stream flow and others across the world. Batrie *et al*. (2011) applied SWAT model to the Upper Blue Nile River basin which has a total area of 184,560 km^2 to simulate soil erosion and the output was successfully calibrated and validated. Helena (2015) applied SWAT model to upper Blue Nile to investigate hydrologic response unit discretization for erosion modelling and reported that the model was successfully calibrated and validated. Setegn (2008) applied SWAT model to Lake Tana basin which has basin area of 15,096 km^2 to model sediment yield and the model was successfully calibrated and validated. The SWAT model was applied for simulation of a sediment yield by Setegn *et al*. (2010) in the Anjeni gauged catchment (110 ha) and the obtained result was quite acceptable. The purpose of the study was to examine the applicability of the SWAT model in a watershed with a high sediment runoff modulus.

The automated calibration process was used to calibrate the model parameters and the model was successfully calibrated and validated.

There many other literatures that reported as the SWAT model has been used for watershed modelling in Blue Nile river basin to predict runoff, stream flow and sediment yield and soil erosion. Therefore, SWAT model is applicable in small and large basin scales of Blue Nile and was used to predict sediment yield in this study.

3.4 Data collection and Sources

The required data for this study included Digital Elevation model (DEM), land use/land cover map, soil map and soil data, weather data, sediment and stream flow data. These data were obtained from various sources as shown in table 3.5.

Table 3. 5 SWAT input data and their sources

Data Type	Source	Scale/Period	Description
DEM	Ministry of Water, Irrigation and Energy (MoWIE)	30m X 30m	Digital Elevation Model
Land Cover	Ministry of Water, Irrigation and Energy (MoWIE)	1998	Land use classification map
Soil	Ministry of Water, Irrigation and Energy (MoWIE)	1998	Soil classification map
Weather	National Meteorological Service Agency (NMSA) and Weather generator (Internet)	1980 - 2014	1. Daily rainfall data 2. Daily Max and min Temperature 3. Daily Wind speed 4. Daily Radiation 5. Daily relative humidity

3.4.1 Digital Elevation Model Data

DEM is any digital representation of a topographic surface and it is specifically made available in a form of a raster or regular grid of spot heights. It is the basic input of the SWAT hydrologic model. The Digital Elevation Model of 30m by 30m resolution of Blue Nile river basin has been obtained from ministry of water, irrigation and energy (MoWIE), GIS department.

3.4.2 Land Cover Map

Land cover is one of the most important factors that affect runoff, evapotranspiration and surface erosion in a watershed. The land cover map of Blue Nile river basin was obtained from ministry of water, irrigation and energy (MoWIE), GIS department, Ethiopia.

3.4.3 Soil Map

SWAT model requires different soil textural and physio-chemical properties such as soil texture, available water content, hydraulic conductivity, bulk density and organic carbon content for different layers of each soil type. Soil map of Blue Nile river basin was obtained from the ministry of water, irrigation and energy (MoWIE), GIS department, Ethiopia.

3.4.4 Weather Data

Climate data is among the most prerequisite parameter of SWAT model. There are various sources of climatic data. In this study, two sources were used to obtain climatic data. The first one is Ethiopian National Metrological Service Agency (ENMSA) from which daily recorded climatic data of 20 stations were collected. However only some of them have long year recorded data. Only seven (7) stations which were with better recorded data has been selected to be used. The second source is internet (http://globalweather.tamu.edu/). Fully recorded daily climatic data from 1979 to 2014 for eighty (80) stations in Didessa watershed are available on this website. Climatic data of these stations were downloaded and only seven stations were selected to be used in this study.

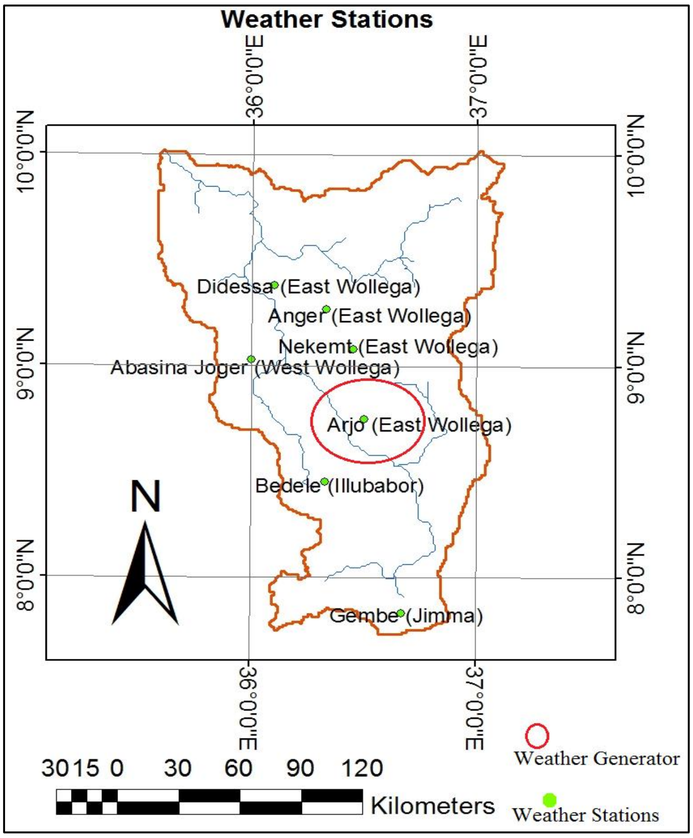

Figure 3. 3 Location of weather stations

The station distribution is not even, very densely in area, few and scares in other area as shown on figure 3.3.

However, weather data obtained from MoWIE contained a lot of missing data and unrecorded data for long period of time up to two years or more. Geographic location of weather stations are described in figure 3.3 and table 3.6.

Table 3. 6 Location and Elevation of weather data stations

No	Station	Zone	Elevation(m)	Longitude	Latitude
1	Anger	East Wollega	1350	36.33	9.27
2	**Arjo**	**East Wellega**	**2565**	**36.50**	**8.75**
3	Bedele	Illubabor	2011	36.33	8.45
4	Didessa	East Wellega	1310	36.10	9.38
5	Abasina Joger	West Wellega	1800	36.00	9.03
6	Nekemte	East Wellega	2080	36.46	9.08
7	Gembe	Jimma	1596	36.67	7.83

3.5 Data Analysis and Processing

3.5.1 Weather Data

Weather data obtained from ENMSA were used for SWAT model and daily data which downloaded from global weather were used to fill missing data (unrecorded data for long period of time). For missing data computation, linear regression method was used. XLSTAT2015 tool (software) has been used for linear regression. In case when daily data of one station was not recorded for long period of time, for example for one year, two years etc. data obtained from global weather were copied and used. Because unexpected results were obtained from linear regression for such cases and coefficient of correlation was very small (closer to zero). Daily data obtained from both sources have similar trend and monthly data were almost the same. Therefore, instead of computed value, daily data obtained from global weather were directly used for long period missed data. For example the similarity between monthly rainfall data obtained from MoWIE and from Global weather at Arjo station was compared and shown on figure 3.4 and figure 3.5

3.5.1.1 Rainfall Data

The SWAT model requires daily rainfall data arranged vertically parallel to time series. For selected seven stations as shown on figure 3.3, Missing data were filled with the help of XLSTAT2015 program and global weather.

Correlation between rain data obtained from MoWE and Global weather at Arjo station for the periods (1984 -2007) is shown on figure 3.4.

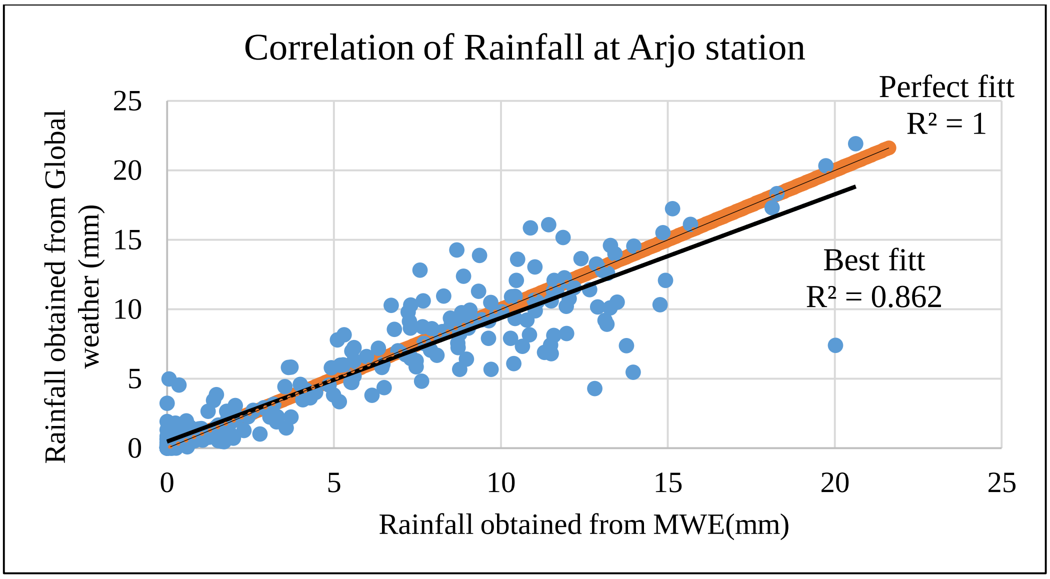

Figure 3. 4 Comparison of rainfall data obtained from MoWE and global weather

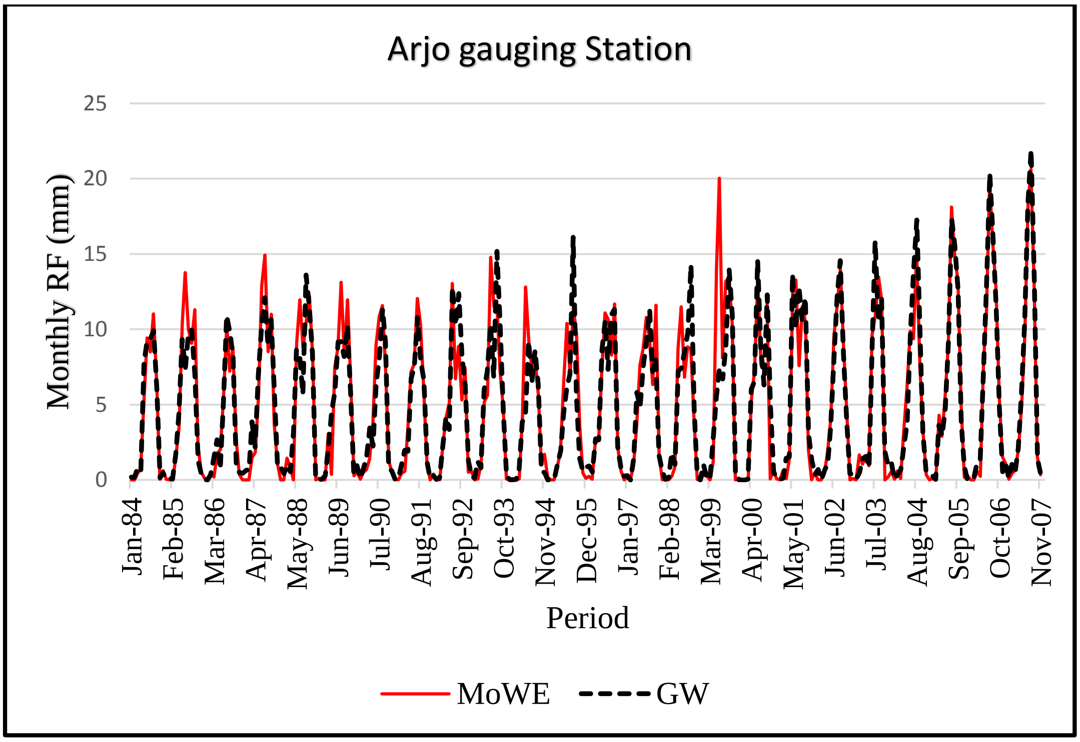

Figure 3. 5 Similarity between Global weather RF data and recorded RF data

Consistency of Rainfall Data

Hydrological data for water-management studies should be stationary, consistent, and Homogeneous when they are used in frequency analyses or system simulations. Double mass curve method was used to check consistency of rain fall data for this study.

Double Mass Curve

Double-mass analysis assumes a linear relation between time series of hydrological data. As this assumption may not be valid at all rates of accumulation, it must be verified. Rainfall data are usually proportional to totals at nearby stations in the same hydrological area.

Double-mass analysis is used not only to verify the relative consistency of a time series, but also to find correction factors for errors and fill in gaps (Dahmen and Hall, 1990). This application is limited to monthly and yearly totals, as it normally does not work with daily ones.

Furthermore, at its best, double-mass analysis preserves the mean and not the standard deviation of the time series, unless a proportional error has been made (e.g. measuring rainfall in a measuring jar that is not calibrated for the sampling area).

A linear relation between two variables that include the pair x = O and y = O can be expressed as:Y = bx

Where b is a proportionality factor.

If yi, is the time series to be tested, xi, the time series of the pattern, and i = 0..., n (The number of data pairs and the index of the time steps), then the plot of $Yi = \sum yi$ (The mass of y) against $Xi = \sum xi$ (the mass of x) will result in a broken line through the origin, with an average slope $b_{av} = \frac{Yn}{Xn}$. The line passes through the origin because the sum of the data at time zero is zero for both X and Y. Defining the average slope as the slope of the line through the points 0, 0 and Yn, Xn will give a good enough estimate of the true mean of the proportionality factors.

Double mass curve was developed for each stations to check their consistency. Double mass curve for Nekemt rain fall station is shown on figure 3.6 and (See Appendix A) for remaining stations.

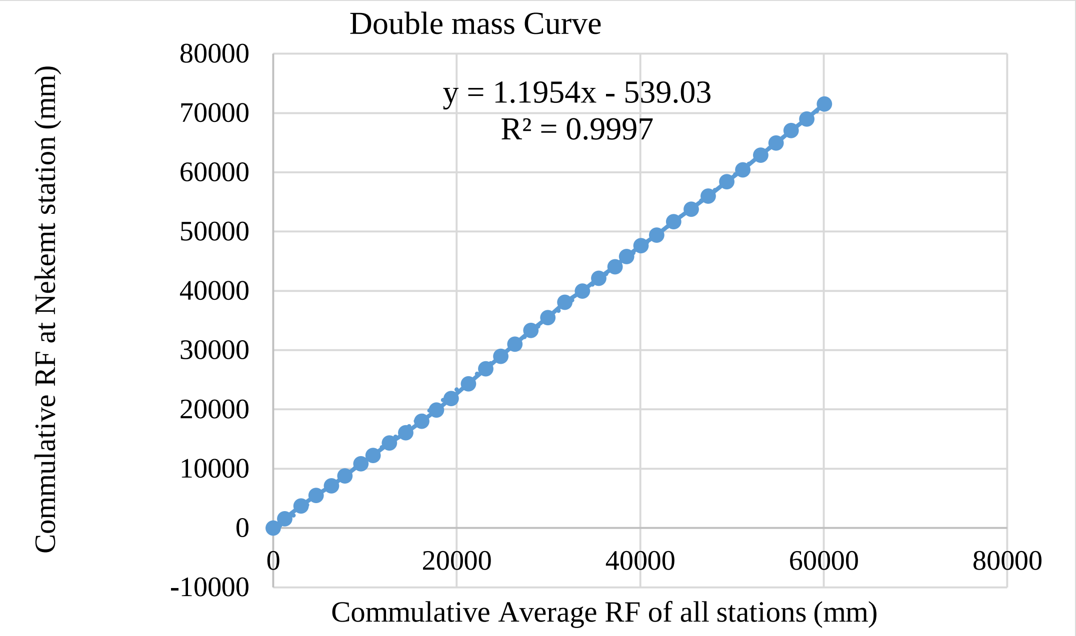

Figure 3. 6 Double mass curve for rainfall at Nekemt gauging station

From the figure 3.6 the line is straight, no change in slope, therefore the rainfall data for Nekemt station has consistency. Similarly double mass curve for other stations were described in Appendix A

3.5.1.2 Temperature Data

For generating of evaporation and evapotranspiration, temperature data is required for SWAT model simulation. The maximum and minimum daily temperature were obtained from ENMSA. Like other weather data even more than rainfall data it was difficult to get continuously recorded many years' data in the Didessa watershed. Like rainfall missed data were filled using XLSTAT2015 tool. After missed data were filled, temperature data was arranged downward parallel to corresponding date of record.

3.5.1.3 Wind speed, Relative Humidity and Sunshine Hours

Wind speed, relative humidity and solar radiation are also the vital parameters for SWAT model to generate weather. Since, very few stations had daily data of wind speed, relative humidity and solar radiation; it was preferred to use downloaded global weather data. Available recorded data were directly used and downloaded data were used in place of missing data.

3.5.2 Hydrological Data

3.5.2.1 Flow Data

Daily flow data is required for SWAT simulated result calibration and validation. Flow data for 15 stations were obtained from ministry of water, irrigation and Energy of Ethiopia. However, only 2 stations which were with better observed flow and sediment concentration sample were selected. Flow data of the two stations were collected and arranged vertically to generate sediment data by using rating curve. Flow data of one station was further prepared as per the requirement of SWAT-CUP for calibration and validation. The selected gauging stations were Toba (Didessa near Denbi) and Gutin (Little Anger). Location and area of these stations are given in table 3.7. These stations were selected because of their long term and reliable data.

Table 3. 7 Location of selected gauging stations

St. No	Station	Location	Longitude	Latitude
114014	Toba (Didessa near dembi)	Jimma	36:27:0	8:3:0
114007	Gutin (Little Anger)	Anger Gutin	36:35:0	9:30:0

One of the measure of stream flow data quality is completeness. Completeness is the percentage of days of available data with respect to total number of days having recorded data.

$$Completness = \frac{\text{Number of days having stream flow data}}{\text{Total number of days in the record}} * 100\% \quad -----3.16$$

Completeness of stream flow data for Toba and Gutin gauging stations were described in table 3.8.

Table 3. 8 Completeness of flow data at Toba and Gutin stations

Gauging Station	Period	Number of days in record	Days of missed data	Completeness (%)
Toba	1996 to 2006	4018	4007	99.73
Gutin	1993 to 2002	3652	3636	99.57

Completeness of stream flow data for both stations were high and missed data were filled by forwarding average method. Monthly observed and simulated flow ware given in Appendix A.

3.5.2.2 Sediment Data

There are few sites which has measured suspended sediment concentration data in Didessa river basin with a very short data. Suspended sediment sample (mg/L) observed at Toba (Didessa near Dembi), Gutin (Little Anger), Didessa (Didessa near Arjo) and Tato (Tato near Gutie) were obtained from MoWE. Relatively Toba and Gutin have better observed suspended sediment concentration than other stations. Months during suspended sediment sample had taken was described in table 3.8 and table 3.9 for Toba and Gutin respectively.

Didessa near Arjo outlet may represent larger watershed area however, observed sediment at this station was very small (only five days recorded) sediment data were obtained. Tato station is located on Wama river which joins Didessa river at downstream of Arjo Didessa dam at which sediment yield was to be determined.

Toba station is located at upstream of Arjo Didessa Reservoir at which sediment yield was to be determined. Gutin (Little Anger) station is located at northern part of Didessa river basin (figure 3.7) from where large quantity of sediment yield is expected to be generated due soil erosion resulted from agricultural expansion. Suspended sediment concentration observed at Toba and Gutin stations were selected to check the validity of SWAT model to predict sediment yield in Didessa river basin.

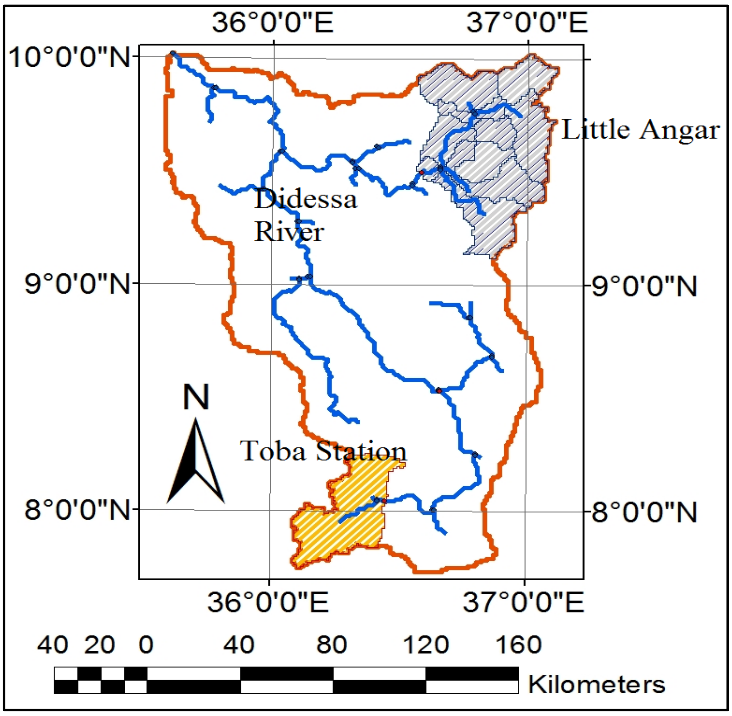

Figure 3. 7 Location of Little Anger and Toba gauging stations

Tato represents small area and Didessa near Arjo has few sediment samples. Therefore, both Tato and Didessa were not used. Even for Toba (table 3.8) and Little Anger (table 3.9) Suspended Sediment concentration was not continuously measured. Since SWAT-CUP needs continuously measured sediment data, the data was not used for calibration and validation. Continuous suspended sediment has been generated by using sediment rating curve and used only for comparison.

Table 3. 9 Months having suspended sediment concentration at Toba

<table>
<tr><th></th><th>Jan</th><th>Feb</th><th>Mar</th><th>Apr</th><th>May</th><th>Jun</th><th>Jul</th><th>Aug</th><th>Sep</th><th>Oct</th><th>Nov</th><th>Dec</th></tr>
<tr><td>1990</td><td></td><td></td><td style="background:yellow"></td><td></td><td></td><td></td><td style="background:yellow"></td><td></td><td style="background:yellow"></td><td></td><td></td><td style="background:yellow"></td></tr>
<tr><td>1993</td><td></td><td></td><td></td><td style="background:yellow"></td><td style="background:yellow"></td><td style="background:yellow"></td><td></td><td></td><td></td><td></td><td></td><td></td></tr>
<tr><td>1998</td><td></td><td></td><td></td><td></td><td></td><td></td><td></td><td></td><td></td><td style="background:yellow"></td><td></td><td></td></tr>
<tr><td>2005</td><td></td><td></td><td></td><td></td><td></td><td></td><td></td><td></td><td style="background:yellow"></td><td></td><td></td><td></td></tr>
<tr><td>2006</td><td></td><td></td><td></td><td></td><td></td><td></td><td style="background:yellow"></td><td></td><td></td><td></td><td></td><td></td></tr>
<tr><td>2010</td><td></td><td></td><td></td><td></td><td></td><td></td><td></td><td></td><td style="background:yellow"></td><td></td><td></td><td></td></tr>
<tr><td>2011</td><td></td><td></td><td></td><td></td><td></td><td></td><td></td><td></td><td style="background:yellow"></td><td></td><td></td><td></td></tr>
<tr><td>2013</td><td></td><td></td><td></td><td></td><td></td><td></td><td></td><td></td><td></td><td></td><td style="background:yellow"></td><td></td></tr>
<tr><td>2014</td><td></td><td></td><td></td><td></td><td></td><td></td><td></td><td></td><td></td><td style="background:yellow"></td><td></td><td style="background:yellow"></td></tr>
</table>

The number of days on which suspended sediment sample was taken during a month ranges from one day to six days. For each day sediment sample was measured three times.

Table 3. 10 Months having suspended sediment concentration at Gutin

<table>
<tr><th></th><th>Jan</th><th>Feb</th><th>Mar</th><th>Apr</th><th>May</th><th>Jun</th><th>Jul</th><th>Aug</th><th>Sep</th><th>Oct</th><th>Nov</th><th>Dec</th></tr>
<tr><td>1990</td><td></td><td style="background:yellow"></td><td style="background:yellow"></td><td style="background:yellow"></td><td></td><td></td><td style="background:yellow"></td><td></td><td></td><td style="background:yellow"></td><td></td><td></td></tr>
<tr><td>1991</td><td></td><td></td><td></td><td></td><td></td><td></td><td></td><td style="background:yellow"></td><td></td><td></td><td style="background:yellow"></td><td></td></tr>
<tr><td>1992</td><td></td><td></td><td></td><td></td><td></td><td></td><td></td><td style="background:yellow"></td><td style="background:yellow"></td><td></td><td></td><td></td></tr>
<tr><td>1994</td><td></td><td></td><td></td><td></td><td></td><td></td><td></td><td style="background:yellow"></td><td></td><td></td><td></td><td></td></tr>
<tr><td>1995</td><td style="background:yellow"></td><td></td><td></td><td></td><td></td><td></td><td></td><td style="background:yellow"></td><td style="background:yellow"></td><td></td><td></td><td></td></tr>
<tr><td>2006</td><td></td><td></td><td></td><td></td><td></td><td></td><td></td><td style="background:yellow"></td><td></td><td></td><td></td><td></td></tr>
<tr><td>2007</td><td></td><td style="background:yellow"></td><td></td><td></td><td></td><td></td><td style="background:yellow"></td><td></td><td></td><td></td><td style="background:yellow"></td><td></td></tr>
<tr><td>2008</td><td></td><td></td><td style="background:yellow"></td><td></td><td></td><td></td><td style="background:yellow"></td><td style="background:yellow"></td><td style="background:yellow"></td><td></td><td></td><td></td></tr>
<tr><td>2011</td><td style="background:yellow"></td><td></td><td></td><td></td><td></td><td></td><td></td><td></td><td></td><td></td><td></td><td></td></tr>
</table>

3.5.2.3 Weather Generator

SWAT includes the weather generator model to generate climatic data or to fill in gaps in measured records. The occurrence of rain on a given day has a major impact on relative humidity, temperature and solar radiation for the day. The weather generator first independently generates precipitation for the day. Once the total amount of rainfall for the day is generated, the distribution of rainfall within the day is computed.

Maximum temperature, minimum temperature, solar radiation and relative humidity are then generated based on the presence or absence of rain for the day. Finally, wind speed is generated independently.

In order to prepare the weather generator the monthly average value of minimum and maximum temperature, wind speed, humidity and sunshine hours (described in table 3.3 and 3.4) were determined using PCPSTAT and dew02 programs. Finally, a statistical weather generator file WXGEN for Arjo station was prepared and added to SWAT data base.

The overall procedure of this methodology can be described by the following flow chart.

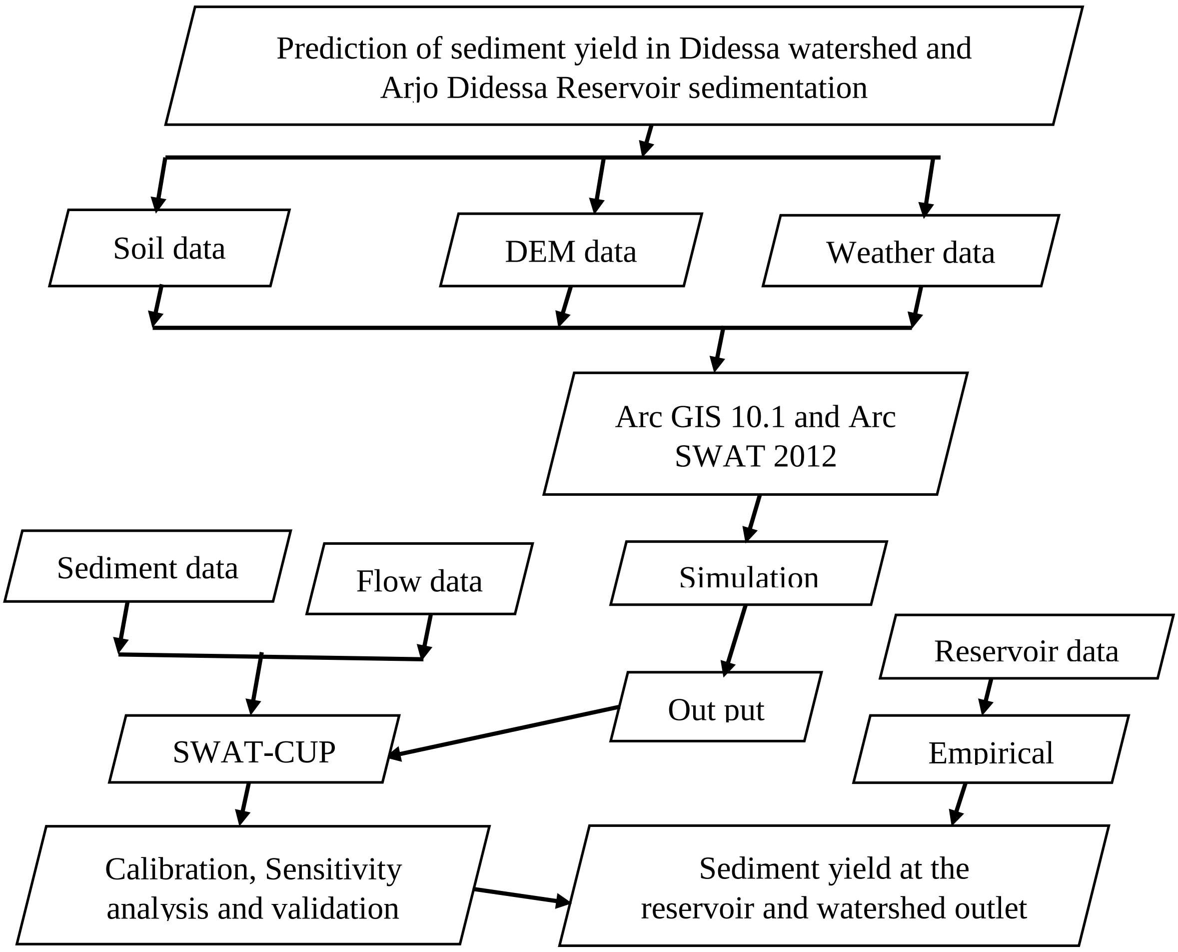

Figure 3. 8 Flow chart of work procedure

3.6 SWAT model Setup

3.6.1 Watershed Delineation

SWAT uses digital elevation model (DEM) data to automatically delineate the watershed into several hierologically connected sub-watersheds. The watershed delineation operation uses and expands Arc GIS and Spatial Analyst extension functions to perform watershed delineation. The first step in the watershed delineation was loading the properly projected DEM. The DEM of Didessa watershed, which is study area was extracted (clipped) by using GIS and loaded to Arc SWAT for further processes as described in figure 3.9.

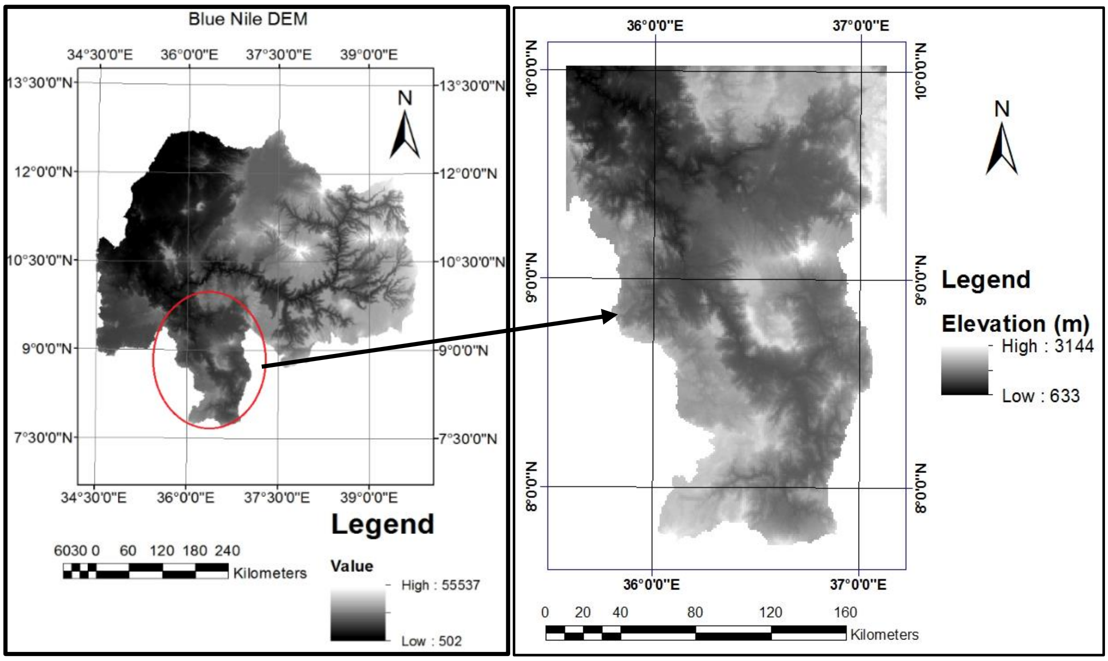

Figure 3. 9 Blue Nile DEM and Extracted Didessa River Basin DEM

After the DEM grid was loaded, the DEM map grid was processed to remove the non-draining zones. Stream network and sub-basin outlets were defined based on drainage area threshold approach. The threshold area defines the minimum drainage area required to form the origin of a stream. The interface lists a minimum, maximum and suggested threshold area. The smaller the threshold area, the more detailed the drainage network delineated by the interface but the slower the processing time and the larger memory space required. In this study, 17,000ha threshold area was used based on minimum and maximum threshold area suggested. The watershed delineation activity was finalized by calculating the geomorphic sub-basin parameter. Number of HRUs and sub-basins produced were 666 and 89 respectively.

3.6.2 Hydrologic response unit analysis

Hydrologic response units (HRUs) are lumped land areas within the sub-basin that are comprised of unique land cover, soil and management combinations. HRUs enable the model to reflect differences in soil erosion, evapotranspiration and other hydrologic conditions for different land covers and soils. The runoff is estimated separately for each HRU and routed to obtain the total runoff for the watershed hence sediment yield. This increases the accuracy in flow prediction and provides a much better physical description of the water balance. Land cover map and soil map are needed to create HRUs.

3.6.2.1 Land Cover Map

Land cover is one of the most important factors that affect runoff, evapotranspiration and surface erosion in a watershed. The land cover map of Didessa river basin was clipped from Blue Nile basin land cover map. The land cover data in a projected shape file format were loaded into the ArcSWAT interface to determine the area and hydrologic parameters of each land-soil category simulated within each sub-watershed. The land cover classes were defined using the look up table. A look-up table that identifies the 4-letter SWAT code for the different categories of land cover/land use was prepared so as to relate the grid values to SWAT land cover/land use classes. Then, the land cover loaded was reclassified and displayed as shown on figure 3.10.

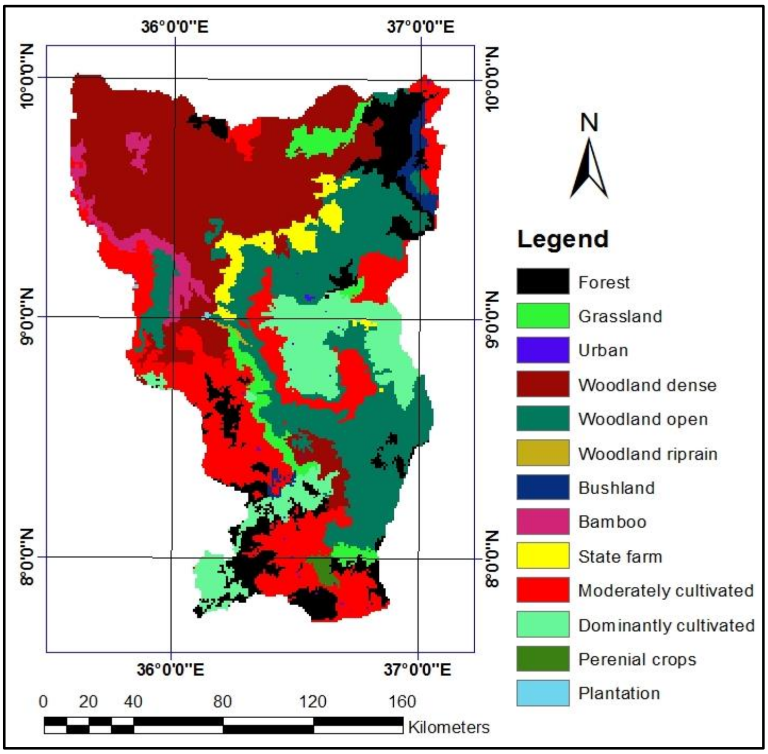

Figure 3. 10 Land cover map of Didessa River basin

After the land cover SWAT code assigned to all map categories, calculation of the area covered by each land use and reclassification were done. The percentage of area covered by each land cover type is described in table 3.10.

Table 3. 11 Land cover map of Didessa River basin

No	Land cover	Area (%)	Area covered (Km^2)
1	Forest	9.77	2707.45
2	Grassland	3.23	895.09
3	Urban	0.13	36.03
4	Woodland dense	28.38	7864.64
5	Woodland open	21.59	5983.00
6	Woodland riprain	0.09	24.94
7	Bushland	1.14	315.92
8	Bamboo	2.59	717.74
9	State farm	2.69	745.45
10	Moderately cultivated	19.81	5489.73
11	Dominantly cultivated	10.08	2793.36
12	Perenial crops	0.45	124.70
13	Plantation	0.05	13.86

3.6.2.2 Soil Map

The obtained soil map shapefile was co-referenced with the FAO (1998) soil data base to obtain the physical description and characteristics of the map. However, SWAT data base has no FAO soil but American soils. In order to add FAO soil into SWAT data base MWSWAT was downloaded from (http://www.waterbase.org/) and installed. Finally, FAO soil was copied from MWSWAT data base and added to ArcSWAT data base for further processes. As of the land cover, the soil layer in the map was linked to the user soil database information by loading the soil look-up table and reclassification applied.

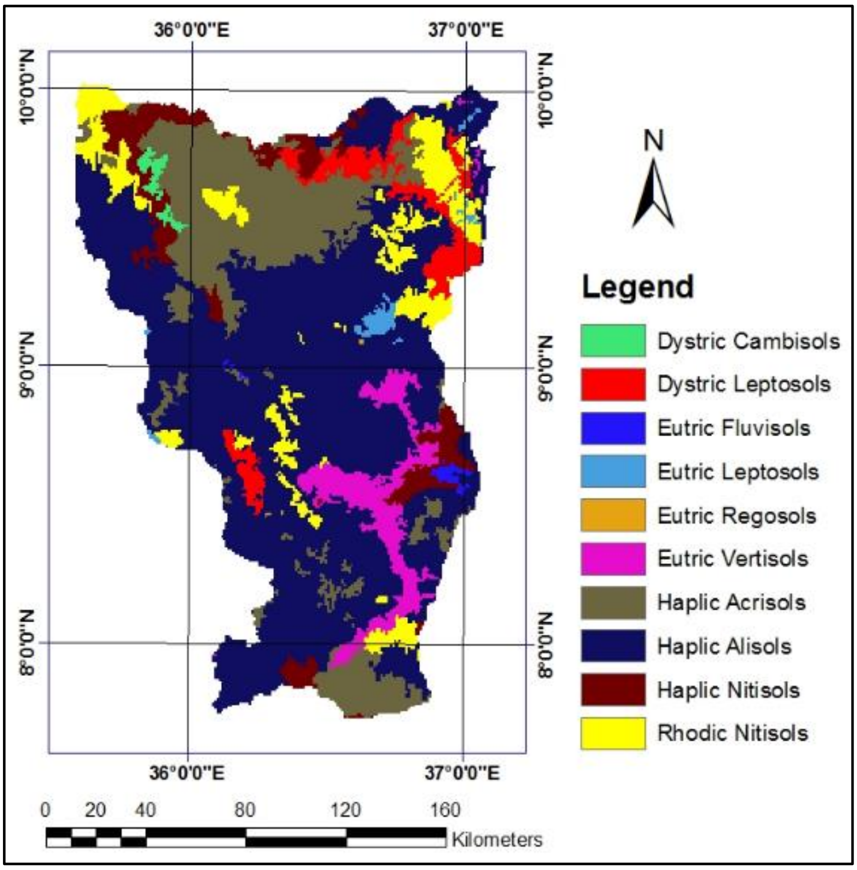

Figure 3. 11 Didessa River basin soil map

Major soil types in the basin are Haplic Alisols, Haplic Acrisols, Rhodic Nitisols, Haplic Nitisols, Eutric Fluvisols and Dystric Leptosols.

Table 3. 12 Soil types and their percentage of area cover

No	Soil	Area (%)	Area Covered (km^2)
1	Dystric Cambisols	0.58	160.73
2	Dystric Leptosols	4.35	1205.47
3	Eutric Fluvisols	5.48	1518.61
4	Eutric Leptosols	0.76	210.61
5	Eutric Regosols	0.03	8.31
6	Eutric Vertisols	0.1	27.71
7	Haplic Acrisols	18.99	5262.49
8	Haplic Alisols	55.11	15272.04
9	Haplic Nitisols	6.12	1695.97
10	Rhodic Nitisols	8.48	2349.97

3.6.2.3 Slope

The land slope classes were also integrated in defining the hydrologic response units. The DEM data used during the watershed delineation was also used for slope classification. The multiple slope discretization operation was preferred over the single slope discretization as the sub-basins have a wide range of slopes between them. Elevation of the Didessa river basin ranges from 3144m to 633m. Multiple slope classes in ArcSWAT was used to classify the slope into three slope classes as shown in the figure 3.6. Based on the suggested min, max, mean and median slope statistics of the watershed, three slope classes (0- 2.5, 2.5 – 6.5, and >6.5 %) were applied and slope grids reclassified.

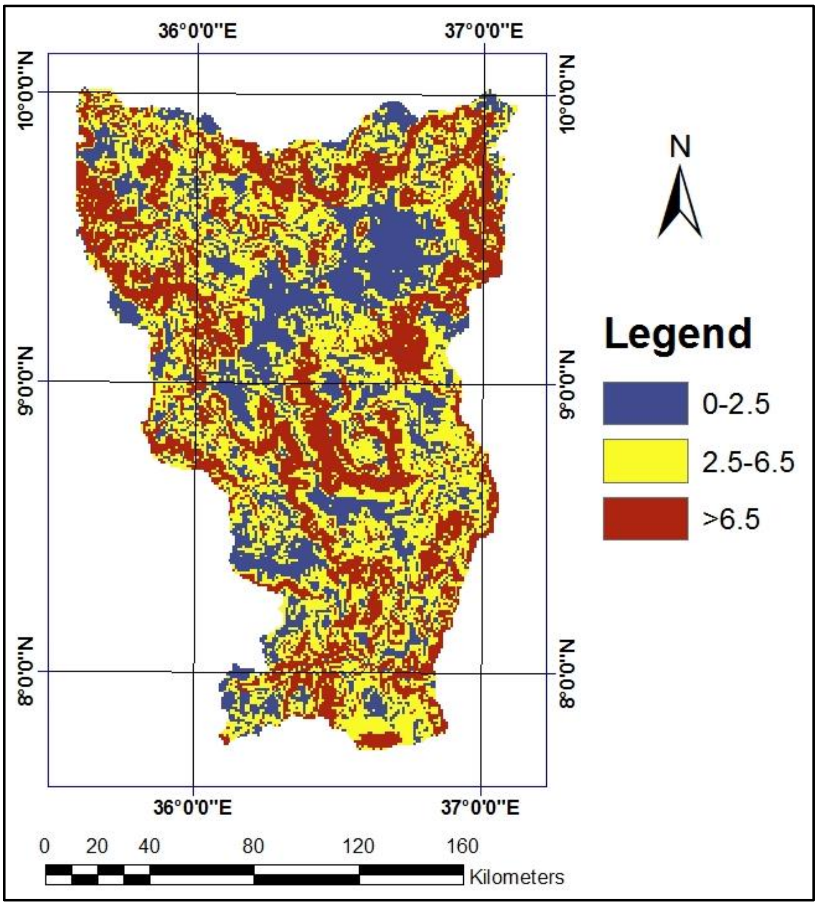

Figure 3. 12 Reclassified Slope in Didessa river basin

After the reclassification of the land use, soil and slope grids overlay operation was performed. When the overlay finished, the catchment was divided into hydrological response units (HRU) based on soil type, land use and slope classes. A detailed report was added to the project. The report describe the land use, soil, and slope class distribution within the watershed and within each sub-watershed unit (sub-basin).

The last step in the HRU analysis was the HRU definition. The HRU distribution in this study was determined by assigning multiple HRU to each sub-watershed. In multiple HRU definition, a threshold level was used to eliminate minor land uses, soils or slope classes in each sub-basin. Land uses, soils or slope classes which cover less than the threshold level are eliminated. After the elimination process, the area of the remaining land use, soil, or slope class was re-portioned so that 100% of the land area in the sub-basin was modelled. The threshold levels set is a function of the project goal and amount of detail required. In the SWAT user manual it is suggested that it is better to use a larger number of sub-basins than larger number of HRUs in a sub-basin; a maximum of 10 HRUs in a sub-basin is recommended. Hence, taking the recommendations in to consideration, 10%, 10%, and 15% threshold levels for the land use, soil and slope classes were applied, respectively so as to encompass most of spatial details.

3.7 SWAT Hydrological Processes

SWAT simulates the hydrology of a watershed in to two phases, the land and water or routing phases of the hydrologic cycle. The land phase of the hydrologic cycle controls the amount of water, sediment, nutrient and pesticide loadings to the main channel. The routing phase of the hydrologic cycle defines the transport of water, sediment, nutrient and pesticide through the channel to the outlet of the sub basin.

The hydrologic cycle as simulated by SWAT is based on the water balance equation:

$$SW_t = SW_o + \sum_{i=1}^{t}\left(R_{day} - Q_{Surf} - E_a - W_{seep} - Q_{gw}\right) ----------- 3.1$$

Where SW_t - is the final soil water content (mm H_2O), SW_0 is the initial soil water content on day I (mm H_2O), t is the time (days), R_{day} is the amount of precipitation on day i (mm H_2O), Q_{surf} is the amount of surface runoff on day i (mm H_2O), Ea is the amount of evapotranspiration on day i (mm H_2O), W_{seep} is the amount of water entering the vadose zone from the soil profile on day i (mm H_2O), and Q_{gw} is the amount of return flow on day i (mm H_2O).

The subdivision of the watershed in to HRU enables the model to reflect differences in evapotranspiration for various crops and soils. Runoff is predicted separately for each HRU and routed to obtain the total runoff for the watershed. This increases accuracy and gives a much better physical description of the water balance.

The climatic variables required by SWAT consist of daily precipitation, maximum and minimum air temperature, solar radiation, wind speed and relative humidity. Surface Runoff Volume is computed using a modification of the SCS curve number method (USDA, 1972) or the Green & Ampt infiltration method (Green and Ampt, 1911).

3.7.1 Runoff Simulation

The SCS curve number equation is used to determine runoff depth (USDA, 1972):

$$Q_{Surf} = \frac{(R_{day} - I_a)^2}{(R_{day} - I_a + S)} \text{-------------------------} 3.2$$

Where Q_{surf} is the accumulated runoff or rainfall excess (mm H_2O), R_{day} is the rainfall depth for the day (mm H_2O), I_a is the initial abstractions which includes surface storage, interception and infiltration prior to runoff (mm H_2O), and S is the retention parameter (mm H_2O). The retention parameter varies spatially due to changes in soils, land use, management and slope, and temporally due to changes in soil water content. The retention parameter is defined as:

$$S = 25.4\left(\frac{1000}{CN} - 10\right) \text{-------------------------} 3.3$$

Where, CN- is the curve number for the day. The initial abstractions, Ia, is commonly approximated as 0.2S and equation 3.2 becomes:

$$Q_{Surf} = \frac{(R_{day} - 0.2S)^2}{(R_{day} + 0.8S)} \text{-------------------------} 3.4$$

3.7.2 Peak Runoff Rate

The peak runoff rate is the maximum runoff flow rate that occurs with a given rainfall event. The peak runoff rate is an indicator of the erosive power of a storm and is used to predict sediment loss. SWAT calculates the peak runoff rate with a modified rational method. The rational method is widely used in the design of ditches, channels and storm water control systems. The rational method is based on the assumption that if a rainfall of intensity i begins at time t = 0 and continues indefinitely, the rate of runoff will increase until the time of concentration, $t = t_{conc}$, when the entire sub-basin area is contributing to flow at the outlet. The rational formula is:

$$q_{peak} = \frac{C * i * Area}{3.6} \text{---------------------} 3.5$$

Where q_{peak} is the peak runoff rate (m^3/s), C is the runoff coefficient, i is the rainfall intensity (mm/hr), Area is the sub-basin area (km^2) and 3.6 is a unit conversion factor.

Equation 3.5 was modified to determine peak runoff rate. The modified rational formula used to estimate peak flow rate is:

$$q_{peak} = \frac{\alpha_{tc} * Q_{surf} * Area}{3.6 * t_{conc}} ----------------------3.6$$

Where α_{tc} is the fraction of daily rainfall that occurs during the time of concentration, Q_{surf} is given in equation 3.4 and t_{conc} is the time of concentration for the sub-basin (hr)

The time of concentration is the amount of time from the beginning of a rainfall event until the entire sub-basin area is contributing to flow at the outlet. The time of concentration is calculated by summing the overland flow time (the time it takes for flow from the remotest point in the sub-basin to reach the channel) and the channel flow time (the time it takes for flow in the upstream channels to reach the outlet):

$$t_{conc} = t_{ov} + t_{ch} ------------------------- 3.7$$

Where t_{conc} is the time of concentration for a sub-basin (hr), t_{ov} is the time of concentration for overland flow (hr), and t_{ch} is the time of concentration for channel flow (hr).

3.7.3 Sediment Yield Simulation

Transport of sediment, nutrients and pesticides from land areas to water bodies is a consequence of weathering that acts on landforms. Soil and water conservation planning requires knowledge of the relations between factors that cause loss of soil and water and those that help to reduce such losses.

Erosion caused by rainfall and runoff is computed with the Modified Universal Soil Loss Equation (MUSLE) (Williams, 1975). MUSLE is a modified version of the Universal Soil Loss Equation (USLE) developed by Wischmeier and Smith (1965, 1978).

The modified universal soil loss equation (Williams, 1995) is given by:

$$\text{Sed} = 11.8\,.\,(Q_{Surf} . q_{peak} . area_{hru})^{0.56} . K_{USLE}\ . C_{USLE} . P_{USLE} . LS_{USLE} . CFRG --- 3.8$$

Where Sed is the sediment yield on a given day (metric tons), Q_{surf} is the surface runoff volume (mm H_2O/ha), q_{peak} is the peak runoff rate (m^3/s), $area_{hru}$ is the area of the HRU (ha), *KUSLE* is the USLE soil erodibility factor (0.013 metric ton m^2 hr/(m^3-metric ton cm)), *CUSLE* is the USLE cover and management factor, *PUSLE* is the USLE support practice factor, *LSUSLE* is the USLE topographic factor and *CFRG* is the coarse fragment factor. Surface runoff and peak rate are given in equation 3.4 and 3.6.

Sediment Routing

Each sub basin has a main routing reach where sediment from upland sub basins is routed and then added to downstream reaches. In SWAT, a simplified version of Bagnold (1977) stream power equation was used to calculate the maximum amount of sediment that can be transported in a stream segment. It does not keep track of sediment pools in various particle sizes.

Bagnold's (1977) steam power equation was simplified by Williams (1980). This simplified equation used to determine degradation as a function of channel slope and velocity. Maximum amount of sediment that can be transported from a reach segment is a function of the peak channel velocity.

The peak channel velocity $V_{ch,pk}$ is given by equation:

$$V_{ch,pk} = \frac{q_{ch,pk}}{A_{ch}} ----------------------------3.9$$

$q_{ch,pk}$ is the peak flow rate (m^3/s) and A_{ch} is the cross sectional area of flow in the channel (m^2).

The peak flow rate is defined as:

$$q_{ch,pk} = P_{rf} \cdot q_{ch} ---------------------------3.10$$

Where p_{rf} is the peak rate adjustment factor, and q_{ch} is average rate of flow (m^3/s).

In current version, four additional stream power equations with more physically based approach have been incorporated for modelling sediment transport, bank and bed erosions in channel containing various bed materials and sediment deposition. If one among these four physically based approach is selected, then sediment pool in six particle sizes are tacked by the model.

The maximum amount of sediment that can be transported from a reach segment is calculated:

$$CONC_{Sed,\ ch,\ mx} = C_{SP}.V_{ch,\ pk}{}^{spexp} --------------------3.11$$

Conc $_{sed,\ ch,\ mx}$ is the maximum concentration of sediment that can be transported by the water (ton/m^3 or kg/L), Csp is a coefficient defined by the user, V ch,pk is the peak channel velocity (m/s), and spexp is an exponent defined by the user. Actually between 1.0 and 2 and average value was used. i.e 1.5.

The maximum concentration of sediment calculated with equation above is compared to the concentration of sediment in the reach at the beginning of time step, $Conc_{sed,ch,i}$.

$If\ Conc_{sed,ch,i} > Conc_{sed,ch,mx}$, deposition is the dominant process in the reach segment and the net amount of sediment deposited, Sed_{dep} is given by

$$Sed_{dep} = (Conc_{sed,ch,i} - Conc_{sed,ch,mx}).V_{ch} --------------3.12$$

Sed_{dep} is the amount of sediment deposited in the reach segment (metric tons), $Conc_{sed,ch,i}$ is the initial sediment concentration in the reach (kg/L or ton/m^3), $Conc_{sed,ch,mx}$ is the maximum concentration of sediment that can be transported by the water (Kg/L or ton/m^3) and V_{ch} is the volume of water in the reach segment (m^3).

$If\ Conc_{sed,ch,i} < Conc_{sed,ch,mx}$, degradation is the dominant process in the reach segment and the net amount of sediment reentrained, Sed_{deg} is given by

$$Sed_{deg} = (Conc_{sed,ch,mx} - Conc_{sed,ch,i}).V_{ch}K_{CH}C_{CH} ----------- 3.13$$

where Sed_{deg} is the amount of sediment re-entrained in the reach segment (metric tons), $conc_{sed,ch,mx}$ is the maximum concentration of sediment that can be transported by the water (kg/L or ton/m^3), $conc_{sed,ch,i}$ is the initial sediment concentration in the reach (kg/L or ton/m^3), Vch is the volume of water in the reach segment (m^3 H_2O), K_{CH} is the channel erodibility factor (cm/hr/Pa), and C_{CH} is the channel cover factor.

Once the amount of deposition and degradation has been calculated, the final amount of sediment in the reach is determined:

$$Sed_{Ch} = Sed_{Ch,i} - Sed_{dep} + Sed_{deg} ----------------3.14$$

Where Sed_{ch} is the amount of suspended sediment in the reach (metric tons), $Sed_{ch,i}$ is the amount of suspended sediment in the reach at the beginning of the time period (metric tons), Sed_{dep} is the amount of sediment deposited in the reach segment (metric tons), and sed_{deg} is the amount of sediment reentrained in the reach segment (metric tons).

The amount of sediment transported out of the reach is calculated:

$$Sed_{out} = Sed_{ch} * \frac{V_{out}}{V_{ch}} ------------------------3.15$$

where sed_{out} is the amount of sediment transported out of the reach (metric tons), sed_{ch} is the amount of suspended sediment in the reach (metric tons), V_{out} is the volume of outflow during the time step (m^3 H_2O), and V_{ch} is the volume of water in the reach segment (m^3 H_2O).

3.8 Sediment Rating Curve

A sediment rating curve consists of a graph or equation, relating sediment concentration or discharge to stream discharge, which can be used to estimate sediment loads from the stream flow record. There is no standard method for rating curve construction. In some cases visual curve fitting give better result than mathematical curve fitting (Morris and Fan, 1998). The most commonly used mathematical rating curve is power function (Walling, 1978; Morris and Fan, 1998).

$$S = aQ^b \text{ ---------------------------- } 3.17$$

Where: Q is stream discharge, S is either suspended sediment concentration or sediment discharge. Values of a and b for particular stream are determined from data via linear regression between (log S) and (Log Q).

Sediment discharge (Kg/s) versus flow rate (m^3/s) produce a better fit than the suspended sediment concentration (mg/L) versus flow rate (m^3/s). A logarithmic plot is commonly used in both cases (Walling, 1977; Morris and Fan, 1998). A regression equation minimizes the sum of squared deviation from log transformed data, which introduces bias that underestimates the concentration at any discharge (Morris and Fan, 1998).

The relationship between discharge and sediment concentration or discharge and sediment load for a particular stream is not a fixed parameter but can considerably vary from one storm to another depending on factors including the intensity and areal distribution of the rainfall, and changes in the sediment supply (Morris and Fan, 1998). To avoid poor relationship between water discharge and sediment discharge separate curves may be developed for winter and summer, fine and course, falling and rising stages of discharge and different ranges of discharge (Morris and Fan, 1998).

For this study, hydrograph for Toba and Little anger stations where developed and to identify rising and falling limp (See Appendix A). From the graph raising limp is from April to August and falling limp is from September to March.

3.8.1 Sediment Rating Curve at Toba Station

Using the very sparse and few data at Toba station rating curve was developed and described in figure 3.13 and figure 3.14 for sediment concentration versus discharge and Sediment discharge versus flow discharge respectively.

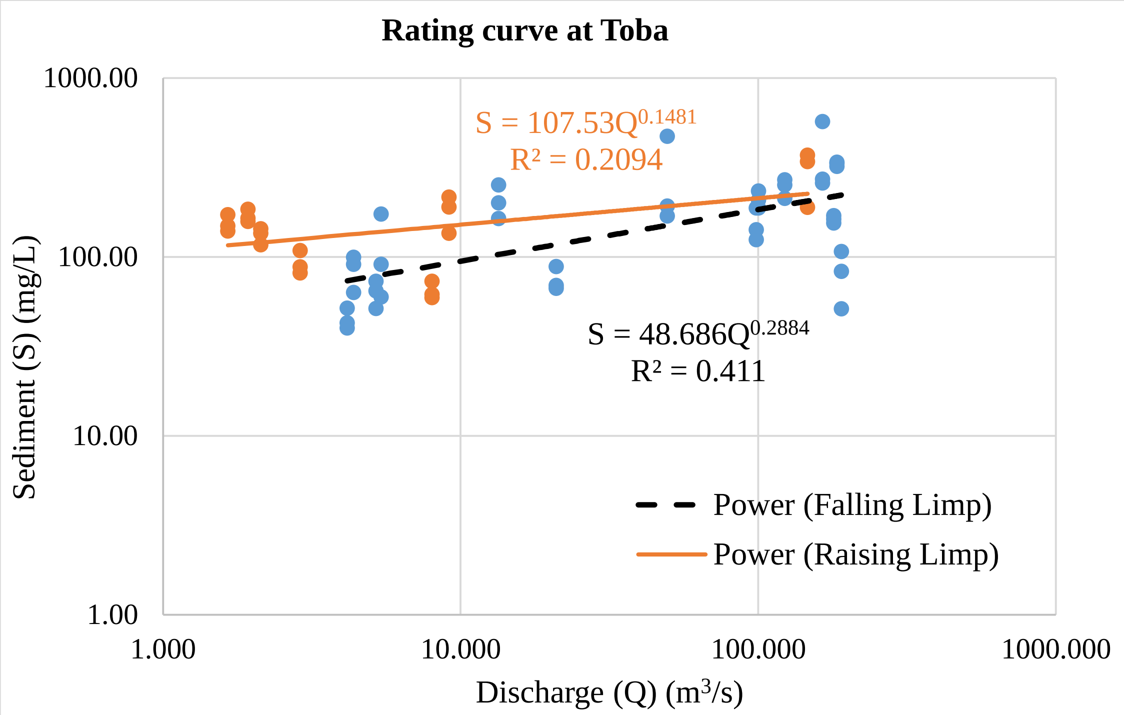

Figure 3. 13 Sediment concentration rating curve at Toba gauging station

Sediment rating curve constructed of sediment concentration (mg/L) versus discharge reveals poor correlation coefficient as shown on figure 3.13 when compared to rating curve developed of sediment discharge (Kg/s) versus discharge as shown in figure 3.14. This indicates that sediment rating curve constructed of sediment yield produce better result.

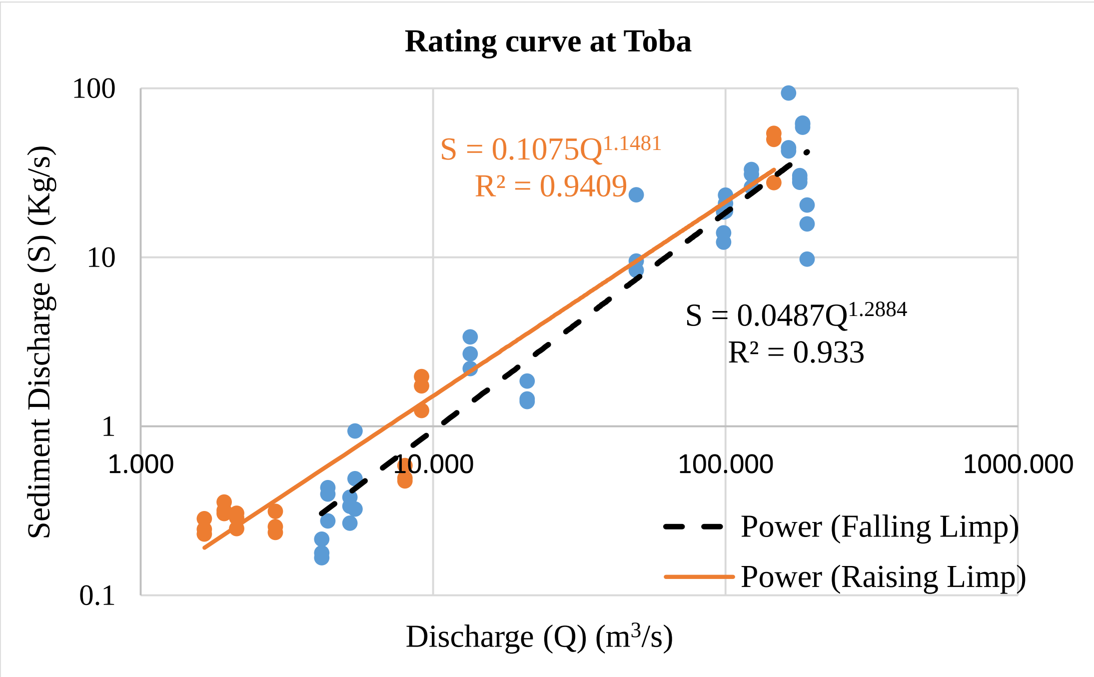

Figure 3. 14 Sediment discharge Rating Curve for Toba station

From the best fit rating curve on figure 3.14, coefficient a is equal to 0.1075, power b is equal to 1.1481 and regression coefficient R^2 is equal to 0.9409 for rising limp (April to August). Similarly, a is equal to 0.0487, power b is equal to 1.2884 and regression coefficient R^2 is equal to 0.933 for falling limp (September to March). Now, to generate sediment discharge for Toba station the following equation were used.

$$S = 0.1075Q^{1.1481} \text{ --------------------------- } 3.18$$

$$S = 0.0487Q^{1.2884} \text{ --------------------------- } 3.19$$

Equation 3.18 and 3.19 were developed for rising limp and falling limp respectively. Where S and Q are previously defined.

3.8.2 Sediment Rating Curve at Little Anger Station

The relationship between discharge and sediment concentration or discharge and sediment load for a particular stream is not a fixed parameter but can considerably vary from one storm to another depending on factors including the intensity and areal distribution of the rainfall, and changes in the sediment supply (Morris and Fan, 1998). Therefore another sediment rating curve was developed for Little Anger station to generate sediment concentration at this station from measured discharge.

The developed rating curve for sediment concentration and sediment discharge is described on figure 3.15.

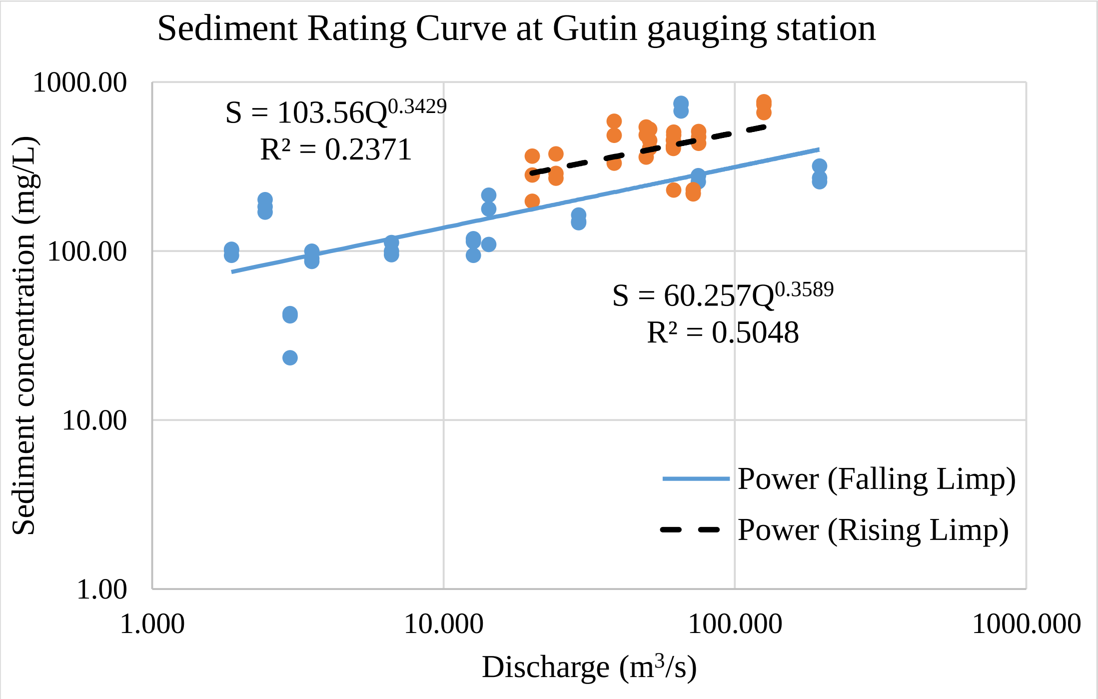

Figure 3. 15 Sediment concentration Rating Curve for Little Anger

And developed rating curve for sediment discharge and sediment discharge is described figure 3.16.

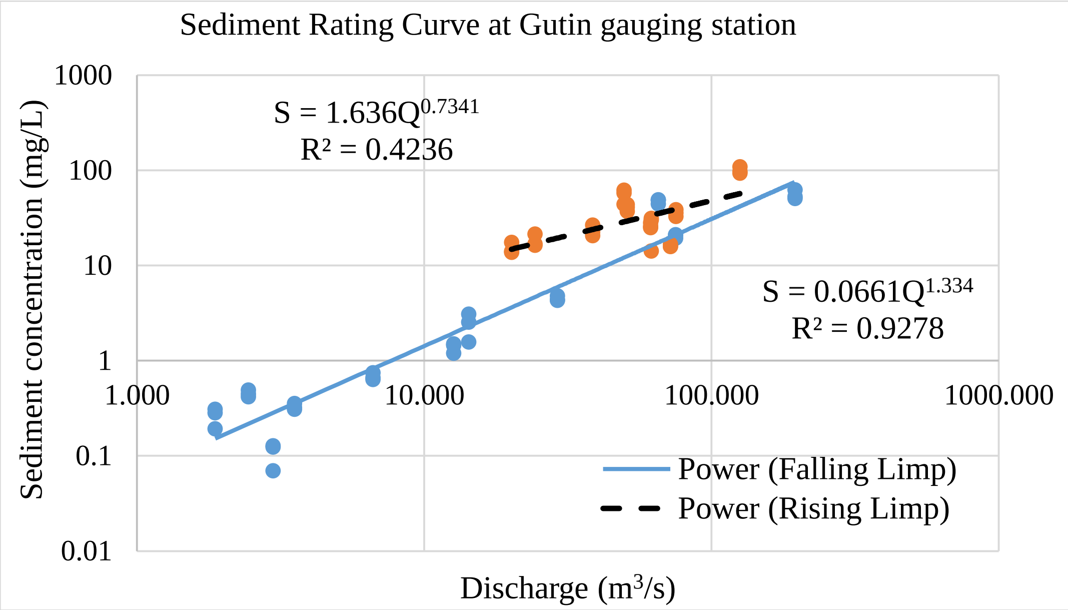

Figure 3. 16 Sediment discharge Rating Curve for Little Anger

From the best fit rating curve on figure 3.16, coefficient a is equal to 1.636, power b is equal to 0.7341 and regression coefficient R^2 is equal to 0.4236 for rising limp (April to August). Similarly, a is equal to 0.0661, power b is equal to 1.1334 and regression coefficient R^2 is equal to 0.9278 for falling limp (September to March). To generate sediment concentration for little Anger at Gutin, the following equation were used.

$$S = 1.636Q^{0.7341} ----------------------------3.20$$

$$S = 0.0661Q^{1.1334} ----------------------------3.21$$

Equation 3.20 and 3.21 were developed for rising limp and falling limp respectively. Where S and Q are previously defined.

3.9 Sensitivity Analysis

Sensitivity analysis is the process of identifying the model parameters that exert the highest influence on model calibration or on model predictions. Model sensitivity is defined as the change in model output per change in parameter input. Sensitivity analysis describes how model output varies over a range of a given input variable. An important aim of the parameter sensitivity analysis is to allow the possible reduction in the number of parameters that must be estimated, thereby reducing the computational time required for model calibration.

The current version of SWAT model provides the algorithmic techniques for sensitivity analysis. Model parameters that have high sensitivity must be chosen with care because small variations in their values can cause large variations in model output, and therefore it is important to ensure that the parameter value is the best possible estimate. Model parameters that have low sensitivity do not require as much examination in their selection because small changes in their values do not cause large changes in model output (Abbaspour, 2014).

In SWAT-CUP, There are two ways to identify the most sensitive parameters. The first one is Global Sensitivity analysis. Parameter sensitivities are determined by calculating the following multiple regression system, which regresses the Latin hypercube generated parameters against the objective function values (Abbaspour, 2014):

$$g = \alpha + \sum_{i=1}^{m} \beta_i b_i \quad ----------------------- 3.22$$

A t-test is then used to identify the relative significance of each parameter bi. The sensitivities given above are estimates of the average changes in the objective function resulting from changes in each parameter, while all other parameters are changing. This gives relative sensitivities based on linear approximations and, hence, only provides partial information about the sensitivity of the objective function to model parameters. t-stat provides a measure of sensitivity (larger in absolute values are more sensitive) P-values determined the significance of the sensitivity. A values close to zero has more

The second method is One-at-a-time sensitivity analysis. One-at-a-time sensitivity shows the sensitivity of a variable to the changes in a parameter if all other parameters are kept constant at some value. The problem here is that we never know what the value of those other constant parameters should be. This is an important consideration as the sensitivity of one parameter depends on the value of other parameters.

In this study, global sensitivity analysis method was used to identify the most sensitive flow parameters from flow parameters listed in table 3.13.

Table 3. 13 Stream flow parameters

No	PARAMETERS	Description
1	ALPHA_BF	Baseflow alpha factor (days)
2	BIOMIX	Biological mixing efficie
3	BLAI	Max leaf area index
4	CAN_MX	Maximum canopy storage
5	CH_K2	Effective hydraulic conductivity in main channel alluvium
6	CH_N2	Manning’s "n" value for the main channel.
7	CN2	SCS runoff curve number f
8	EPCO	Plant uptake compensation factor
9	ESCO	Soil evaporation compensation factor
10	GW_DELAY	Groundwater delay (days)
11	GW_ REVAP	Groundwater "revap" coefficient
12	GWQMN	Treshold depth of water in the shallow aquifer required for return flow to occur (mm).
13	REVAPMN	Threshold depth of water in the shallow aquifer for "revap" to occur (mm)
14	SFTMP	Snowfall temperature
15	DEEPST	Initial depth of water in the deep aquifer (mm)
16	SLSUBBSN	Average slope length.
17	SMFMN	Minimum melt rate for snow during the year
18	SMTMX	Maximum melt rate for snow during year
19	SMTMP	Snow melt base temperature
20	SOL_ALB	Moist soil albedo
21	SOL_AWC	Available water capacity of the soil layer
22	SOL_K	Saturated hydraulic conductivity
23	SOL_Z	Depth from soil surface to bottom of layer
24	SURLAG	Surface runoff lag time
25	TIMP	Snow pack temperature lag factor
26	SOL_ZMX	Maximum rooting depth of soil profile
27	SHALLST	Manning's "n" value for overland flow Initial depth of water in the shallow aquifer (mm)

From parameters listed in table 3.13, only 17 most sensitive parameters were used for calibration and validation.

3.10 Model Calibration and Validation

Model calibration is the process of estimating model parameters by comparing model outputs for a given set of assumed conditions with observed data for the same conditions whereas model validation involves running a model using input parameters measured or determined during calibration process (Moriasi *et al.*, 2007).

To perform such studies as the evaluation of the impact of alternative land management practices on stream water quality and quantity, and sediment transport, first the model must be calibrated and validated for existing conditions. Proper model calibration is important in hydrologic modelling studies to reduce uncertainty in model simulations (Moriasi *et al*., 2007).

There are three steps in calibration/validation processes (Neitsch *et al*. 2011):

1. Selecting some portion of observed data
2. Running the model at different values for unknown parameters until fit to observations is good
3. Applying model with calibrated parameters to remaining observations.

The SWAT model for Didessa River basin, stream flow was calibrated for recorded data at Toba flow monitoring station. As no automatic calibration procedure can substitute for actual physical knowledge of the watershed, which can translate into corrected parameter range for different parts of the watershed (Arnold *et al.*, 2012), the calibration procedure involved sensitivity analysis followed by semi-automated calibration procedure by SWAT-CUP, where at times, manual manipulation on the selection of calibration parameters was necessary.

Observed suspended sediment concentration (mg/L) at Toba (Didessa near Dembi) and Gutin (Little Anger) were used to compare with simulated suspended sediment. Toba station is an outlet of 1400.50km^2 (5.05 %) of the total basin area. Monthly flow data for 1996 to 2001 were used for calibration and 2002 to 2006 used for validation. Sediment concertation generated by rating curve (1990 to 2006) used for comparison only.

Gutin (Little Anger) station is an outlet of 3844.54km^2 (13.87%) of the total basin area. Monthly suspended sediment concentration generated by using sediment rating curve was compared with simulated total suspended sediment concentration to evaluate the performance of model.

The determination coefficient R^2 and Nash-Sutcliffe Efficiency (NSE) were used as an objective functions to calibrate and validate the model using 17 flow sensitive input parameters. The model was calibrated using the Sequential Uncertainty Fitting (SUFI-2) algorithm of SWAT-CUP, an interface developed for SWAT (Abbaspour, 2014).

3.3.1 Model Efficiency

Model simulations efficiency can be evaluated by using root mean square error (RMSE), observations standard deviation ratio (RSR), regression coefficient (R^2), Nash-Sutcliffe simulation efficiency (E_{NS}) and percent bias (PBIAS). In this study, regression coefficient (R^2) and Nash-Sutcliffe simulation efficiency (E_{NS}) were used to evaluate model efficiency during calibration and validation.

Nash-Sutcliffe Efficiency (N_{SE}): The Nash-Sutcliffe Efficiency (N_{SE}) is a normalized statistic that determines the relative magnitude of the residual variance compared to the measured data variance.

NSE indicates how well the plot of observed versus simulated data fits the line with 1:1 slope. NSE is computed by:

$$E_{NS} = \frac{\sum_{i=1}^{n}(q_{oi} - q_{si})^2}{\sum_{i=1}^{n}(q_{oi} - q_o)^2} \quad \text{------------------} 3.23$$

With these values, model performance can be judged based on general performance ratings as proposed by Moriasi *et al.* (2007).

Coefficient of determination (R^2): the index of correlation of measured and simulated values, has been used to evaluate the accuracy of the overall model calibration and validation. The value of R^2, ranges between 0 and 1. The more value of R^2, approaches 1, the better is the performance of the model and the values of R^2 less than 0.5 indicates poor performance of the model.

$$R^2 = \frac{[\sum_{i=1}^{n}(q_{si} - q_s)(q_{oi} - q_o)]}{\sum_{i=1}^{n}(q_{si} - q_s)^2 \sum_{i=1}^{n}(q_{oi} - q_o)^2} \quad \text{-------------} 3.24$$

Where: q_{si} is the simulated values of the quantity in each model time step, q_{oi} is the measured values of the quantity in each model time step , q_s is the average simulated value of the quantity in each model time step and q_o is the average measured value of the quantity in each model time step. After each calibration, the regression coefficient (R^2), and the simulation efficiency (E_{NS}) were also checked in accordance to Santhi *et al.* (2001) recommendation ($R^2 > 0.6$ and $E_{NS} > 0.5$).

3.11 Specific Weight of Sediment Deposit

Conversion of sediment mass into volume is important to know the storage depleted per period of time. Specific weight of sediment deposited is a conversion factor. Specific weight is determined by grain size, deposit thickness, and whether the deposit has been exposed to the air and allowed to dry. Consolidation is a time-dependent process which increases specific weight, and reservoir sediments may consolidate for decades because of self-weight plus overburden from additional loads.

By taking grain size distribution and reservoir operation into account an empirical method for estimating the initial specific weight of sediment deposits was developed (Lara and Pemberton, 1963; Tadesse, 2013). Lara-Pamberton equation is given as:

$$W = WcPc + WmPm + WsPs \text{ ---------------------- } 3.25$$

Where, W is the deposit specific weight in kg/m^3; Wc, Wm and Ws are initial weights for clay, silt and sand respectively; Pc, Pm and Ps are percentages of clay, silt and sand.

Table 3. 14 Initial weight of clay, silt and sand for different mode of operations

Operational condition	Initial weight kg/m^3		
	Wc	Wm	Ws
Continuously submerged	416	1120	1154
Periodic draw down	561	1140	1154
Normally empty reservoir	641	1150	1154
Riverbed sediment	961	1170	1154

The average density of all sediment deposited during *t* years of consolidation may be calculated by equation given by Milller (1953) (Morris and Fan, 1997).

$$W1 = W + 0.4343B\left(\frac{t}{t-1}lnt - 1\right) \text{ --------------------- } 3.26$$

Where, W1 is specific weight of a deposit with an age of t years, W is initial specific weight and B is constant which depends on particle size and reservoir operation.

Table 3. 15 Coefficient B for different sediment content

Operational condition	B in kg/m^3		
	Sand	Silt	Clay
Continuously submerged	0	91	256
Periodic draw down	0	29	135
Normally empty reservoir	0	0	0

Arjo Didessa reservoir was under construction so sediment data deposited sediment data was not available.

Specific sediment of Blue Nile River was taken from other literature for prediction of sediment rate of Arjo Didessa reservoir. For the composition of sediment in the Blue Nile; Sand (0.02-0.2 mm) ~22%, Silt (0.002-0.02 mm) ~ 38% and Clay (< 0.002 mm) ~ 40% (Tadesse, 2013) and reservoir was assumed to be continuously submerged. For this condition, initial specific weight can be estimated as 0.846 t/m^3. According to the U.S. Natural Resources Conservation Service the specific weight of deposit with clay-silt mixture sediment dominating and submerged reservoir ranges from 0.64 to 1.04 t/m^3.

Different density of deposited sediment has been used by different Authors. Ahmed, 2008 stated that the most common density is 1.12 t/m^3 which was used for Mandaya reservoir sedimentation study.

Tadesse (2013) used 1.12 average density of sediment deposit in GERD and reported as this value over estimate sedimentation rate. Therefore, 1.12t/m^3 was used to compute the sedimentation rate of Arjo Didessa reservoir.

3.12 Reservoir Trap Efficiency

Trap efficiency (TE) is the proportion of the incoming sediment that is deposited or trapped in a reservoir or pond (verstraeten and poesen, 2000):

$$TE = \frac{S_{inflow} - S_{outflow}}{S_{inflow}} = \frac{S_{settled}}{S_{inflow}} \text{---------------} 3.27$$

S_{inflow} is the sediment mass entering reservoir (the sediment yield or delivery), $S_{outflow}$ is the sediment mass leaving the reservoir with the outflowing water and $S_{settled}$ is the sediment mass deposited within the reservoir.

The reservoir trap efficiency refers to the percentage of incoming sediment that is retained in the reservoir. Given the many parameters that influence the sedimentation process, it is very difficult to predict the Trap Efficiency in a simple manner. To make an accurate prediction, an extensive and complex model has to be developed which is based on theoretical relations and incorporates all the influencing factors (Koen Bronsvoort, (2013). This is a very time-consuming process. Different empirical relations have been developed to estimate the trapping efficiency. Some of them are discussed as follows.

1. **Brown Empirical Equation**

This method determine the Trap Efficiency by using the ratio between the capacities of a reservoir to the watershed. Given its good performance for large reservoirs and low data requirements the relation proposed by Brown (1943) is used for determination of reservoir trap efficiency. Brown developed a curve that relates TE to capacity-watershed area ratio (C/W) based on data from 15 reservoirs:

$$TE = \left[1 - \frac{1}{\left(1 + D * \frac{C}{A}\right)}\right] * 100 ------------------------ 3.28$$

Where C is the storage capacity expressed in acres and W the catchment area expressed in miles.

$$TE = \left[1 - \frac{1}{\left(1 + 0.0021 * D * \frac{C}{A}\right)}\right] * 100 -------------------- 3.29$$

Where C stands for the capacity of reservoir (m^3) and A for drainage area of the catchment (km^2). D is constant between 0.046 and 1. It depends on the characteristics of the reservoir operation and 0.1 has been used. For large reservoirs, the trapping efficiency will always be close to 100 percent (verstraeten and poesen, 2000).

When using empirical methods, one should always be aware of the fact that the parameters are very dynamic and change during the sedimentation process. The storage capacity (C), m^3 for instance, changes during the sedimentation process and therefore influences the C/I ratio during time (Koen Bronsvoort, 2013). For that, Brown developed Curves based on capacity/watershed ratio as shown on figure 3.17. The Trap Efficiency is in this figure described as CT and the capacity/watershed ratio is expressed in the capacity of the reservoir SR per square mile of drainage area.

The use of the capacity/watershed ratio (C/W), has the disadvantage that this parameter is not very reliable. The run-off production of the watershed (W) is highly depending on the soil characteristics, which differs heavily per watershed. This is the reason why for low C/W ratios (and therefore a relatively high W) the span of the Trap Efficiency is large (Koen Bronsvoort, 2013).

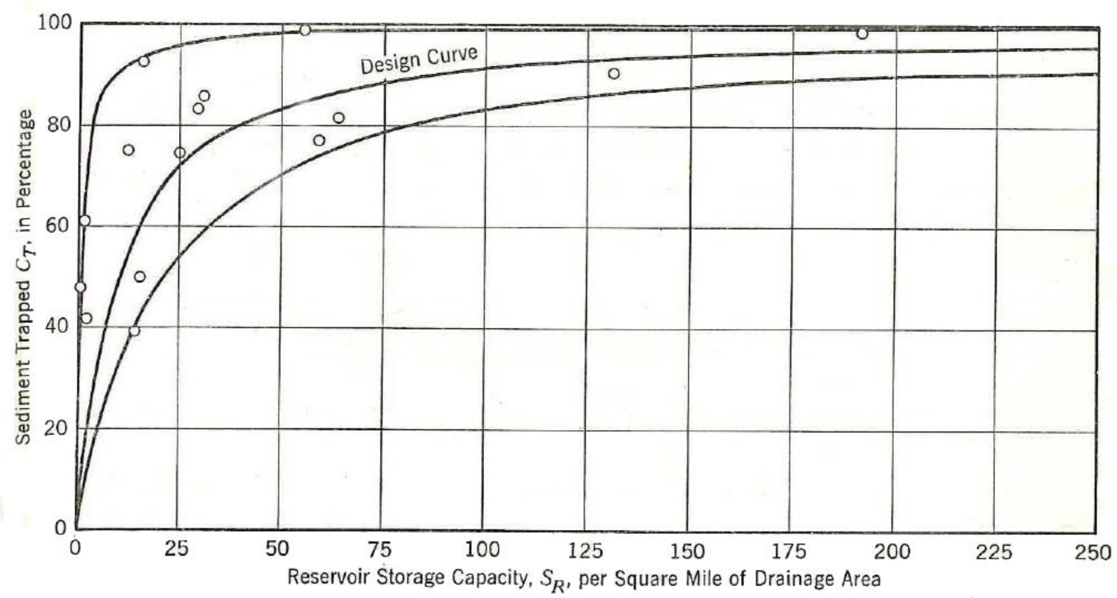

Figure 3. 17 Brown Curves for Calculating the Trap Efficiency (Brown, 1943)

This method therefore is not preferred if an estimation of the Trap Efficiency has to be made. However if other methods can't be used, a considerable uncertainty has got to be taken into account if the Brown curves are considered.

2. Brune Curves

It is the most widely used method to empirically determine the Trap Efficiency. The curves of this method are based on data from 44 reservoirs and are used worldwide to determine the Trap Efficiency. The curves are based on the capacity-inflow ratio of reservoirs and are presented in figure 3.18. These curves were modified by (Verstraeten, and Poesen, 2000).

It must be emphasised that these curves should only be used for normally situated reservoirs (reservoirs which are completely filled by water and have their outlet at the top of the embankment). These curves are not suitable for floodwater-retarding structures, desilting ponds or semi-dry reservoirs. Misusing these simplified curves may lead to large errors in the calculation of the Trap Efficiency.

On figure 3.18, the horizontal axis is C/I ratio, where C represents the capacity of the reservoir and I the average annual water inflow.

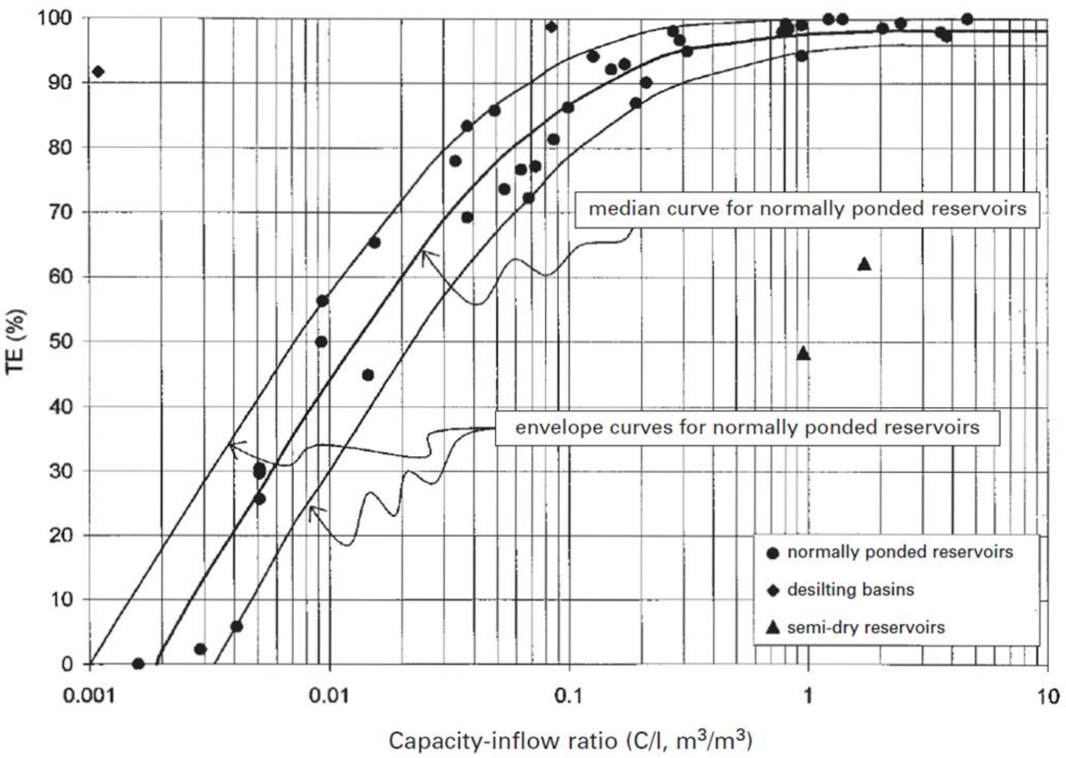

Figure 3. 18 Modified Brune Curves (Verstraeten, G. And Poesen, J., 2000)

Because the unity of C is (m^3) and I is (m^3/year), the C/I ratio is expressed in years (which is incorrectly presented in figure 3.18). When the C/I ratio is smaller than 1 year, it means that the amount of water in the reservoir is replaced totally during one year.

If the C/I ratio is bigger than 1 year, it means that the amount of water in a reservoir is bigger than the total amount of water that yearly flows into the reservoir. The C/I ratio therefore describes the average retention time of the water in a reservoir. The upper curve yields for predominantly coarse-grained sediments, the median curve yields for mixtures of grain sizes and the lower curve yields for primarily fine sediments.

3. Churchill Curves

Another widely used method is the method developed by Churchill (Churchill, 1948). Churchill suggested that there is a relationship between the amount of sediments that passes a reservoir (100-TE (%)) and the sedimentation index.

The sedimentation index of a reservoir is defined as:

$$\text{Sedimentation Index} = \frac{\text{Period of retention}}{\text{Mean velocity}} - - - - - - - - - - - - - - - - 3.30$$

With the Sedimentation Index, a ratio is added of two reservoir characteristics which both have a significant influence on the reservoir sedimentation. The bigger the retention time of the pool and the lower the mean velocity, the higher will be the sedimentation rate of the reservoir and with that the Sedimentation Index as shown on figure 3.19.

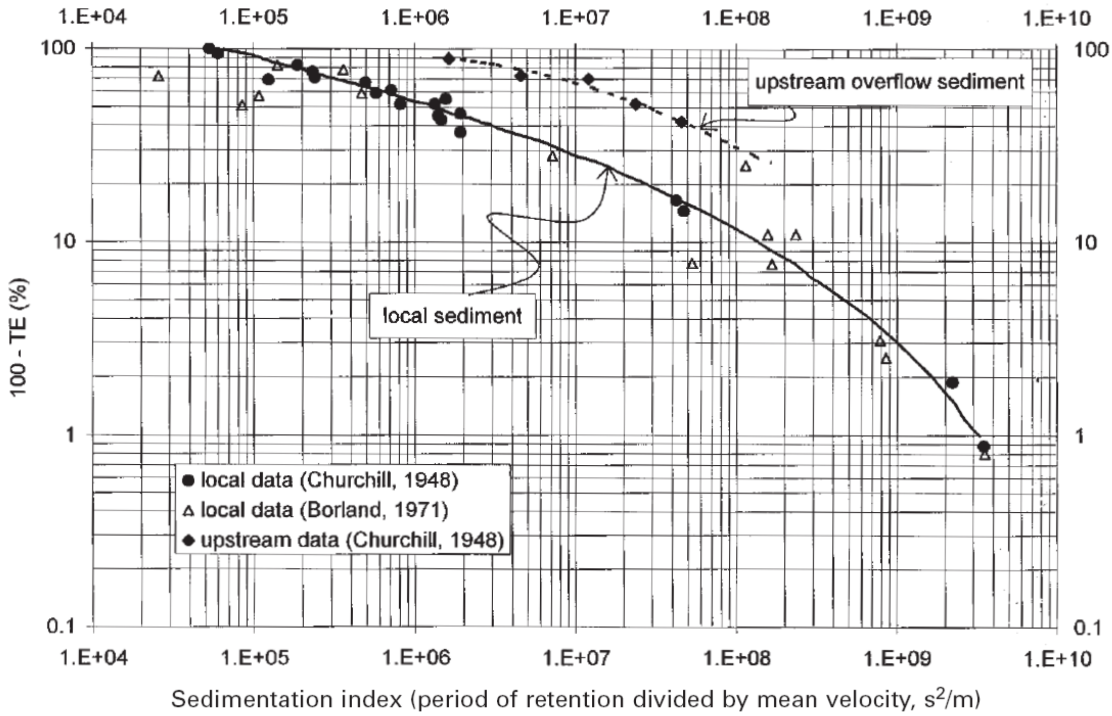

Figure 3. 19 Churchill's Curves After (Verstraeten, G. And Poesen, J., 2000)

The Churchill curves may give a better prediction of Trap Efficiency than the Brune curves, the big disadvantage of this method is that it is very difficult to determine the Sedimentation Index.

The data necessary to calculate the Sedimentation Index is often not available, which makes the method in that case useless. This is the main reason why the Brune curves are more widely used to determine the Trap Efficiency (Koen Bronsvoort (2013). For the same reason, Churchill Curve method was not used in this study.

4. Determination of TE using SWAT model

A reservoir is an impoundment located on the main channel network of a watershed. No distinction is made between naturally occurring and manmade structures (Neitsch *et al.*, 2011). The water balance for a reservoir is:

$$V = V_{Stored} + V_{flow\ in} - V_{flow\ out} + V_{pcp} - V_{evap} - V_{Seep} \quad ----------3.31$$

Where V is volume of the water in the reservoir at the end of the day (m^3), V_{Stored} is the volume of water stored in the reservoir at the beginning of the day (m^3),
$V_{flow\ in}$ is the volume of water entering in the reservoir during the day (m^3), $V_{flow\ out}$ is the volume of water flowing out of the reservoir during the day (m^3), V_{pcp} is the volume of precipitation falling on the water body during the day (m^3), V_{evap} is the volume of water removed from the reservoir by evaporation (m^3), V_{seep} is the volume of water lost from reservoir by seepage during the day (m^3).

Surface area of the reservoir is needed to calculate the amount of precipitation falling on the water body as well as the amount of evaporation and seepage. Surface area varies with change in the volume of water stored in the reservoir.

The surface area is updated daily using the equation:

$$SA = \beta_{sa} * V^{expsa} \quad (3.32)$$

Where SA is the Surface area of the water body (ha), V is the volume of water in the impoundment (m^3) and expsa is an exponent and β_{sa} is coefficient.

The volume of precipitation falling on the reservoir during a day is calculated:

$$V_{pcp} = 10 * R_{day} * SA \quad (3.33)$$

Where R_{day} is the amount of precipitation falling on a given day (mm) and other parameters are previously defined.

The volume of water lost to evaporation on a given day is calculated:

$$V_{evap} = 10 * \eta * E_o * SA \quad (3.34)$$

Where η is the evaporation coefficient (0.6) and E_o is a potential evaporation for a given day (mm).

The volume of water lost by seepage through the bottom of the reservoir on a given day is calculated:

$$V_{seep} = 240 * K_{sat} * SA \quad (3.35)$$

Where K_{sat} is the effective saturated hydraulic conductivity of the reservoir bottom (mm/hr).

Sediment in the reservoir

SWAT incorporates a simple mass balance model to simulate the transport of sediment into and out of the reservoirs. SWAT defines four different types of water bodies: ponds, wetlands, reservoirs and potholes. Sediment processes modelled in ponds, wetlands, reservoirs and potholes are identical. When calculating sediment through a water body, SWAT assumes the system is completely mixed (i.e sediment enters the water body is instantaneously distributed throughout the volume).

The mass balance equation for sediment in a reservoir is:

$$Sed_{wb} = Sed_{wbi} + Sed_{flow\ in} - Sed_{stl} - Sed_{flow\ out} \quad 3.36$$

Where Sed_{wb} is the amount of sediment in the reservoir at the end of the day (metric tons) Sed_{wbi} is the amount of sediment in the reservoir at the beginning of the day (metric tons), Sed_{flowin} is the amount of sediment added to the reservoir with inflow (metric tons), Sed_{stl} is the amount of sediment removed from the water by settling (metric tons) and $Sed_{flowout}$ is the amount of sediment transported out of the reservoir with outflow (metric tons)

Incoming sediment is deposited using a modified overflow rate model (EPA, 1986; Neitch *et al*., 2011). For each day the deposition routine begins with the computation of the detention times. The actual detention time is based upon the ratio of impoundment volume to the outflow rate.

$$t_D = \frac{C_t(1 - DS)Vol}{Q_o} \quad 3.37$$

Where t_D is detention time (sec), Ct is empirical parameter to account for impoundment geometry, hydraulic response, and stratification of the suspended sediment, DS is the dead storage (the portion of the pond that does not contribute to settling), Vol is the average impoundment volume over the time step (ft^3) and Qo is the average outflow rate over the time step (ft^3/sec).

Then the trapping efficiency (TE) of the reservoir is calculated as:

$$TE = \frac{V_{set}}{V_{ovfl}} \quad 3.38$$

Where V_{set} is the settling velocity (m/d), V_{ovfl} is the overflow velocity (m/d) and V_{ovfl}, overflow velocity (m/d) is defined as

$$\frac{Q_o/SA}{10{,}000} \quad 3.39$$

Qo is reservoir outflow (m^3) and SA is reservoir surface area (ha)

4. RESULT AND DISCUSION

4.1. Sensitivity Analysis

Sensitivity analysis was carried out to identify sensitive parameters that significantly affected stream flow. Groundwater delay (GW_DELAY), Curve number (CN2), Snowfall temperature (SFTMP), Manning's "n" value for the main channel (CH_N2), Maximum canopy storage (CANMX), soil evaporation compensation factor (ESCO), saturated hydraulic conductivity (SOL_K), Effective hydraulic conductivity in main channel alluvium (CH_K2), Groundwater "revap" coefficient (GW_REVAP), Threshold depth of water in the shallow aquifer for "revap" to occur (REVAPMN), Biological mixing efficiency (BIOMIX), Plant uptake compensation factor (EPCO), soil depth (SOL_Z), average slope steepness (SLSUBBSN), Threshold depth of water in a shallow aquifer for return flow (GWQMN), available water capacity (SOL_AWC), and Base flow alpha factor (ALPHA_BF) were relatively high sensitive parameters that significantly affect stream flow.

Table 4. 1: Sensitive parameters ranks for calibration

Parameter Name	t-Stat	P-Value	Rank
GW_DELAY	-18.07	0	1
CN2	-11.37	0	2
SFTMP	-5.33	0	3
CH_N2	2.42	0.02	4
CANMX	-2.05	0.04	5
ESCO	-1.77	0.08	6
SOL_K	1.47	0.14	7
CH_K2	1.45	0.15	8
GW_REVAP	-1.44	0.15	9
REVAPMN	1.4	0.16	10
BIOMIX	1.32	0.19	11
EPCO	1.25	0.21	12
SOL_Z	0.96	0.34	13
SLSUBBSN	0.59	0.56	14
GWQMN	0.41	0.68	15
SOL_AWC	0.4	0.69	16
ALPHA_BF	0.06	0.95	17

4.2.Calibration and validation

Once the most sensitive parameters were identified, values of selected model parameters were varied iteratively within a reasonable range during various calibration runs until a satisfactory agreement between observed and simulated stream flow obtained. There was no observed streamflow and sediment data near to the basin outlet which integrates a number of sub basins for better calibration and validation.

Rather observed streamflow and few suspended sediment data for small tributaries on the periphery of the basin were obtained. From obtained streamflow and sediment data only one gauging station (Toba) with better recorded data was used for stream flow calibration and validation. Toba gauging station is located at upstream of Arjo Didessa Dam reservoir which covers 140049.7614ha (17%) of 825012.6495ha which is Arjo Didessa reservoir watershed.

Stream flow of twelve years (1995 to 2006) measured daily flow was converted into monthly flow and prepared as per SWAT-CUP requirement for calibration and validation. The period was divided into two for calibration and validation. Seven years monthly stream flow data from (1995 to 2001) was used for calibration and five years (2002 to 2006) monthly stream flow data was used for validation using 17 sensitive parameters listed in table 4.1.

Sediment data generated from observed suspended sediment concentration using rating curve at both gauging stations were used for comparison only. In this study the SWAT model was calibrated and validated for stream flow at Toba (Didessa near Dembi) gauging station. However, the objective of this study was to predict sediment yield at Arjo Didessa dam and at the whole basin outlet. Due to lack of observed sediment data, the model output was calibrated and validated for the sediment driving force stream flow. The result is indicative since the most driving force was calibrated and validated.

4.2.1.Evaluation of flow simulation at Toba gauging station

The observed and simulated monthly flow for the calibration period from 1995–2001 is shown in figure 4.1. The statistical results for the model performance displayed satisfactory (R^2 is 0.79 and N_{SE} is 0.76) between the simulated and observed flow. However, the simulated stream flow was generally lower than the corresponding observed values during periods with high rainfall.

The calibrated model was then run from 2002–2006 to validate the model. During validation period, the observed and simulated monthly stream flow closely match for most part, except during some high-flow events that underestimated by the model (figure 4.3). The statistical analysis results also demonstrated good agreement between the observed and simulated stream flow with R^2 value of 0.66 and NSE value of 0.65.

Although the statistical evaluation showed the satisfactory, for both calibration and validation periods, SWAT tended to underestimate the stream flow during high-flow periods and underestimated during low flow periods. This could be partly because the present curve number technique is unable to generate accurate stream flow prediction for a day that experience several storms. When several storms occur during a single day, the soil moisture level and the corresponding stream flow curve number vary from storm to storm. However, SCS-CN methods define a rainfall event as the sum of all rainfall that occurs during one day, and this might lead to underestimation of runoff hence stream flow.

The result showed that there was good agreement between observed and simulated flow compared to previous studies Adgolign (2015) calibrated stream flow at Didessa near Arjo and reported that the result showed very good agreement between observed and simulated value R^2 and E_{NS} were 0.87 during calibration and 0.8 during validation respectively. Several authors calibrated and validated SWAT model in Blue Nile river basin and their report showed that the statistical parameters (R^2 and E_{NS}) varied between 0.53 and 0.92. Therefore SWAT model is applicable in Didessa river basin and for this study simulated values was reasonably acceptable.

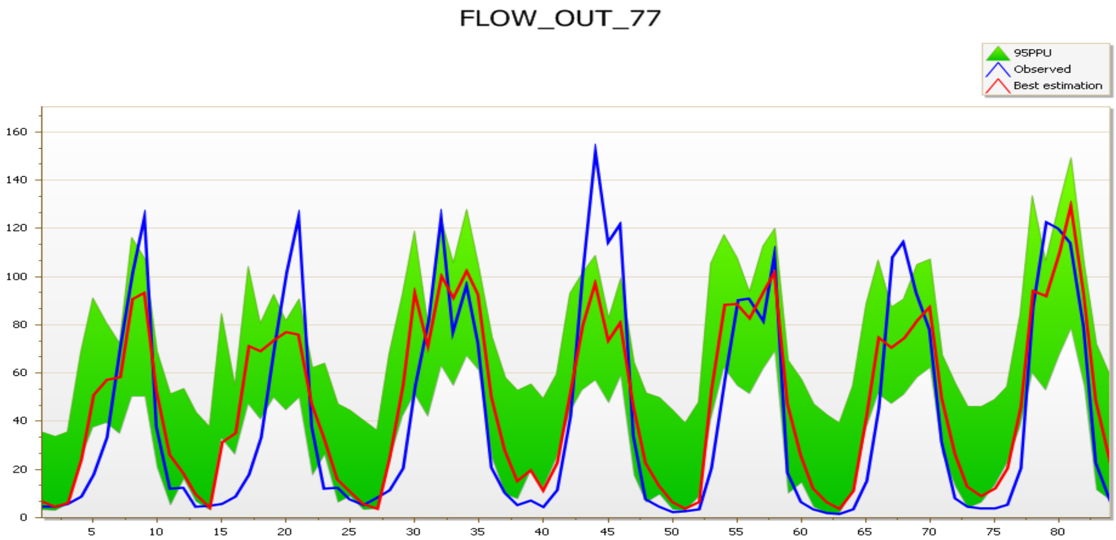

Figure 4. 1 Calibrated monthly stream flow by SUFI-2 at Toba station

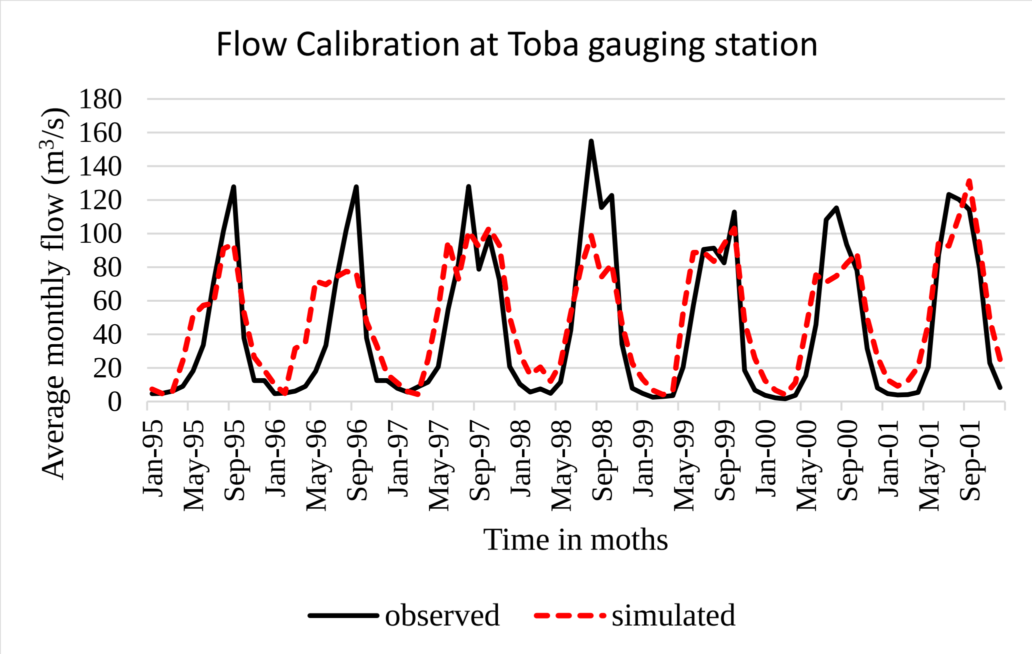

Figure 4. 2: Calibration results of monthly measured and simulated flow

Generally SWAT model underestimated the flow rate except during low flow (winter season) at Toba station. Summary of statistical parameters for calibration and validation were given in table 4.2.

Table 4. 2: Calibration and validation statistic parameters

Parameter	**Calibrated(1996-2001)**	**Validated (2002-2006)**
R^2	0.79	0.66
E_{NS}	0.76	0.65
PBIAS	-13	-3.3

Deviation of SWAT model simulation from actually measured flow was crearly described on figure 4.2. For low flow condition the best fit line deviate to simulated value that indicated overestimation and for high flow condition the line deviate to the observed value that indicates SWAT model underestimated.

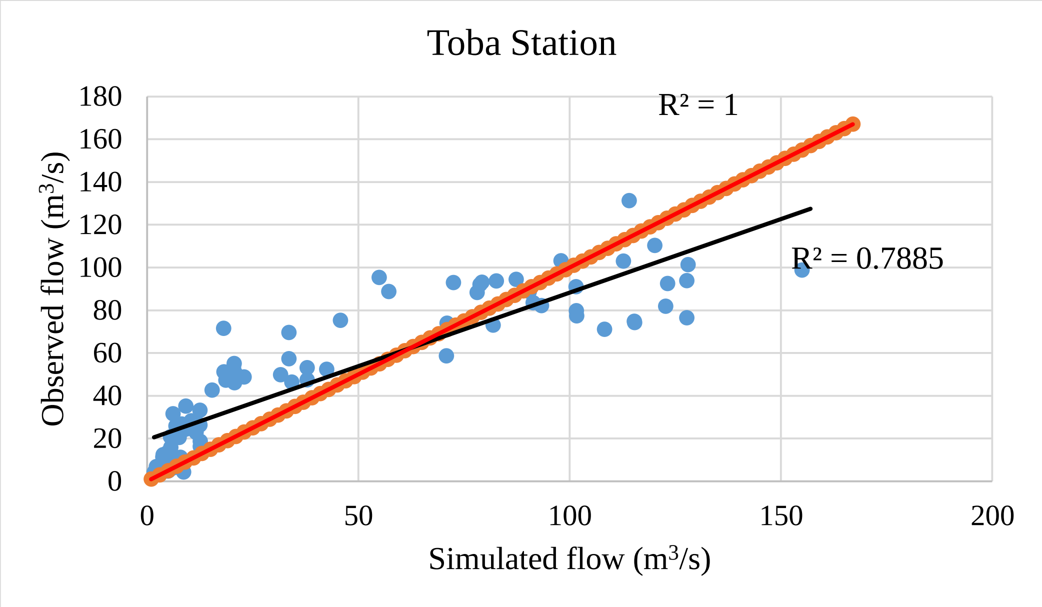

Figure 4. 3: Comparison of monthly simulated and observed stream flow during calibration

Average monthly flow simulated and observed at Toba gauging station during calibration and validation were summarized in table 4.3. The result SWAT model overestimated flow rate by 11.5% and 3.2% during calibration and validation period respectively.

Table 4. 3: Comparison of monthly measured and simulated flows

Period	Average flow (m^3/s)	
	measured	simulated
Calibration (1996-2001)	43.88	49.58
Validation (2002-2006)	47.67	49.23

The result in table 4.3 indicated that the average simulated runoff during calibration and validation period was closer.

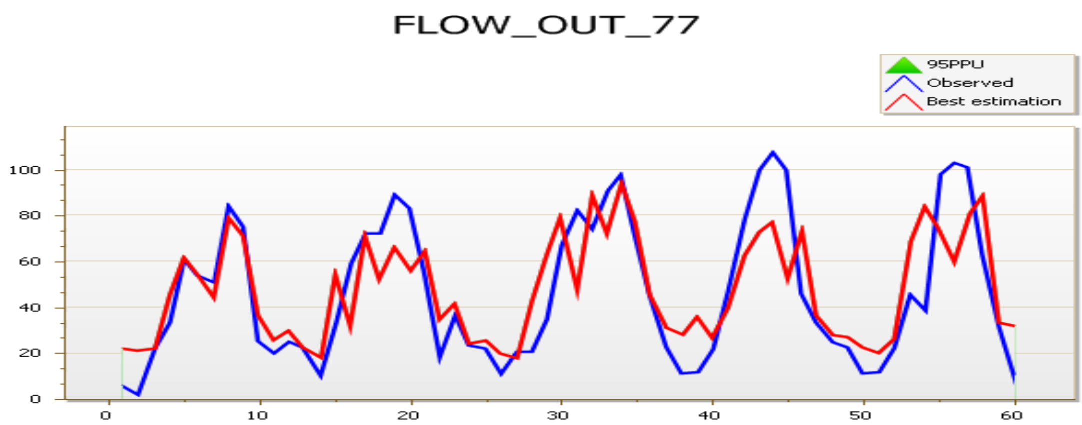

Figure 4. 4 Stream flow validation by SUFI-2 at Toba Station

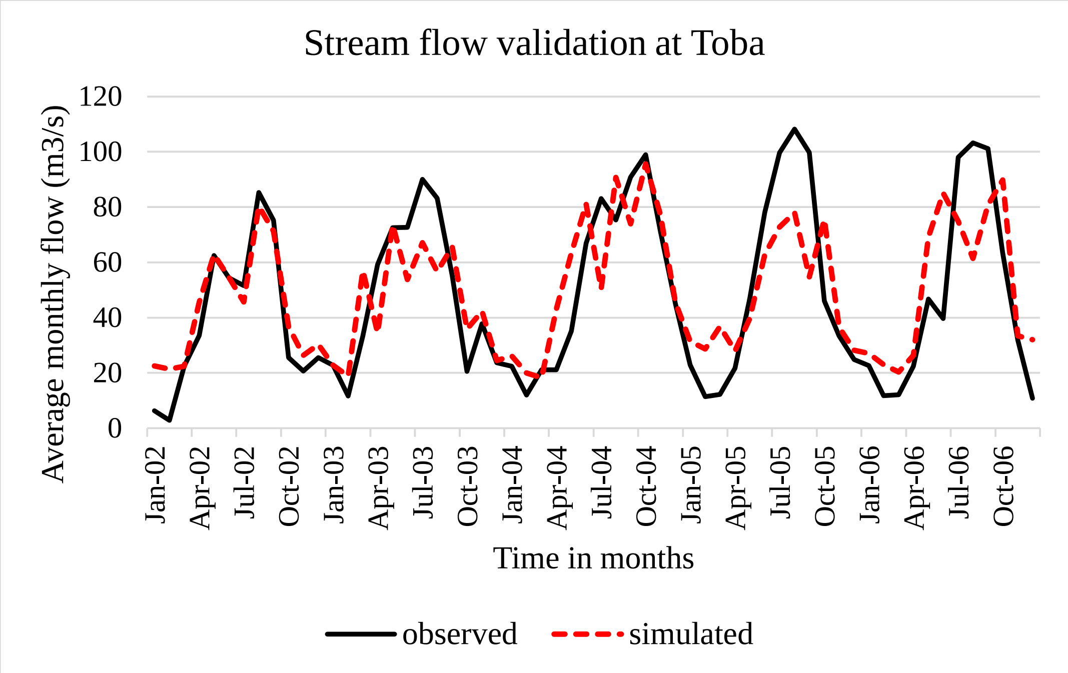

Figure 4. 5: Validation results of average monthly measured and simulated flow

Deviation of SWAT model simulation from actually observed stream flow during validation period was described on figure 4.4. For low flow condition the best fit line deviate to simulated value that indicated overestimation and for high flow condition the line deviate to the observed value that indicates SWAT model underestimated.

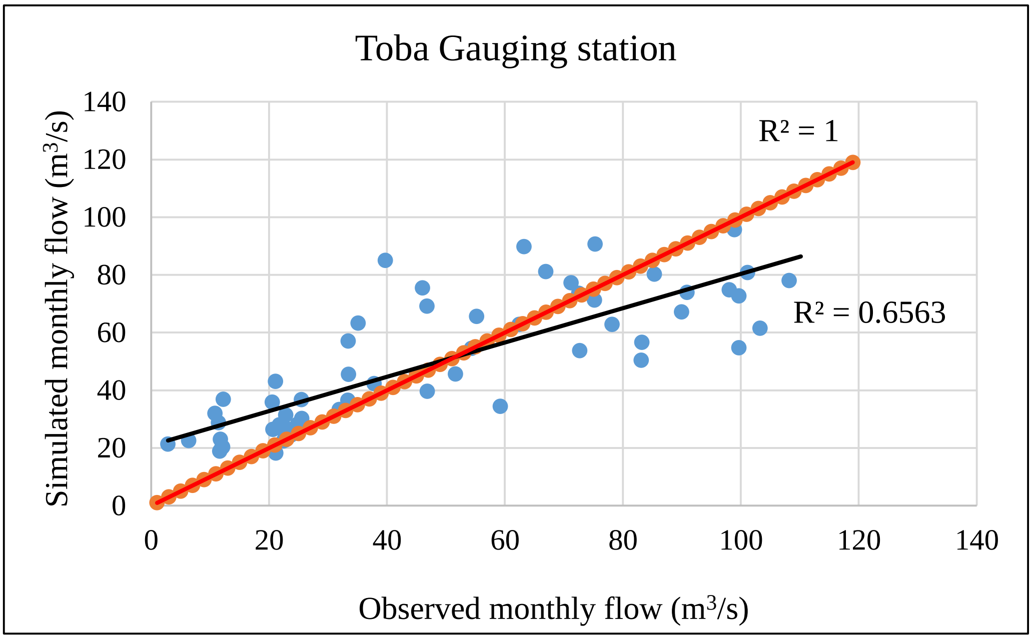

Figure 4. 6: Comparison of monthly simulated and observed streamflow during validation

4.2.2.Evaluation of Simulated Sediment Load at Toba and Gutin

The obtained suspended sediment concentration data was not sufficient for calibration and validation of SWAT model. Calibration and validation need continuously observed data. It is possible to generate continuous sediment concentration data using few observed sediment for a given stream by using sediment rating curve. Accordingly sediment concentration data for Toba and Little Anger streams were generated using observed data.

However sediment data obtained from rating is not recommended for calibration and validation since it does not represent actual observed sediment. Most river loads estimated by this method have been underestimated and the degree of underestimation increases with the degree of scatter about the rating curve and can reach 50% (Ferguson, 1986; Walling, 1977; Tadesse, 2013). Therefore, sediment load obtained from rating curve was not used for calibration and validation but only for comparison.

The best fit line of scattered plot (figure 4.5) for simulated suspended sediment concentration (TSS) and sediment concentration generated by using rating curve showed the precision of SWAT model in predicting sediment yield. Figure 4.5 plotted for only observed flow from 1990 to 2006 removing days with missing data to avoid double error. During this period SWAT model overestimated than rating curve by 37%. Since rating curve underestimates up to 50% by its nature the accuracy of simulated sediment was believed to be high.

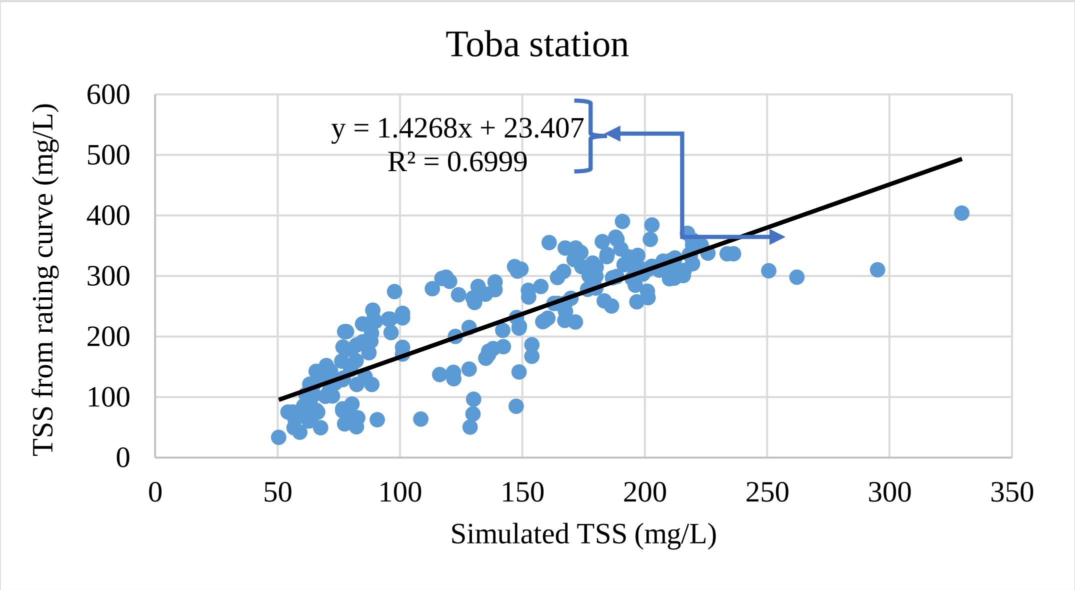

Figure 4. 7: Comparison between TSS simulated and obtained from rating curve

Monthly simulated and computed suspended sediment concentration at Toba gauging station during 1990 to 2006 was shown on figure 4.6 have similar trend but for high flow period SWAT model highly overestimated and during low flow period slightly underestimated.

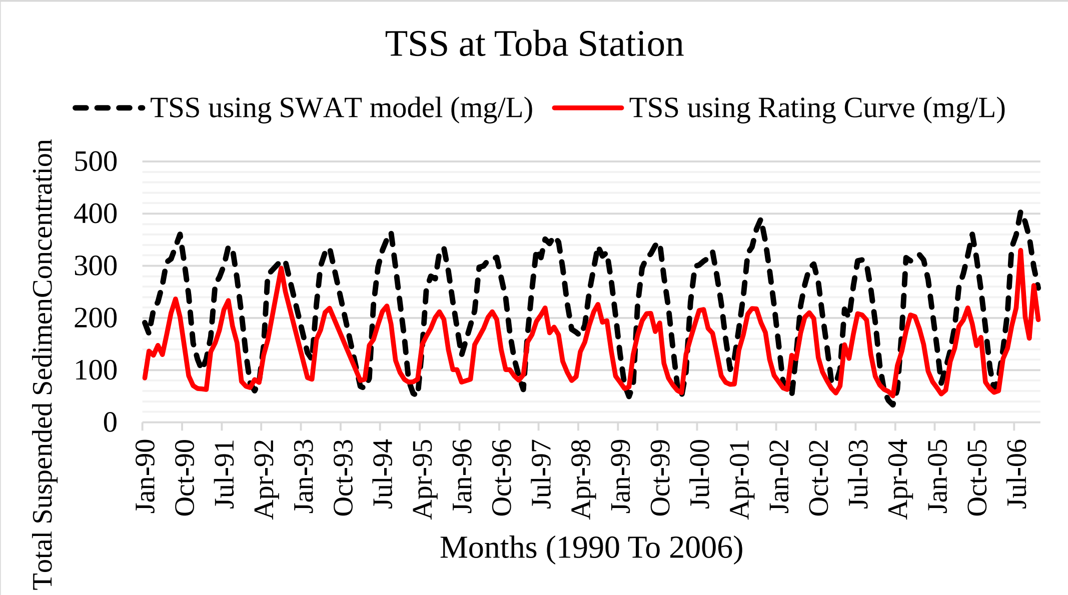

Figure 4. 8: Simulated and computed monthly suspended sediment concentration

Similarly, suspended sediment concentration at Gutin (Little Anger) gauging station was computed for periods of available flow (1990 to 2011) by using rating curve. Computed suspended sediment concentration was plotted against simulated suspended sediment concentration as shown on figure 4.7. SWAT model slightly overestimated compared to the computed value using rating curve.

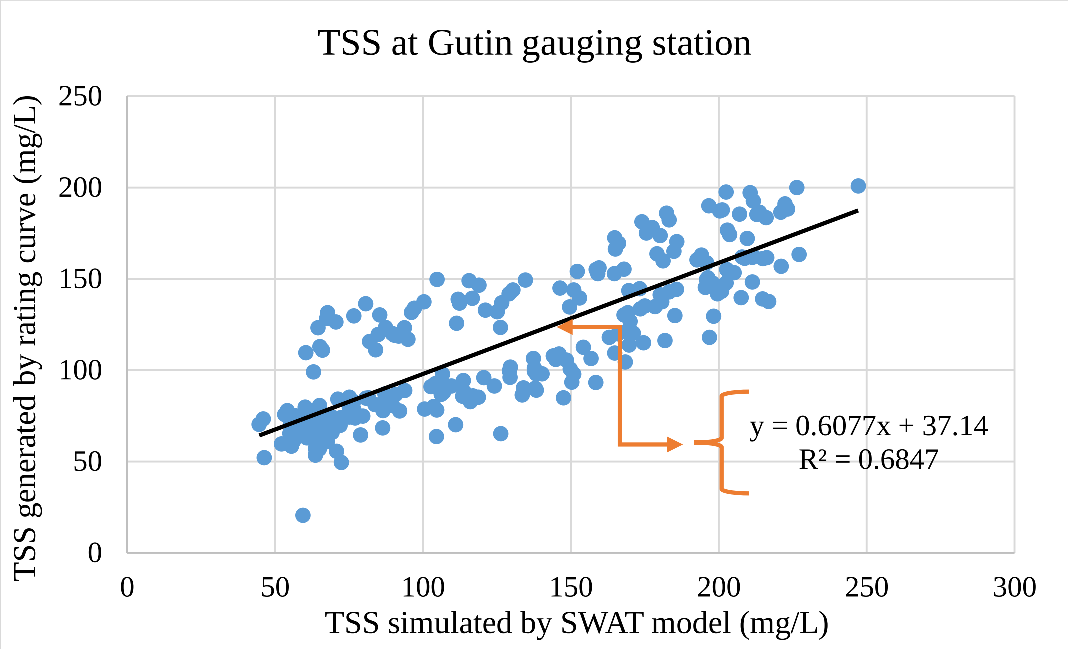

Figure 4. 9: comparison between TSS simulated and obtained from rating curve

During this period SWAT model overestimated than rating curve by 33.34% which was closer to value obtained from rating curve at Gutin station than that of Toba station. This shows that simulated total suspended sediment concentration at Gutin gauging station was better than that obtained at Toba gauging station.

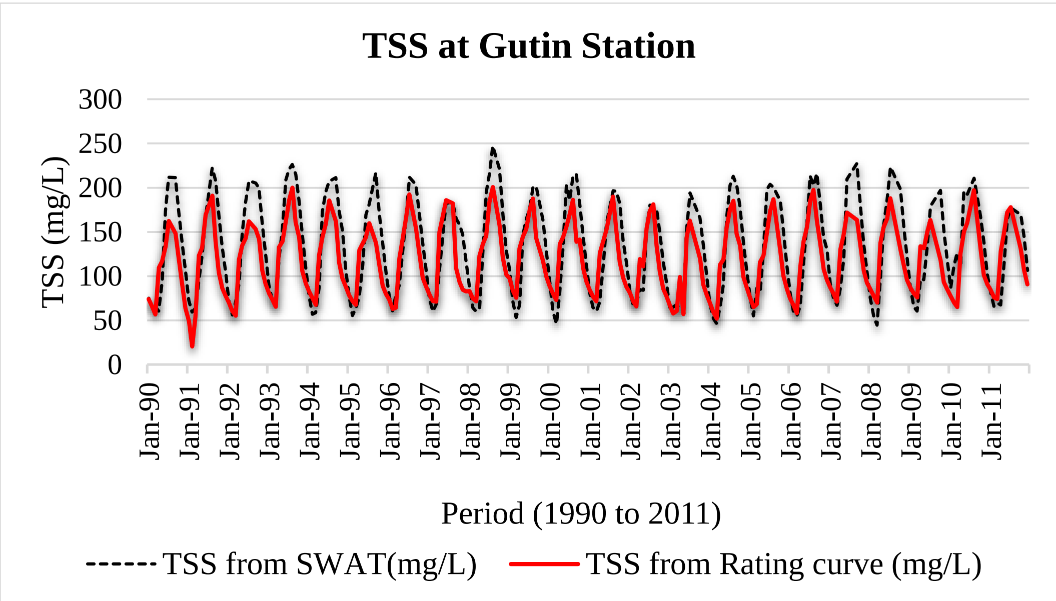

Figure 4. 10: Simulated and computed monthly suspended sediment concentration

Generally, the result obtained at both gauging stations showed that there was good agreement between rating curve and SWAT model on predicting sediment load and concluded that sediment yield simulated by SWAT model acceptable.

4.3. Sediment Yield

One of the objective of this study was to predict sediment yield at the out let of Didessa river basin and Arjo Didessa Reservoir. Each sub-basin has corresponding reach in which SWAT model simulated annual sediment enter and out flow from each reach. The whole basin outlet is represented by RCH 1 (See table 4.4) and the Arjo Didessa dam outlet is represented by reach (RCH 71). Sediment yield inflow to and outflow from each reach is shown in table 4.4.

SWAT simulation show that the average sediment yield of the basin as measured at the outlet was 8.29Mton/year and average sediment yield at Arjo Didessa dam was 0.99Mton/year.

Batrie *et al*. (2011) predicted average sediment yield at the outlet of the Upper Blue Nile as 117Mt per year and (Ndorimana *et al.* (2005) estimated sediment load of upper Blue Nile as 131Mt per year. (Betrie *et al*., 2011) reported that the observed sediment yield at upper Blue Nile was 140Mt per year. When compared to these literatures, Didessa River contributes only (5 to 7%) sediment yield to Blue Nile River. However, in terms of area, it covers about 15% of the basin.

Table 4. 4: Sediment yield at outlet of each sub-basin

RCH	Area (km^2)	Sediment yield at outlet (Mton/yr)	RCH	Area (km^2)	Sediment yield at outlet (Mton/yr)	RCH	Area (km^2)	Sediment yield at outlet (Mton/yr)
1	27710	8.29	31	456	6.44	61	170.8	0.12
2	27390	12.00	32	5445	3.33	62	2308	0.68
3	246.8	4.04	33	4767	1.81	63	9974	2.85
4	370.6	0.05	34	738.7	0.28	64	538	0.18
5	555.9	1.64	35	15630	7.47	65	170.8	1.84
6	1035	0.32	36	246.8	1.22	66	187	2.56
7	769.4	0.26	37	261.3	2.82	67	8649	2.58
8	234	4.73	38	288.6	2.93	68	3237	1.19
9	1689	0.42	39	334.8	2.89	69	1.708	0.00
10	210.1	0.23	40	648.2	6.48	70	359.5	5.46
11	316	3.48	41	15320	4.15	71	4984	0.99
12	26430	12.87	42	383.4	3.15	72	269	1.34
13	178.5	3.46	43	386	2.17	73	2018	0.64
14	471.4	6.08	44	439.8	1.58	74	4577	0.99
15	493.6	10.32	45	14550	7.80	75	443.2	3.22
16	560.2	4.96	46	13800	5.12	76	412.5	0.13
17	25050	10.31	47	333.9	0.76	77	1400	0.46
18	1179	0.38	48	454.3	5.47	78	951.3	0.26
19	5994	3.56	49	3068	0.92	79	173.4	0.08
20	2230	0.60	50	10730	4.20	80	3566	0.85
21	7909	3.04	51	10320	4.14	81	1694	0.23
22	885.6	0.26	52	177.6	0.44	82	2023	0.81
23	3845	1.09	53	290.3	0.74	83	762.6	0.21
24	307.4	0.83	54	388.6	0.35	84	175.1	0.04
25	540.6	0.18	55	2569	0.97	85	880.4	0.12
26	3878	1.15	56	345.9	0.81	86	176.8	0.35
27	17100	6.80	57	294.6	1.41	87	294.6	0.25
28	543.1	8.73	58	795	0.35	88	451.7	0.10
29	1048	0.35	59	953	2.29	89	677.2	0.43
30	212.6	0.71	60	1918	0.49			

(Betrie *et al*., 2011) reported that sediment transport to the main river decreases from the north-east to the south-west of the Blue Nile basin which is agree with this result. Location of delineated stream flows and Dam were shown on figure 4.9.

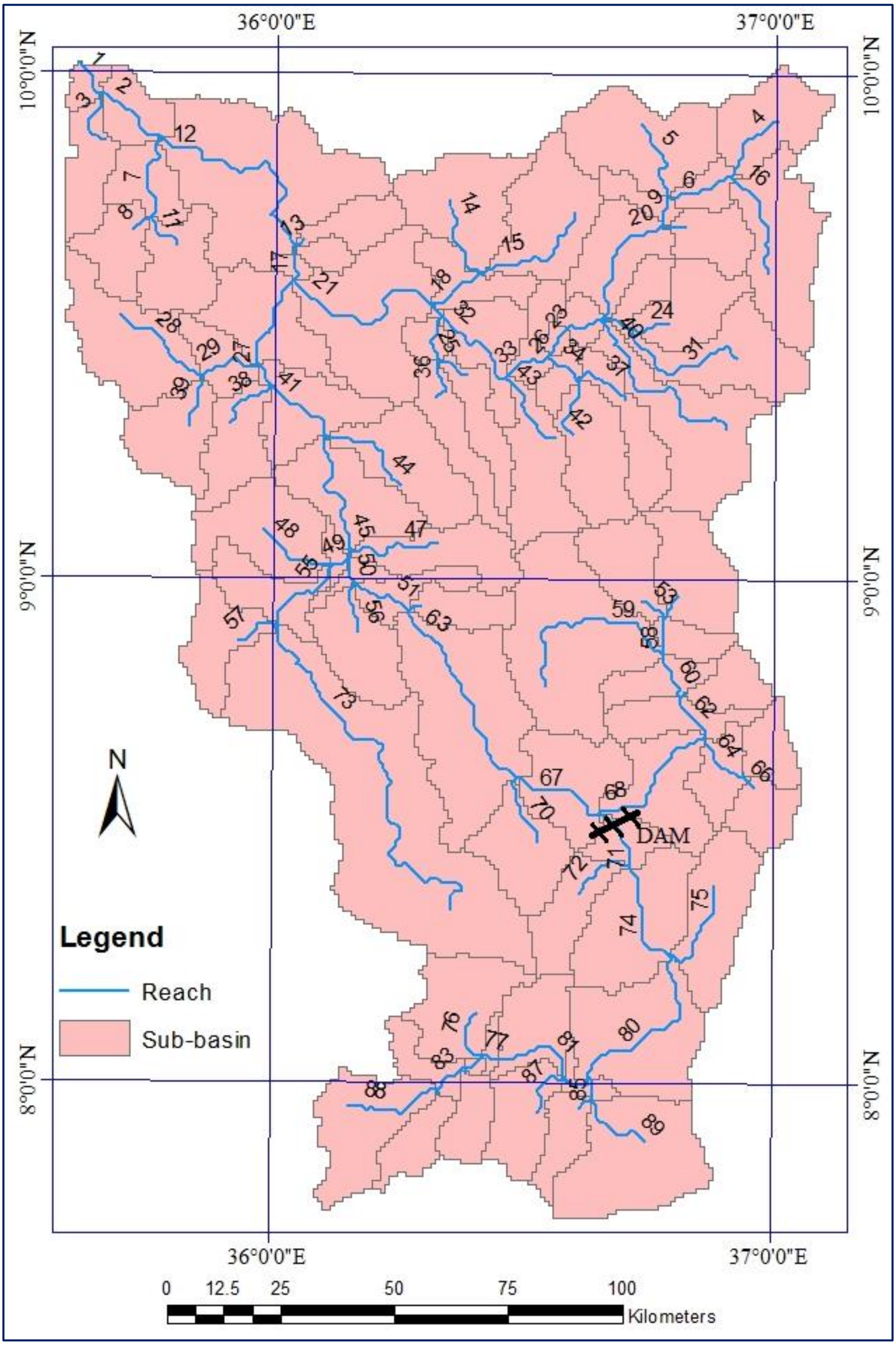

Figure 4. 11: Location of Arjo Didessa Dam and Reaches

Considering 1.12t/m^3 sediment density to be deposited and 0.99Mton/yr in Arjo Didessa reservoir, sedimentation rate becomes:

$$Sedimentation\ rate = \frac{0.99Mton/yr}{1.12t/m^3} = 0.88\text{Mm}^3/\text{year}$$

4.4. Reservoir Trap Efficiency

Brown equation and curves were used to determine Arjo Didessa reservoir trap efficiency.

For Arjo Didessa Reservoir, Catchment area (A) = 8250.126495km^2 and Reservoir capacity (C) = 1924.6*10^{6}m^3 trap efficiency by Brown will be:

$$TE = \left[1 - \frac{1}{\left(1 + 0.0021 * 0.1 * \frac{1924.6 * 10^{\wedge}6}{8250.126495}\right)}\right] * 100$$

TE = 97.99956%

Assuming that Arjo Didessa reservoir is normally ponded and sediment is mixture of grain size, C/I ratio will be

I = 4,067,889,811m^3/year

C =1924.6*10^{6}m^3

$$\frac{C}{I} = \frac{1924.6\text{M}m^3}{4067.9Mm^3/year} = 0.4731$$

From figure 3.18, TE = 97.82%

Assuming that, the reservoir was operating starting from Jan, 2014 and using inflow and outflow data obtained from (OWWDSE), the model was run adding the reservoir with required data. SWAT predicted trap efficiency of the reservoir as 97.39%.

Generally comparing Trap efficiency of Arjo Didessa reservoir obtained in three methods, 98% trap efficiency was adopted. The sediment yield expected to be deposited in the reservoir is 0.98*0.88Mm^3/year which 0.86Mm^3/year. The annual sediment load had been estimated to be 0.7756 Mm^3/year at the Dam site during the Feasibility Study for Irrigation Project.

4.5.Soil Erosion Prone Area

The other objective of this study is to identify the soil erosion prone area in the Didessa river basin. It is very important to know soil erosion prone area in the basin for catchment management planning.

SWAT model divided Didessa river basin into 89 sub-basin during stream network delineation and simulated soil erosion in the basin as shown in (table 4.6). The result varied from 0 to 200ton/ha. The average annual soil loss for whole watershed was 69.78ton/ha. Soil loss is a critical problem throughout the whole country, with sheet and rill erosion being the most important forms. It reaches levels of up to 100-200 ton/ha/yr throughout Ethiopia (FAO, 1986; Helena Huber, 2015).

The extent of soil erosion was classified into low (0 – 25t/ha/yr), moderate (25 – 75 t/ha/yr), severe (75 – 150t/ha/yr) and extreme for over 150t/ha/yr. The low class represents the erosion extent less than the soil formation rates, which is 22 t/ha/yr in the Ethiopian highlands, the moderate class represents erosion level less than the average soil loss from cultivated land, which is (72 t/ha/yr) and extreme class represents one fold higher than the average soil loss and the severe class represents two folds higher than average soil loss (Hurni, 1985; Betrie *et al*., 2011).

According to the above classification, Extreme erosion was dominant in the northern part of the basin, severe soil erosion was dominant in northern and central parts of sub-basins, Moderate erosion was dominant in eastern and north-east parts of basin and low erosion was dominant in the southern and central parts of the basin. Area coverage of each classification is given in Table 4.5.

Table 4. 5: Severity of soil erosion corresponding area in Didessa river basin

Soil Erosion condition	Sediment yield (ton/ha/yr)	Percent of area coverage (%)	Area (km^2)
Low erosion	0 - 25	31.43	8710.38
Moderate erosion	25 - 75	20.07	5561.89
Severe erosion	75 - 150	38.08	10553.29
Extreme erosion	Over 150	10.42	2886.40

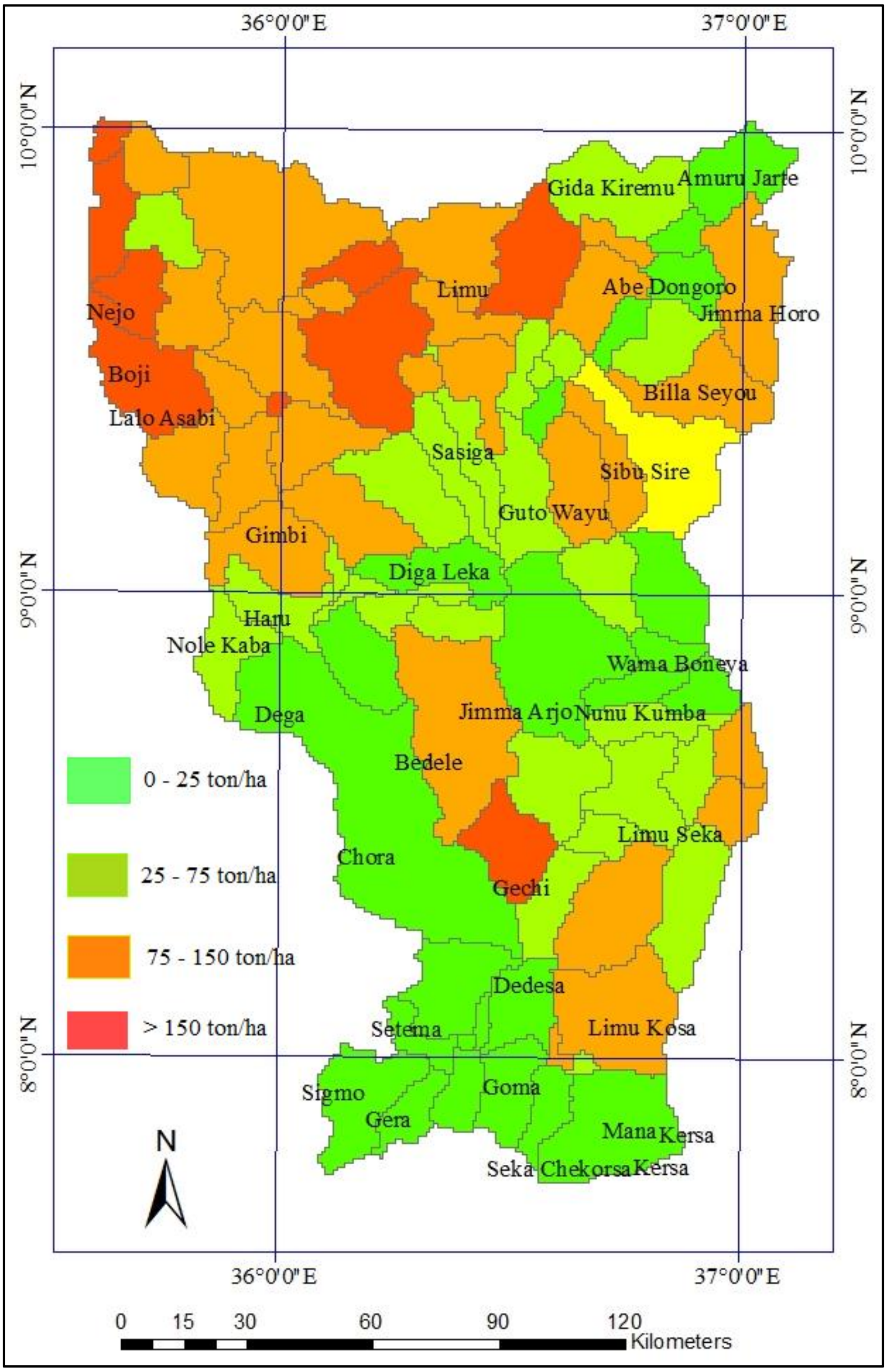

Figure 4. 12: spatial distribution of soil erosion in Didessa river basin

Arjo Didessa Dam reservoir is located at the outlet of sub-basin 71. Out of 89 sub-basins only 17 sub-basins contribute sediment to the reservoir. Average soil loss from these sub-basins was 33ton/ha/yr. For all sub-basins the corresponding soil erosion were described in table 4.6.

Table 4. 6: Simulated upload sediment yield of Didessa watershed sub-basins

Sub-basin	Area (Km^2)	SYLD (ton/ha)	Sub-basin	Area (Km^2)	SYLD (ton/ha)	Sub-basin	Area (Km^2)	SYLD (ton/ha)
1	70.88	167.59	31	456.02	141.24	61	170.79	7.07
2	196.41	127.15	32	292.05	139.98	62	219.47	34.39
3	246.80	163.52	33	150.30	32.50	63	965.83	129.56
4	370.62	1.22	34	93.94	21.32	64	180.19	62.69
5	555.93	29.53	35	24.77	166.47	65	170.79	107.98
6	104.18	0.34	36	246.80	49.27	66	187.02	137.09
7	219.47	51.61	37	261.31	108.00	67	426.13	66.74
8	233.99	202.32	38	288.64	101.58	68	391.11	62.53
9	98.21	132.11	39	334.75	86.40	69	1.71	28.57
10	210.07	11.18	40	648.16	100.00	70	359.52	151.85
11	315.97	110.18	41	330.48	134.23	71	137.49	40.24
12	1197.30	106.55	42	383.43	82.16	72	269.00	49.93
13	178.48	193.78	43	385.99	56.12	73	2017.90	3.18
14	471.39	129.01	44	439.79	35.99	74	567.88	100.55
15	493.59	208.99	45	418.44	138.99	75	443.21	72.68
16	560.20	88.61	46	2.56	21.00	76	412.46	3.20
17	39.28	119.17	47	333.90	22.83	77	36.72	6.78
18	214.34	126.23	48	454.31	120.32	78	15.37	7.28
19	8.54	53.32	49	45.26	26.89	79	173.35	4.72
20	330.48	105.30	50	64.05	36.16	80	662.67	88.00
21	735.26	150.42	51	165.67	45.96	81	293.76	7.72
22	122.12	17.68	52	177.62	24.96	82	34.16	83.14
23	81.13	62.46	53	290.35	25.65	83	135.78	3.18
24	307.43	26.87	54	388.55	9.13	84	175.06	2.40
25	81.13	91.53	55	256.19	59.38	85	26.47	63.34
26	33.31	49.83	56	345.85	23.44	86	176.77	20.05
27	422.71	87.05	57	294.62	47.80	87	294.62	8.43
28	543.12	160.74	58	116.14	9.73	88	451.75	2.26
29	169.94	128.47	59	953.02	24.06	89	677.19	6.34
30	212.64	33.23	60	169.94	21.24			

The result of the SWAT output indicated that significant portions of the area which are known to be highly cultivated area are more vulnerable to soil erosion. Moreover, areas at a higher slope condition have shown higher contribution of sediment yield. Some parts of the watershed which have higher erodibility characteristics because of poor soil physical properties contributed for a higher sediment yield than others. Many of the places which are very near to rivers and stream has shown a considerable contribution for higher soil erosion and sediment yield (Appendix B).

5. CONCLUSION AND RECOMMENDATION

5.1 Conclusion

The annual sediment yield of Didessa river basin as measured at the Didessa river outlet and Arjo Didessa reservoir has been predicted using SWAT model. Sediment yield at each major tributaries outlet also determined and the soil erosion prone area has been identified. The trap efficiency of Arjo Didessa reservoir and sedimentation rate which are very important to estimate the reservoir has been estimated.

SWAT model is a good approach to determine sediment yield of river basin as it considers many factors affecting soil erosion and sediment transport. The model output was evaluated in two ways and the result indicated that the SWAT model performed well in predicting sediment yield of the basin. Suspended sediment concentration simulated by SWAT model was compared with sediment concentration obtained from rating curve and showed very good agreement. In other way the simulated stream flow has been calibrated and validated. The model performance indicators coefficient of determinant (R^2) and Nash-Sutcliffe (E_{NS}) were found to be 0.79 and 0.76 during calibration and 0.66 and 0.65 during validation. This shows that SWAT model simulates well sediment yield of Didessa river basin.

In this study attempts were made to classify the river basin in terms of sediment yield per hectare which is very important data for watershed plan and management. Accordingly, the downstream area and part of middle of the basin were identified as erosion prone area.

In general swat model performed well in predicting sediment yields from Didessa river basin and the results were reasonably acceptable. Therefore, SWAT model is a capable tool for further analysis of the hydrological responses in Didessa river basin. It can be applied to similar basins in Ethiopia to predict sediment yield and water yield.

5.2 Recommendation

The model was calibrated and validated on tributary (Toba) which covers only 5% of the basin area and the simulated sediment was compared with sediment generated from rating curve developed by scarcely available sediment sample for the validation of the model. Therefore, it has to be emphasised that the outputs presented in this study have to be treated with caution and the model could be further tested when the data on the sediment load is available.

Since Arjo Didessa dam was under construction during this study, there was no data on deposited sediment and reservoir operational conditions. Assumptions has been made and data has been taken from literatures to predict reservoir trap efficiency. When the reservoir become operate, bathometric survey has to conduct to determine the actual reservoir trap efficiency.

Sub-basin 15, 8, 13, 1, 28 and 35 showed alarming sediment yield which cause severe soil erosion (>150ton/ha). This area needs soil erosion mitigation measures such as land slope stabilization, construction of bench terraces, changing the land use of the steep area from agriculture to plantation or afforestation. Therefore, government and policy makers have to give priority to watershed management of this area.

Sediment yield predicted during feasibility study of Arjo Didessa reservoir was 0.775Mm^3 per year but this study shows sediment yield at the dam exceed this value which is 0.86Mm^3 per year. Since the dam is still under construction this output has to be taken into consideration to overcome the problems to be aroused due to reservoir sedimentation.

References

Abdalla Abdelsalam Ahmed, (2008). Sediment in the Nile River System UNESCO International Hydrological Programme, International Sediment Initiative.

Abdi Boru Ayana, Desalegn Chemeda Edossa and Ekasit Kositsakulchai, (2012). Simulation of Sediment Yield using SWAT Model in Finchaa Watershed, Ethiopia Kasetsart J. (Nat. Sci.) 46 : 283 – 297.

Admasu Amare, (2005). Study of Sediment Yield from the Watershed of Angereb Reservoir, M.Sc. Thesis, Aramaya University.

Arnold, J. G., Srinivasan, R., Muttiah R. S., Williams J. R. (1998). Large area hydrologic modeling and assessment Part I: Model development. J. Am. Water Resour. Assoc. 34(1):73-89.

Arnold, J. G., D. N. Moriasi, P. W. Gassman, K. C. Abbaspour, M. J. White, R. Srinivasan, C. Santhi, R. D. Harmel, A. van Griensven, M. W. Van Liew, N. Kannan, M. K. Jha (2012). SWAT: Model Use, Calibration, And Validation Transactions of the ASABE (American Society of Agricultural and Biological Engineer), ISSN 2151-0032, 55(4): 1491-1508.

Awulachew, S. B., McCartney, M., Steenhuis, T. S, Ahmed, A. A. 2008. A review of hydrology, sediment and water resource use in the Blue Nile Basin. Colombo, Sri Lanka: International Water Management Institute. 87p. (IWMI Working Paper 131).

Bagnold, R. A. (1977). Bedload transport in natural rivers. Water resources research, 13(2): 3030 – 312.

Beasley, D. B. and L. F. Huggins, (1982). ANSWERS (Areal Nonpoint Source Watershed Environment Response Simulation): User's Manual. U.S. Environmental Protection Agency, Chicago, Illinois.

Beven, K. and Binley A. (1992). The future of distributed models: model calibration and uncertainty prediction. Hydrological. Process; 6: 279–298.

Betrie, G. D., Mohamed Y. A., van Griensven A. and Srinivasan R., (2011). Sediment management modelling in the Blue Nile Basin using SWAT model. Hydrology and Earth System Sciences, 15, 807–818.

Bronsvoort K. (2013). Sedimentation in Reservoirs. Investigating Reservoir Preservation Options and the Possibility of Implementing Water Injection Dredging In Reservoirs. Msc. Thesis, Delft University of Technology.

Brown, C. (1943). Discussion of Sedimentation in Reservoirs, by J. Witzig. Proceedings of the American Society of Civil Engineers 69, 1493-1500.

Churchill, M. (1948). Discussion of Analysis and use of reservoir sedimentation data by L.C. Gottschalk. Proceedings of the federal interagency sedimentation conference, Denver, Colorado, Washington, DC: US Geological Survey, 131-141.

Conway, D. (2000), "The Climate and Hydrology of the Upper Blue Nile River." The Geographical Journal 166(1): 49-62.

Dahmen, E.R. and Hall M.J. (1990). Screening of Hydrological Data: Tests for Stationarity and Relative Consistency. International Institute for Land Reclamation and Improvement/ILRI, Wageningen, The Netherlands.

Dereje Dargie Haile, (2010) Impact of Land Use Change on Reservoir Sedimentation (Case Study of Karadobi). M.Sc Thesis, Addis Ababa University.

Desale Kidane and Binyam Alemu, (2015).The Effect of Upstream Land Use Practices on Soil Erosion and Sedimentation in the Upper Blue Nile Basin, Ethiopia. Research Journal of Agriculture and Environmental Management. Vol. 4(2), pp. 055-068.

FAO (1998). The Soil and Terrain Database for northeastern Africa (CDROM) FAO, Rome.

Gebremicael, T, Mohamed, Y, Betrie, G, van der Zaag, P, & Teferi, E. (2013). Trend Analysis of runoff and sediment fluxes in the Upper Blue Nile basin: A combined analysis of statistical tests, physically-based models and landuse maps. Journal of Hydrology, 482: 57-68.

Green, W. H. and Ampt G. A. (1911) Studies on soil physics, 1. The flow of air and water through soils. Journal of Agricultural Sciences 4: 1-24.

Guzman, C. D., Tilahun S. A., Zegeye A. D., and Steenhuis T. S., (2013). Suspended sediment concentration–discharge relationships in the (sub-) humid Ethiopian highlands, Hydrology and Earth System Sciences, 17, 1067–1077.

Haregeweyn, N., Poesen J., Nyssen J., DE Wit J., Haile M., Govers G. and Deckers S., (2006). Reservoirs in Tigray (Northern Ethiopia): Characteristics and Sediment Deposition Problems. Land Degradation & Development; 17: 211–230.

Helena Huber (2015). Investigation of Hydraulic Response Unit Discretization for Erosion Modelling with SWAT in the Upper Blue Nile Basin, Msc. Thesis, Munchen University.

Joris de VenteT. and Jean Poesen, (2005). Predicting soil erosion and sediment yield at the basin scale: Scale issues and semi-quantitative models. Physical and Regional Geography Research Group, Katholieke Universiteit Leuven, Redingenstraat 16, 3000 Leuven, Belgium. Earth-Science Reviews 71 (2005) 95–125.

http://www.idp-uk.org/OurProjects/ Environment/ Environment Project.htm (accessed: 27/10/2015).

Karim C. Abbaspour, (2014). SWAT-CUP 2012: SWAT Calibration and Uncertainty Programs - A User Manual. Eawag: Swiss Federal Institute of Aquatic Science and Technology.

Kebede Wolka Wolancho, (2012). Watershed Management: An Option to Sustain Dam and Reservoir Function in Ethiopia. Journal of Environmental Science and Technology, 5: 262-273.

Knisel, W. G. (1980). CREAMS: A Field-scale Model for chemical, runoff, and erosion from Agricultural Management Systems. USDA Conservation Research Report No. 26, Washington, D.C.

Leonard, R. A, Knisel W. G., Still D. A. (1987). GLEAMS: Groundwater loading effects of agricultural management systems. Trans. ASAE 30(5):1403-1418.

Mahmood, K. (1987) Reservoir Sedimentation, Impact, Extent, and Mitigation. Washington, DC: World Bank, World Bank Technical Paper No. 71.

Mequanint Tenaw and Seleshi Bekele Awulachew, (2008). Soil and Water Assessment Tool (SWAT)-Based Runoff and Sediment Yield Modelling: A Case of the Gumera Watershed in Lake Tana Sub basin. International Water Management Institute, Addis Ababa, Ethiopia.

Moriasi, D. N., Arnold, J. G., Van Liew, M. W., Bingner, R. L., Harmel, R. D., and Veith, T. L. , (2007). Model evaluation guidelines for systematic quantification of accuracy in watershed simulations, T. ASABE, 50, 885–900.

Morris, G. L., & Fan, J. (1998). Reservoir sedimentation handbook: design and management of dams, reservoirs, and watersheds for sustainable use (Vol. 9). New York: McGraw-Hill.

Ndorimana, L., Saad, S. A., Eldaw, A. K., Naggar, O. M., Nindamutsa, A., Chane, B., Fadul, H. (2005). "Watershed Erosion and Sediment Transport". Group III, Nile Basin Capacity Building Network for River Engineering (NBCBN-RE), River Morphology, Research Cluster, Sudan.

Neitsch S. L., Arnold J. G., Kiniry J. R., Williams J. R. (2005). Soil and Water Assessment Tool: Theoretical Documentation. Blackland Research Center, Grassland, Soil and Water Research Laboratory, Agricultural Research Service: Temple, TX, USA.

Neitsch, S. L., Arnold J. G., Kiniry J. R. and Williams J. R. (2011). Soil and Water Assessment Tool, Theoretical Documentation: Version 2009. Temple, TX. USDA Agricultural Research Service and Texas A & M Blackland Research Center.

Nigussie Teklie and Yared Ashenafi, (2010). Effect of land use/land cover management on Koga Reservoir sedimentation. NBCBN Ethiopia Node, Addis Ababa University.

Oromia Water Works Design and Supervision Enterprise. (2009). Arjo Didessa Irrigation and Hydro Electric Project Studies Feasibility Report. Finfinne: Unpublished report.

Rabin Bhattarai & Dushmata Dutta (2007). Estimation of Soil Erosion and Sediment Yield Using GIS at Catchment Scale, Water Resource Management; 21:1635–1647.

Refsgaard, J.C. and Storm, B. (1996), Construction, calibration and validation of hydrological models, Distributed Hydrological Modelling (eds. M.B. Abbott and J.C. Refsgaard), Kluwer Academic Publishers.

Santhi, C., J.G. Arnold, J.R. Williams, W.A Dugas, R. Srinivasan, and L.M. Hauck. 2001. Validation of the SWAT model on a large river basin with point and nonpoint sources: Journal of the American Water Resources Association 37(5): 1169-1188.

Shiferaw, B. and Holden, S. (1999). Soil erosion and smallholders conservation decisions in the highlands of Ethiopia. World Development 27(4): 739-752.

Shimelis, G. Setegn, Bijan Dargahi, Ragahavan Srinivasan, and Assefa M. Melesse (2010). Modeling of Sediment Yield from Anjeni-Gauged Watershed, Ethiopia Using SWAT Model. Journal of the American Water Resources Association, Vol. 46, No. 3.

Shimelis Gebriye Setegn, (2008). Hydrological And Sediment Yield Modelling In Lake Tana Basin, Blue Nile Ethiopia. M.Sc. Thesis, Royal Institute of Technology (KTH). SE-100 44 Stockholm, Sweden.

Shimelis, G. Setegn, Ragahavan Srinivasan, Bijan Dargahi and Assefa M. Melesse, (2009). Spatial Delineation of Soil Erosion Vulnerability in the Lake Tana Basin, Ethiopia. Hydrological Processes. Spatial Science Laboratory, Texas A & M University, College Station, TX, USA.

Sima Bizuneh Admasu, (2011). Flow Regime and Land Cover changes in the Didessa Sub-Basin of the Blue Nile River, MS.c, Swedish University of Agricultural Science (SLU).

Singh, V, Bankar, N, Salunkhe, S. S, Bera, A. K, & Sharma, J. R. (2013). Hydrological stream flow modelling on Tungabhadra catchment: parameterization and uncertainty analysis using SWAT-CUP. Current Science, 104-9: 1187-1199.

Tadesse Tufa Borji, (2013). Sedimentation and Sustainability of Hydropower Reservoirs: Cases of Grand Ethiopian Renaissance Dam on the Blue Nile River in Ethiopia. M.Sc Thesis, Norwegian University of Science and Technology, Norway.

Tamene, L., Park S.J., Dikau R. and Vlek P.L.G., (2006). Analysis of factors determining sediment yield variability in thehighlands of northern Ethiopia. Center for Development Research (ZEF), University of Bonn, Walter-Flex-Str.3, 53113, Bonn, Germany. Geomorphology 76, 76– 91.

Tena Bekele Adgolign, G. V. R. Srinivasa Rao and Yerramsetty Abbulu, (2015). Assessment of Spatio-Temporal Occurrence of Water Resources in Didessa Sub-Basin, West Ethiopia. International Journal of Civil, Structural, and Environmental and Infrastructure Engineering Research and Development (IJCSEIERD) ISSN (P): 2249-6866; ISSN (E): 2249-7978 Vol. 5, Issue 1, Feb 2015, 105-120.

Tesfaye Muluneh and Wondimu Mamo (2014). Morphometric Analysis of Didessa River Catchment in Blue Nile Basin, Western Ethiopia. Science, Technology and Arts Research Journal, 3(3): 191-197.

Thomas, C. C. Huang and Kwong Fai A. Lo, (2015). Effects of Land Use Change on Sediment and Water Yields in Yang Ming Shan National Park, Taiwan Institute of Geography, Chinese Culture University, Taipei 11114, Taiwan. Environments, 2, 32-42.

Tyagi, J. V., Rai S. P., Nuzhat Qazi and Singh M. P., (2014). Assessment of discharge and sediment transport from different forest cover types in lower Himalaya using Soil and Water Assessment Tool (SWAT). International Journal of Water Resources and Environmental Engineering, National Institute of Hydrology, Jal Vigyan Bhawan, Roorkee - 247 667, Uttarakhand, India. Vol. 6(1), pp. 49-66.

USDA Soil Conservation Service (1972). National Engineering Handbook. Hydrology Section 4 (Chapters 4–10).

Verstraeten, G. and Poesen, J., 2000. Estimating trap efficiency of small reservoirs and ponds: methods and implications for the assessment of sediment yield. Progress in Physical Geography, 24(2): 219-251.

Williams, J.R. and H.D. Berndt, 1977. Sediment Yield Prediction Based on Watershed Hydrology. Transactions of American Society of Agricultural Engineers 20(6):1100-1104.

Williams, J.R. (1975). Sediment-yield prediction with universal equation using runoff energy factor. p. 244-252. In Present and prospective technology for predicting sediment yield and sources: Proceedings of the sediment yield workshop, USDA Sedimentation Lab., Ox-ford, MS, November 28-30, 1972. ARS-S-40.

Williams, J. R., Nicks A. D. and Arnold J.G. (1985). SWRRB, a simulator for water resources in rural basins. ASCE Hydrol. J. 111(6):970-986.

Williams, J. R., (1995). Chapter 25: The EPIC Model. In: Computer Models of Watershed Hydrology 1, V.P. Singh (Editor), Water Resources Publications, Colorado, pp. 909-1000.

Williams, J., (1980). SPNM, a model for predicting sediment, phosphorus, and nitrogen yields from agricultural basins, J. Am. Water. Resource. As., 16, 843–848.

Winchel, M., Srinivasan R., Di Luzio M., Arnold J., (2013). ArcSWAT Interface for SWAT2012. Grassland, Soil and Water Research Laboratory USDA Agricultural Research Service 808 East Blackland Road – Temple, Texas 76502.

Wischmeier, W. H., and Smith, D. D. (1965). Predicting rainfall-erosion losses from cropland east of the Rocky Mountains. Agricultural Handbook No. 282, U.S. Dept. Agriculture, Washington, DC.

Young, R. A., Onstad D. D. and Anderson W. P. (1989). AGNPS: A nonpoint source pollution model for evaluating agricultural watersheds. Soil and Water Cons. 44(2): 168-173.

Appendix

Appendix A: Rainfall Data Analysis

Table: Annual rain fall data and average value

Yearly RF (mm)								
Year	ABSJ	Anger	Arjo	Bedele	Didessa	Gembe	Nekemte	Average
1980	1506.94	978.59	1328.01	1217.42	871.03	1262.89	1578.04	1248.99
1981	2035.79	1709.54	1633.78	1831.16	1171.47	1964.68	2177.55	1789.14
1982	1829.50	1315.36	1736.28	1888.10	1312.10	1668.70	1769.75	1645.68
1983	1962.81	1737.86	1360.53	1981.00	1641.65	1373.08	1595.04	1664.57
1984	1297.50	1353.40	1396.10	1713.11	1503.30	1442.90	1674.01	1482.90
1985	1912.30	1569.50	1791.59	1824.90	1750.30	1301.88	2069.40	1745.70
1986	1202.00	1057.60	1506.00	1392.70	1274.10	1434.04	1420.60	1326.72
1987	1856.30	1463.30	1891.40	1991.80	1688.30	1393.28	2075.38	1765.68
1988	1929.50	1737.57	1643.50	2001.50	2119.93	1329.96	1727.60	1784.22
1989	1844.90	1235.80	1854.50	1810.30	1877.67	1672.30	1935.70	1747.31
1990	1429.80	1644.30	1571.40	1711.50	1324.40	1651.10	1889.70	1603.17
1991	1499.20	1741.54	1608.50	1686.20	1327.40	1375.30	1962.50	1600.09
1992	1662.00	1708.30	2001.40	1909.20	1146.40	2230.40	2479.10	1876.69
1993	1901.90	1914.50	1952.40	1783.40	1347.70	1819.10	2512.50	1890.21
1994	1491.83	2098.80	1452.98	1594.40	1180.90	1418.50	2090.00	1618.20
1995	1585.31	1544.80	1317.40	1838.80	1043.10	1423.10	2059.20	1544.53
1996	1565.20	1448.00	1908.78	1735.00	1877.00	1511.80	2320.90	1766.67
1997	1859.70	1399.30	1881.60	2001.60	1478.40	2147.60	2190.00	1851.17
1998	1518.80	2137.54	1750.91	1941.00	1744.60	1239.00	2551.40	1840.46
1999	2477.10	1928.30	1877.01	2322.50	1484.70	1364.10	1919.70	1910.49
2000	1611.20	1709.10	1929.90	1827.80	1836.60	1492.10	2150.20	1793.84
2001	1830.40	1490.10	1873.30	2165.00	1266.30	1755.35	1942.20	1760.38
2002	1278.00	1056.00	1353.60	1449.50	907.20	1049.40	1706.00	1257.10
2003	1537.40	1504.00	1780.90	1445.50	1571.90	1246.66	1837.50	1560.55
2004	1492.00	1562.50	2360.70	1867.50	1472.20	1446.90	1792.10	1713.41
2005	1893.90	1716.60	2143.00	2187.90	1601.10	1147.77	2248.70	1848.42
2006	1715.41	1611.70	1991.20	2358.30	1717.00	1955.20	2139.40	1926.89
2007	1286.50	1713.00	2766.50	1982.40	1520.50	1576.10	2173.00	1859.71
2008	1796.40	1692.70	2626.00	2048.90	2098.10	1346.79	2441.30	2007.17
2009	1655.30	1625.70	2588.00	1776.80	1447.00	1201.03	2022.80	1759.52
2010	1861.50	1929.70	2061.60	2106.00	1641.70	1487.54	2482.10	1938.59
2011	1485.20	1462.45	2461.30	1737.94	1304.70	1304.80	2010.40	1680.97
2012	1315.00	1996.40	1666.00	1770.97	1357.30	1318.80	2109.30	1647.68
2013	1949.45	1542.63	1521.00	1990.46	1420.10	1436.50	1965.30	1689.35
2014	1921.10	1830.00	1972.50	1935.80	1909.10	1457.70	2527.10	1936.19

Graphical representation of annual rainfall

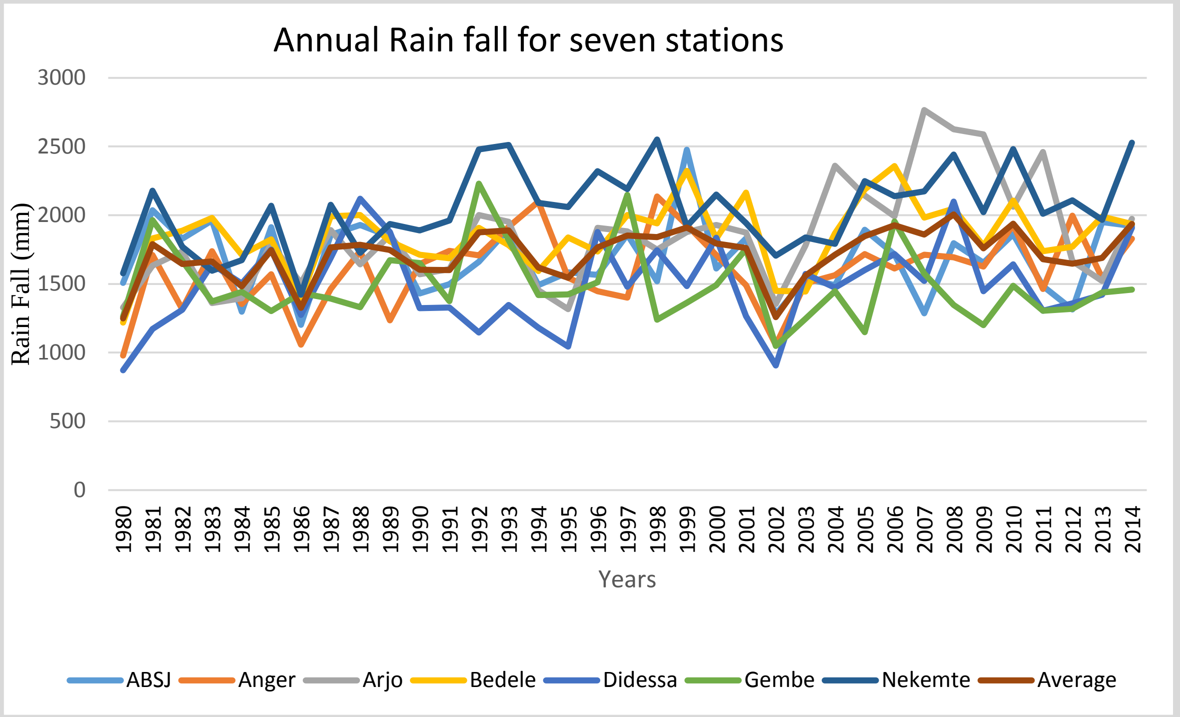

Table: Cumulative annual rain fall for seven stations

Cummulative RF (mm)								
Year	ABSJ	Anger	Arjo	Bedele	Didessa	Gembe	Nekemte	Average
1980	1506.94	978.59	1328.01	1217.42	871.03	1262.89	1578.04	1248.99
1981	3542.73	2688.13	2961.79	3048.58	2042.50	3227.57	3755.59	3038.12
1982	5372.23	4003.48	4698.07	4936.67	3354.60	4896.27	5525.33	4683.81
1983	7335.04	5741.35	6058.60	6917.67	4996.25	6269.35	7120.37	6348.37
1984	8632.54	7094.75	7454.69	8630.78	6499.55	7712.25	8794.39	7831.28
1985	10544.84	8664.25	9246.29	10455.68	8249.85	9014.14	10863.79	9576.97
1986	11746.84	9721.85	10752.29	11848.38	9523.95	10448.18	12284.39	10903.69
1987	13603.14	11185.15	12643.69	13840.18	11212.25	11841.45	14359.76	12669.37
1988	15532.64	12922.71	14287.19	15841.68	13332.18	13171.41	16087.36	14453.59
1989	17377.54	14158.51	16141.69	17651.98	15209.84	14843.71	18023.06	16200.91
1990	18807.34	15802.81	17713.09	19363.48	16534.24	16494.81	19912.76	17804.08
1991	20306.54	17544.35	19321.59	21049.68	17861.65	17870.11	21875.26	19404.17
1992	21968.54	19252.65	21322.99	22958.88	19008.05	20100.51	24354.36	21280.85
1993	23870.44	21167.15	23275.39	24742.28	20355.75	21919.61	26866.86	23171.07
1994	25362.27	23265.95	24728.37	26336.68	21536.65	23338.11	28956.86	24789.27
1995	26947.58	24810.75	26045.77	28175.48	22579.75	24761.21	31016.06	26333.80
1996	28512.78	26258.75	27954.55	29910.48	24456.75	26273.01	33336.96	28100.47
1997	30372.48	27658.05	29836.15	31912.08	25935.15	28420.61	35526.96	29951.64

1998	31891.28	29795.59	31587.06	33853.08	27679.75	29659.61	38078.36	31792.10
1999	34368.38	31723.89	33464.07	36175.58	29164.45	31023.71	39998.06	33702.59
2000	35979.58	33432.99	35393.97	38003.38	31001.05	32515.81	42148.26	35496.44
2001	37809.98	34923.09	37267.27	40168.38	32267.35	34271.17	44090.46	37256.81
2002	39087.98	35979.09	38620.87	41617.88	33174.55	35320.57	45796.46	38513.91
2003	40625.38	37483.09	40401.77	43063.38	34746.45	36567.23	47633.96	40074.47
2004	42117.38	39045.59	42762.47	44930.88	36218.65	38014.13	49426.06	41787.88
2005	44011.28	40762.19	44905.47	47118.78	37819.75	39161.90	51674.76	43636.30
2006	45726.68	42373.89	46896.67	49477.08	39536.75	41117.10	53814.16	45563.19
2007	47013.18	44086.89	49663.17	51459.48	41057.25	42693.20	55987.16	47422.91
2008	48809.58	45779.59	52289.17	53508.38	43155.35	44039.99	58428.46	49430.08
2009	50464.88	47405.29	54877.17	55285.18	44602.35	45241.02	60451.26	51189.59
2010	52326.38	49334.99	56938.77	57391.18	46244.05	46728.55	62933.36	53128.18
2011	53811.58	50797.44	59400.07	59129.12	47548.75	48033.35	64943.76	54809.15
2012	55126.58	52793.84	61066.07	60900.08	48906.05	49352.15	67053.06	56456.84
2013	57076.04	54336.47	62587.07	62890.55	50326.15	50788.65	69018.36	58146.18
2014	58997.14	56166.47	64559.57	64826.35	52235.25	52246.35	71545.46	60082.37

Double mass curve for Rainfall gauging stations

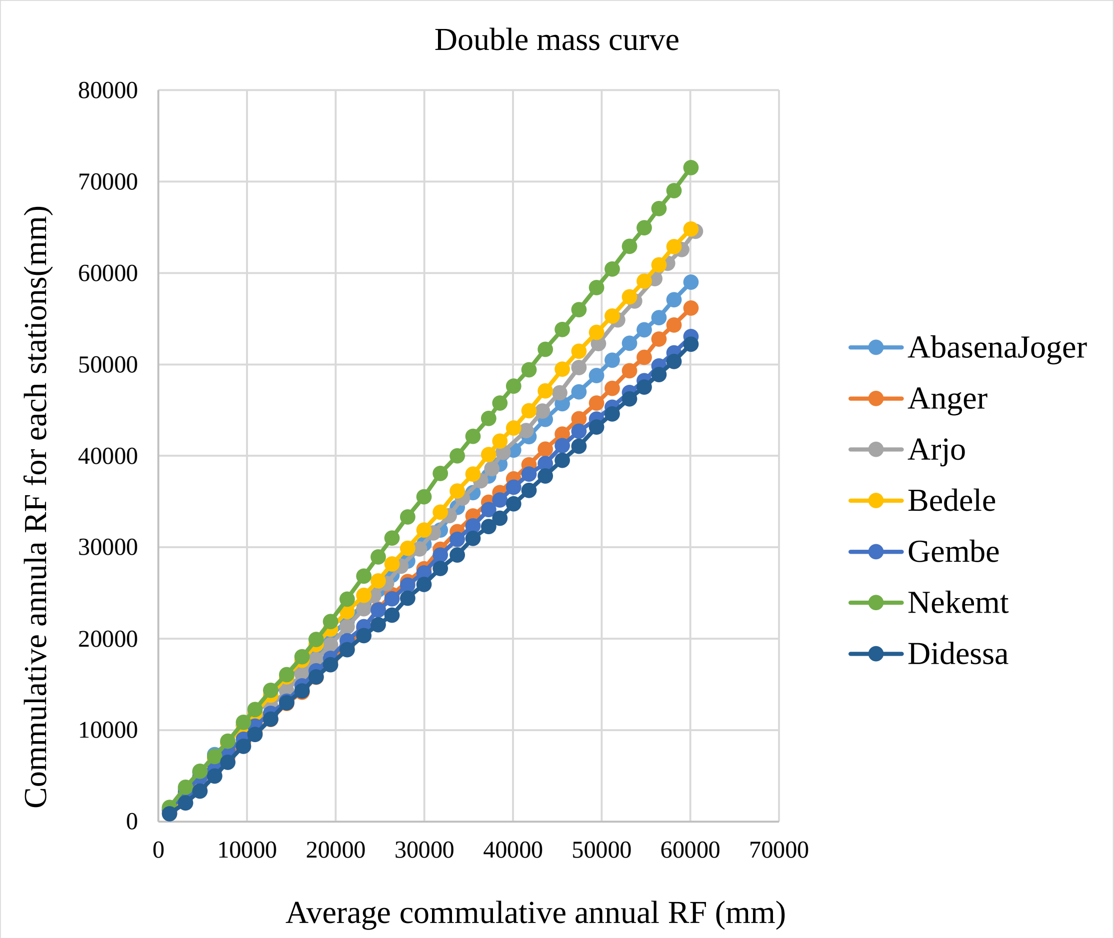

Table: monthly maximum temperature of each gauging station

Monthly Maximum Temprature							
Months	ABSJ	Anger	Arjo	Bedele	Didessa	Gembe	Nekemt
January	32.99	31.21	23.03	26.99	31.21	28.00	26.59
February	34.23	32.65	24.05	28.20	32.65	29.81	27.79
March	35.33	32.92	24.08	28.17	32.92	30.13	27.94
April	34.75	32.14	23.58	27.52	32.14	29.16	27.16
May	32.38	29.75	22.31	25.92	29.75	27.52	25.20
June	29.73	27.48	20.35	23.59	27.48	24.28	22.73
July	27.56	25.46	18.99	21.97	25.46	21.03	21.18
August	27.95	25.56	18.88	22.45	25.56	20.89	21.17
September	29.32	26.68	19.95	23.66	26.68	22.47	22.62
October	30.77	27.91	21.30	24.71	27.91	23.45	24.11
November	31.94	29.17	21.77	25.35	29.17	24.99	24.92
December	32.54	30.03	22.39	26.11	30.03	26.26	25.46

Graphical representation of maximum monthly temperature

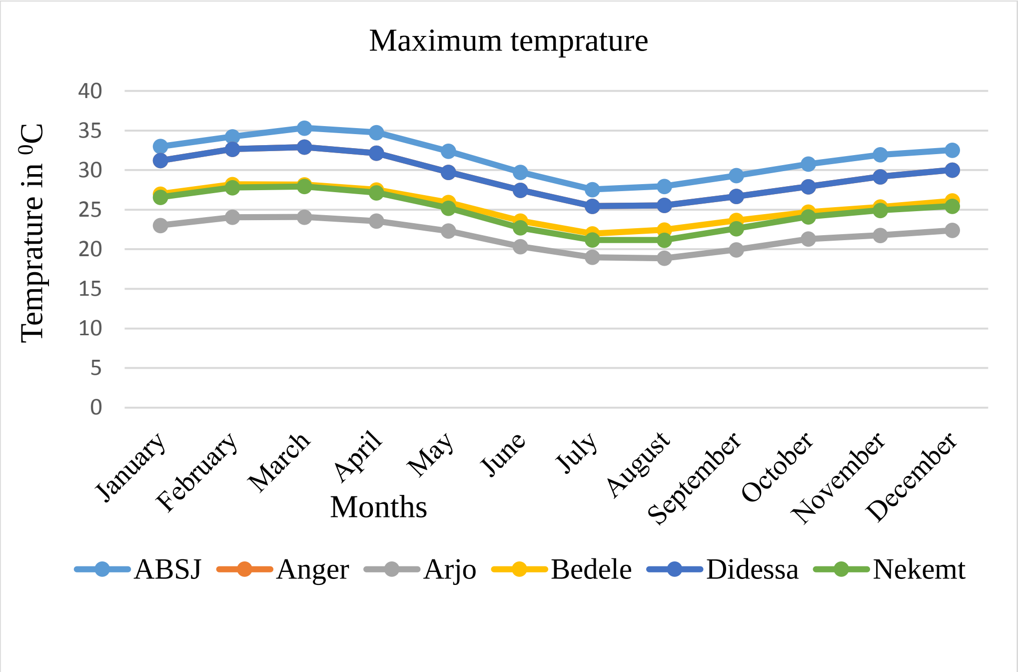

Table: Monthly minimum temperature of each gauging station

Monthly Minimum Temprature							
Months	ABSJ	Anger	Arjo	Bedele	Didessa	Gembe	Nekemt
January	12.60	14.71	11.23	11.65	11.43	8.25	12.24
February	14.10	16.01	12.04	12.57	13.13	10.10	12.94
March	16.04	17.29	12.63	13.44	15.24	11.36	13.86
April	16.91	17.64	12.50	13.81	16.30	11.93	14.06
May	16.62	17.00	12.19	13.37	16.17	11.94	13.61
June	16.29	16.35	11.61	12.87	15.44	11.68	12.80
July	15.69	15.96	11.24	12.72	15.15	11.27	12.62
August	15.74	15.74	11.36	12.62	14.87	10.90	12.75
September	15.62	15.64	11.26	12.22	14.61	9.63	12.70
October	15.05	15.81	11.67	11.99	13.69	7.40	12.78
November	14.06	15.48	11.65	11.65	12.28	6.58	12.74
December	13.05	14.78	11.36	11.29	11.30	7.05	12.17

Graphical representation of maximum monthly temperature

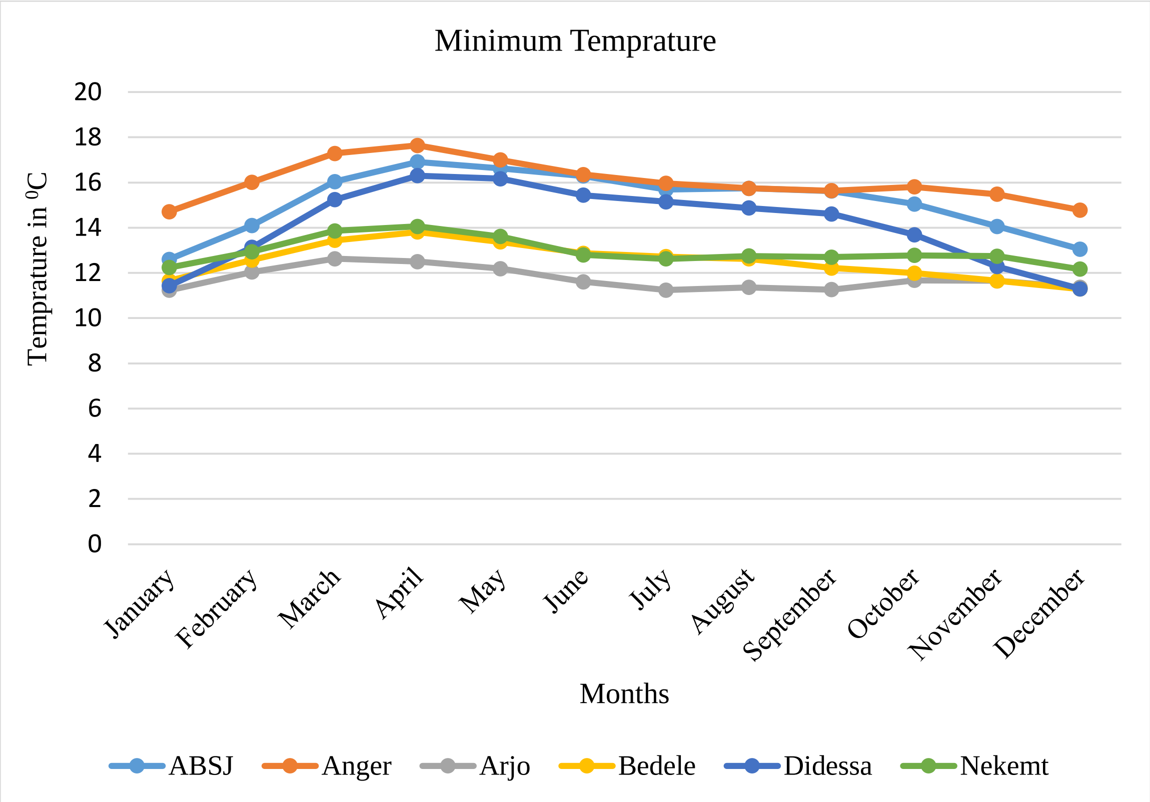

Table: Monthly flow at Toba gauging station to identify rising falling limp

months	Jan	Feb	Mar	Apr	May	Jun	Jul	Aug	Sep	Oct	Nov	Dec
flow	4.87	3.32	4.08	5.49	12.40	42.22	89.98	114.03	106.81	65.05	23.35	8.95

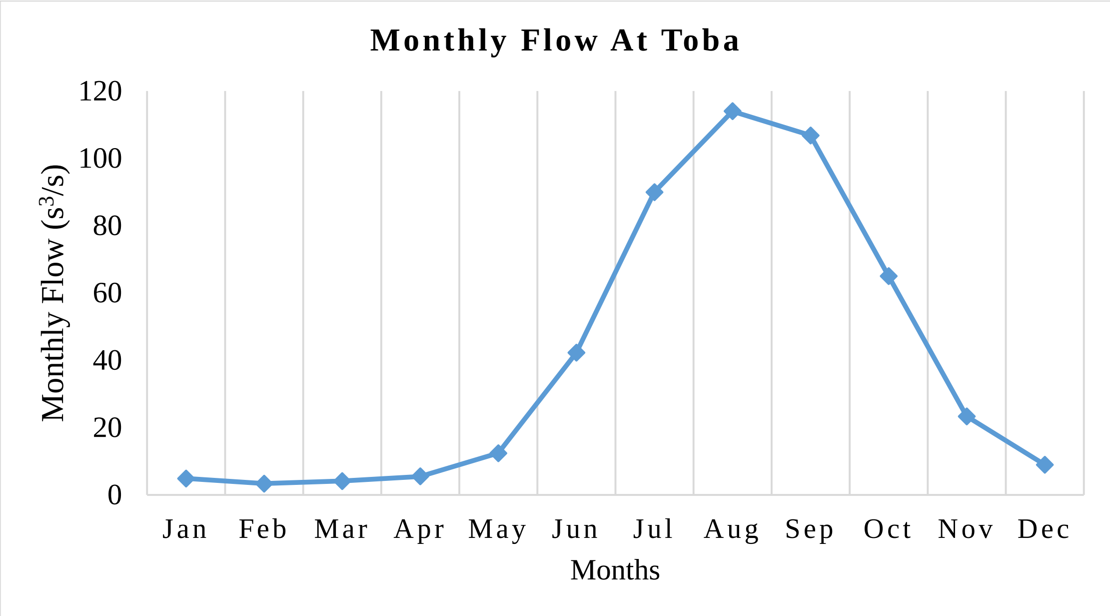

Figure: Toba Hydrograph

Table: Monthly flow at Toba gauging station to identify rising falling limp

Months	Jan	Feb	Mar	Apr	May	Jun	Jul	Aug	Sep	Oct	Nov	Dec
Flow m^3/s)	6.52	4.41	3.47	3.80	7.36	14.77	33.40	51.24	45.79	31.27	13.16	8.38

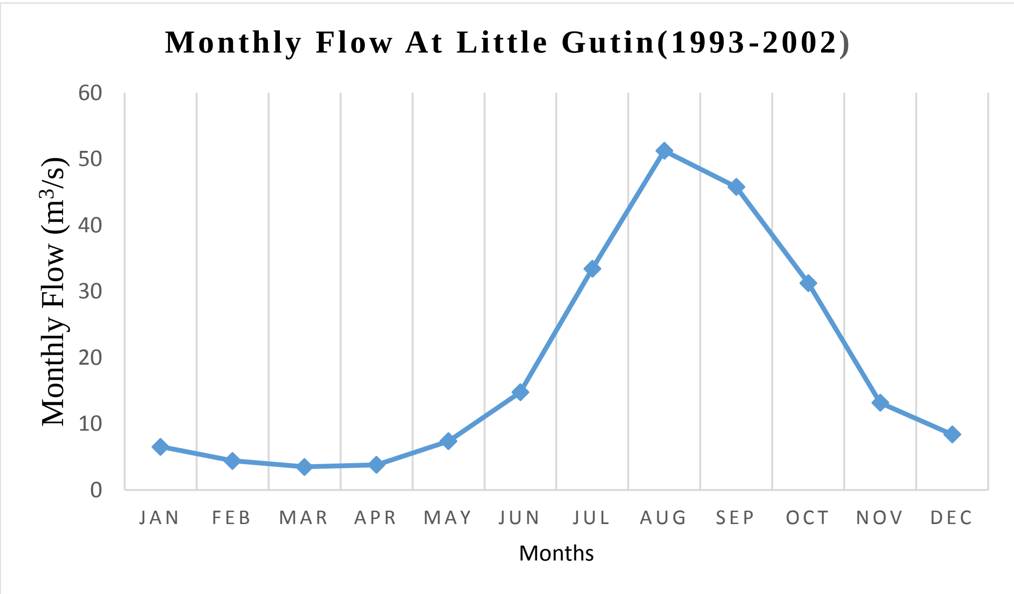

Figure: Little Anger Hydrograph

Table: Samples of suspended Sediment Data determined at little Anger

No.	Samp. No.	River (Stream)	Station	Date of sampling	Time taken (sec)	Flow (m^3/s)	Sediment Conc. (mg/L)
1	1	Didessa	Toba	15-Mar-90	_	4.160	51.56
2	2	Didessa	Toba	15-Mar-90	_	4.160	40.00
3	3	Didessa	Toba	15-Mar-90	_	4.160	42.81
4	1	Didessa	Toba	21-Mar-90	_	5.410	59.69
5	2	Didessa	Toba	21-Mar-90	_	5.410	173.13
6	3	Didessa	Toba	21-Mar-90	_	5.410	90.63
7	1	Didessa	Toba	2-Jul-90	_	9.140	215.31
8	2	Didessa	Toba	2-Jul-90	_	9.140	135.62
9	3	Didessa	Toba	2-Jul-90	_	9.140	190.00
10	1	Didessa	Toba	22-Dec-90	50	4.370	90.94
11	2	Didessa	Toba	22-Dec-90	50	4.370	99.37
12	3	Didessa	Toba	22-Dec-90	50	4.370	63.13
13	1	Didessa	Toba	18-Sep-90		98.500	141.56
14	2	Didessa	Toba	18-Sep-90		98.500	187.82
15	3	Didessa	Toba	18-Sep-90		98.500	124.69
16	1	Didessa	Toba	16-May-93	45	2.890	87.90
17	2	Didessa	Toba	16-May-93	45	2.890	108.63
18	3	Didessa	Toba	16-May-93	40	2.890	81.40
19	1	Didessa	Toba	12-Apr-93	_	8.010	73.05
20	2	Didessa	Toba	12-Apr-93	_	8.010	61.59
21	3	Didessa	Toba	12-Apr-93	_	8.010	59.20
22	1	Didessa	Toba	2-Oct-98	16	5.200	51.40
23	2	Didessa	Toba	2-Oct-98	19	5.200	64.60
24	3	Didessa	Toba	2-Oct-98	21	5.200	73.00
25	1	Didessa	Toba	4-Nov-02	5	20.953	66.76
26	2	Didessa	Toba	4-Nov-02		20.953	69.31
27	3	Didessa	Toba	4-Nov-02	6	20.953	88.27
28	1	Didessa	Toba	30-May-03	8	2.129	116.67
29	2	Didessa	Toba	30-May-03	8	2.129	135.17
30	3	Didessa	Toba	30-May-03		2.129	143.60
31	1	Didessa	Toba	31-May-03	6	1.929	184.80
32	2	Didessa	Toba	31-May-03	8	1.929	157.89
33	3	Didessa	Toba	31-May-03	12	1.929	164.53
34	1	Didessa	Toba	2-Jun-03	6	1.652	139.42
35	2	Didessa	Toba	2-Jun-03	6	1.652	172.00
36	3	Didessa	Toba	2-Jun-03	8	1.652	149.00

49	1	Didessa	Toba	15-Sep-05	29	122.80	252.22
50	2	Didessa	Toba	14-Sep-05	28	122.80	269.45
51	3	Didessa	Toba	15-Sep-05	39	122.80	211.83
52	1	Didessa	Toba	16-Sep-05	34	100.12	207.89
53	2	Didessa	Toba	16-Sep-05	31	100.12	233.19
54	3	Didessa	Toba	16-Sep-05	22	100.12	187.73
61	1	Didessa	Toba	23-Jul-06	36	146.40	189.16
62	2	Didessa	Toba	23-Jul-06	22	146.40	340.23
63	3	Didessa	Toba	23-Jul-06	35	146.40	370.35
70	1	Didessa	Toba	2-Sep-10	16	179.54	162.50
71	2	Didessa	Toba	2-Sep-10	17	179.54	154.48
72	3	Didessa	Toba	2-Sep-10	19	179.54	169.88
73	1	Didessa	Toba	16-Sep-11	33	183.73	332.34
74	2	Didessa	Toba	16-Sep-11	25	183.73	338.14
75	3	Didessa	Toba	16-Sep-11	37	183.73	320.82
76	1	Didessa	Toba	17-Sep-11	39	190.20	107.16
77	2	Didessa	Toba	17-Sep-11	23	190.20	82.83
78	3	Didessa	Toba	17-Sep-11	35	190.20	51.30
79	1	Didessa	Toba	25-Nov-13	45	49.493	169.38
80	2	Didessa	Toba	25-Nov-13	43	49.493	472.53
81	3	Didessa	Toba	25-Nov-13	47	49.493	192.31
82	1	Didessa	Toba	17-Oct-14	19	164.45	570.36
83	2	Didessa	Toba	17-Oct-14	20	164.45	259.05
84	3	Didessa	Toba	17-Oct-14	21	164.45	271.11
91	1	Didessa	Toba	4-Dec-14	38	13.410	163.78
92	2	Didessa	Toba	4-Dec-14	35	13.410	251.90
93	3	Didessa	Toba	4-Dec-14	35	13.410	

Table: conversion of sediment concentration into discharge for Toba

Falling Limp				Raising Limp			
Date of Sampling	Flow (m^3/s)	Sediment Conc. (mg/l)	Sediment Disch. (Kg/s)	Date of Sampling	Flow (m^3/s)	Sediment Conc. (mg/l)	Sediment Disch. (Kg/s)
15-Mar-90	4.160	51.56	0.21449	2-Jul-90	9.140	215.31	1.967933
15-Mar-90	4.160	40.00	0.1664	2-Jul-90	9.140	135.62	1.239567
15-Mar-90	4.160	42.81	0.17809	2-Jul-90	9.140	190.00	1.7366
21-Mar-90	5.410	59.69	0.32292	16-May-93	2.890	87.90	0.254031
21-Mar-90	5.410	173.13	0.93663	16-May-93	2.890	108.63	0.313941
21-Mar-90	5.410	90.63	0.49031	16-May-93	2.890	81.40	0.235246
22-Dec-90	4.370	90.94	0.39741	12-Apr-93	8.010	73.05	0.585131
22-Dec-90	4.370	99.37	0.43425	12-Apr-93	8.010	61.59	0.493336
22-Dec-90	4.370	63.13	0.27588	12-Apr-93	8.010	59.20	0.474192
18-Sep-90	98.500	141.56	13.9437	30-May-03	2.129	116.67	0.24839
18-Sep-90	98.500	187.82	18.5003	30-May-03	2.129	135.17	0.287777
18-Sep-90	98.500	124.69	12.282	30-May-03	2.129	143.60	0.305724
2-Oct-98	5.200	51.40	0.26728	31-May-03	1.929	184.80	0.356479
2-Oct-98	5.200	64.60	0.33592	31-May-03	1.929	157.89	0.30457
2-Oct-98	5.200	73.00	0.3796	31-May-03	1.929	164.53	0.317378
4-Nov-02	20.953	66.76	1.39882	2-Jun-03	1.652	139.42	0.230322
4-Nov-02	20.953	69.31	1.45225	2-Jun-03	1.652	172.00	0.284144
4-Nov-02	20.953	88.27	1.84952	2-Jun-03	1.652	149.00	0.246148
15-Sep-05	122.800	252.22	30.9726	23-Jul-06	146.400	189.16	27.69302
14-Sep-05	122.800	269.45	33.0885	23-Jul-06	146.400	340.23	49.80967
15-Sep-05	122.800	211.83	26.0127	23-Jul-06	146.400	370.35	54.21924
16-Sep-05	100.122	207.89	20.8144				
16-Sep-05	100.122	233.19	23.3474				
16-Sep-05	100.122	187.73	18.7959				
2-Sep-10	179.540	162.50	29.1753				
2-Sep-10	179.540	154.48	27.7353				
2-Sep-10	179.540	169.88	30.5003				
16-Sep-11	183.730	332.34	61.0608				
16-Sep-11	183.730	338.14	62.1265				
16-Sep-11	183.730	320.82	58.9443				
17-Sep-11	190.200	107.16	20.3818				
17-Sep-11	190.200	82.83	15.7543				
17-Sep-11	190.200	51.30	9.75726				
25-Nov-13	49.493	169.38	8.38304				
25-Nov-13	49.493	472.53	23.3867				
25-Nov-13	49.493	192.31	9.5179				
17-Oct-14	164.450	570.36	93.7959				
17-Oct-14	164.450	259.05	42.6004				

Table: Samples of suspended Sediment Data determined at little Anger

No.	Sam No.	River (Stream)	Station	Date of Sampling	Time Taken (Sec)	Flow (m^3/s)	Sediment Conc. (mg/l)
419	1	Little Angar	Gutin	26-Feb-90	10	3.530	100.31
420	2	Little Angar	Gutin	26-Feb-90	10	3.530	87.19
421	3	Little Angar	Gutin	26-Feb-90	10	3.530	90.63
431	1	Little Angar	Gutin	29-Mar-90	9	2.976	23.44
432	2	Little Angar	Gutin	29-Mar-90	9	2.976	42.81
433	3	Little Angar	Gutin	29-Mar-90	9	2.976	41.56
587	1	Little Angar	Gutin	29-Apr-90	9	2.486	107.40
588	2	Little Angar	Gutin	29-Apr-90	9	2.486	136.88
589	3	Little Angar	Gutin	29-Apr-90	9	2.486	162.50
787	1	Little Angar	Gutin	24-Jun-90	10	10.784	6906.99
788	2	Little Angar	Gutin	24-Jun-90	10	10.784	6887.67
789	3	Little Angar	Gutin	24-Jun-90	10	10.784	6955.99
1007	1	Little Angar	Gutin	28-Jul-90	12	38.539	686.56
1008	2	Little Angar	Gutin	28-Jul-90	12	38.539	533.12
1009	3	Little Angar	Gutin	28-Jul-90	12	38.539	587.81
1725	1	Little Angar	Gutin	21-Oct-90	12	29.103	147.94
1726	2	Little Angar	Gutin	21-Oct-90	12	29.103	150.00
1727	3	Little Angar	Gutin	21-Oct-90	12	29.103	164.12
1770	1	Little Angar	Gutin	2-Nov-91	10	12.669	118.75
1771	2	Little Angar	Gutin	2-Nov-91	10	12.669	114.38
1772	3	Little Angar	Gutin	2-Nov-91	10	12.669	94.69
1785	1	Little Angar	Gutin	31-Aug-91	11	71.903	231.88
1786	2	Little Angar	Gutin	31-Aug-91	11	71.903	219.06
1787	3	Little Angar	Gutin	31-Aug-91	11	71.903	221.25
2186	1	Little Angar	Gutin	15-Aug-92	12	75.132	435.00
2187	2	Little Angar	Gutin	15-Aug-92	12	75.132	476.00
2188	3	Little Angar	Gutin	15-Aug-92	12	75.132	512.00
2204	1	Little Angar	Gutin	5-Sep-92	12	74.902	279.00
2205	2	Little Angar	Gutin	5-Sep-92	12	74.902	281.00
2206	3	Little Angar	Gutin	5-Sep-92	12	74.902	258.00

3283	1	Little Angar	Gutin	31-Aug-94	50	125.63	863.44
3284	2	Little Angar	Gutin	31-Aug-94	45	125.63	769.33
3285	3	Little Angar	Gutin	31-Aug-94	60	125.63	739.60
3819	1	Little Angar	Gutin	7-Aug-95	20	61.690	230.20
3820	2	Little Angar	Gutin	7-Aug-95	22	61.690	487.40
3821	3	Little Angar	Gutin	7-Aug-95	25	61.690	108.00
3822	1	Little Angar	Gutin	31-Aug-95	20	50.930	807.40
3823	2	Little Angar	Gutin	31-Aug-95	22	50.930	726.80
3824	3	Little Angar	Gutin	31-Aug-95	25	50.930	853.50
3834	1	Little Angar	Gutin	5-Sep-95	50	195.18	319.00
3835	2	Little Angar	Gutin	5-Sep-95	48	195.18	272.00
3836	3	Little Angar	Gutin	5-Sep-95	46	195.18	258.00
3837	1	Little Angar	Gutin	5-Sep-95	49	58.450	659.00
3838	2	Little Angar	Gutin	5-Sep-95	45	58.450	567.70
3839	3	Little Angar	Gutin	5-Sep-95	40	58.450	572.80
3931	1	Little Angar	Gutin	28-Jan-95	14	6.62	95.53
3932	2	Little Angar	Gutin	28-Jan-95	9	6.62	100.00
3933	3	Little Angar	Gutin	28-Jan-95	8	6.62	112.67
4646	1	Little Angar	Gutin	7-Aug-96	31	1.340	959.40
4647	2	Little Angar	Gutin	7-Aug-96	36	1.340	1391.30
4648	3	Little Angar	Gutin	7-Aug-96	30	1.340	1223.80
7841	1	Little Angar	Gutin	2-Sep-04	22	1.000	1710.40
7842	2	Little Angar	Gutin	2-Sep-04	19	1.000	1217.60
7843	3	Little Angar	Gutin	2-Sep-04	20	1.000	2460.45
10612	1	Little Angar	Gutin	31-Aug-06	11	49.600	1444.92
10613	2	Little Angar	Gutin	31-Aug-06	10	49.600	1361.12
10614	3	Little Angar	Gutin	31-Aug-06	10	49.600	887.20
10693	1	Little Angar	Gutin	1-Feb-07	10	1.869	364.84
10694	2	Little Angar	Gutin	1-Feb-07	9	1.869	202.82
10695	3	Little Angar	Gutin	1-Feb-07	8	1.869	451.58
11299	1	Little Angar	Gutin	19-Jul-07	6	61.433	420.00
11300	2	Little Angar	Gutin	19-Jul-07	6	61.433	455.88
11301	3	Little Angar	Gutin	19-Jul-07	5	61.433	406.78

11302	1	Little Angar	Gutin	17-Nov-07	7	14.272	178.08
11303	2	Little Angar	Gutin	17-Nov-07	8	14.272	110.00
11304	3	Little Angar	Gutin	17-Nov-07	6	14.272	215.38
11526	1	Little Angar	Gutin	18-Mar-08	5	2.438	201.90
11527	2	Little Angar	Gutin	18-Mar-08	3	2.438	170.73
11528	3	Little Angar	Gutin	18-Mar-08	5	2.438	184.00
11607	1	Little angar	Gutin	28-Jun-08	4	20.138	865.88
11608	2	Little angar	Gutin	28-Jun-08	4	20.138	683.50
11609	3	Little angar	Gutin	28-Jun-08	4	20.138	697.75
11949	1	Little Angar	Gutin	30-Aug-08	8	24.320	689.52
11950	2	Little Angar	Gutin	30-Aug-08	9	24.320	877.38
11951	3	Little Angar	Gutin	30-Aug-08	9	24.320	670.75
11952	1	Little Angar	Gutin	2-Sep-08	8	65.262	676.56
11953	2	Little Angar	Gutin	2-Sep-08	9	65.262	1444.13
11954	3	Little Angar	Gutin	2-Sep-08	8	65.262	745.81
12316	1	Little Angar	Gutin	26-Aug-09	32	1.130	2448.81
12317	2	Little Angar	Gutin	26-Aug-09	43	1.130	3131.67
12318	3	Little Angar	Gutin	26-Aug-09	44	1.130	2647.24
12936	1	Little Angar	Gutin	3-Jan-11	35	0.715	107.64
12937	2	Little Angar	Gutin	3-Jan-11	30	0.715	101.06
12938	3	Little Angar	Gutin	3-Jan-11	28	0.715	104.62

Table: conversion of sediment concentration into discharge for Toba

Date of Sampling	Flow (m^3/s)	Sed. Conc. (mg/s)	Sed. Disch. (mg/s)	Date of Sampling	Flow (m^3/s)	Sed. Conc. (mg/s)	Sed. Disch. (mg/s)
26-Feb-90	3.530	100.31	0.354	28-Jul-90	38.539	686.56	26.459
26-Feb-90	3.530	87.19	0.308	28-Jul-90	38.539	533.12	20.546
26-Feb-90	3.530	90.63	0.320	28-Jul-90	38.539	587.81	22.654
29-Mar-90	2.976	23.44	0.070	31-Aug-91	71.903	231.88	16.673
29-Mar-90	2.976	42.81	0.127	31-Aug-91	71.903	219.06	15.751
29-Mar-90	2.976	41.56	0.124	31-Aug-91	71.903	221.25	15.909
21-Oct-90	29.103	147.94	4.306	15-Aug-92	75.132	435.00	32.682
21-Oct-90	29.103	150.00	4.365	15-Aug-92	75.132	476.00	35.763
21-Oct-90	29.103	164.12	4.776	15-Aug-92	75.132	512.00	38.468
2-Nov-91	12.669	118.75	1.504	31-Aug-94	125.632	863.44	108.476
2-Nov-91	12.669	114.38	1.449	31-Aug-94	125.632	769.33	96.652
2-Nov-91	12.669	94.69	1.200	31-Aug-94	125.632	739.60	92.917
5-Sep-92	74.902	279.00	20.898	7-Aug-95	61.690	230.20	14.201
5-Sep-92	74.902	281.00	21.047	7-Aug-95	61.690	487.40	30.068
5-Sep-92	74.902	258.00	19.325	7-Aug-95	61.690	508.00	31.339
5-Sep-95	195.180	319.00	62.262	31-Aug-95	50.930	807.40	41.121
5-Sep-95	195.180	272.00	53.089	31-Aug-95	50.930	726.80	37.016
5-Sep-95	195.180	258.00	50.356	31-Aug-95	50.930	853.50	43.469
28-Jan-95	6.62	95.53	0.632	31-Aug-06	49.600	1244.92	61.748
28-Jan-95	6.62	100.00	0.662	31-Aug-06	49.600	1161.12	57.592
28-Jan-95	6.62	112.67	0.746	31-Aug-06	49.600	887.20	44.005
1-Feb-07	1.869	164.84	0.308	19-Jul-07	61.433	420.00	25.802
1-Feb-07	1.869	102.82	0.192	19-Jul-07	61.433	455.88	28.006
1-Feb-07	1.869	151.58	0.283	19-Jul-07	61.433	406.78	24.990
17-Nov-07	14.272	178.08	2.542	28-Jun-08	20.138	865.88	17.437
17-Nov-07	14.272	110.00	1.570	28-Jun-08	20.138	683.50	13.764
17-Nov-07	14.272	215.38	3.074	28-Jun-08	20.138	697.75	14.051
18-Mar-08	2.438	201.90	0.492	30-Aug-08	24.320	689.52	16.769
18-Mar-08	2.438	170.73	0.416	30-Aug-08	24.320	877.38	21.338
18-Mar-08	2.438	184.00	0.449	30-Aug-08	24.320	670.75	16.313
2-Sep-08	65.262	676.56	44.154				
2-Sep-08	65.262	750.13	48.955				
2-Sep-08	65.262	745.81	48.673				
3-Jan-11	0.715	107.64	0.077				
3-Jan-11	0.715	101.06	0.072				
3-Jan-11	0.715	104.62	0.075				

Comparison of sediment concentration obtained by rating curve and SWAT model

Months	Toba Gauging Station (mg/L)		Gutin Gauging Station (mg/L)	
	Rating Curve	SWAT Model	Rating Curve	SWAT Model
Jan	74.03	125.95	80.74	124.61
Feb	73.56	89.44	64.32	109.63
Mar	75.21	98.99	65.85	104.92
Apr	136.81	146.79	83.27	213.68
May	152.12	230.84	124.73	243.69
Jun	184.74	292.75	176.47	322.27
Jul	209.28	309.63	199.54	394.57
Aug	229.26	331.83	207.62	457.30
Sep	193.35	336.91	204.57	246.45
Oct	154.62	310.29	178.61	198.28
Nov	122.63	256.13	144.25	158.66
Dec	92.94	191.47	111.71	138.53

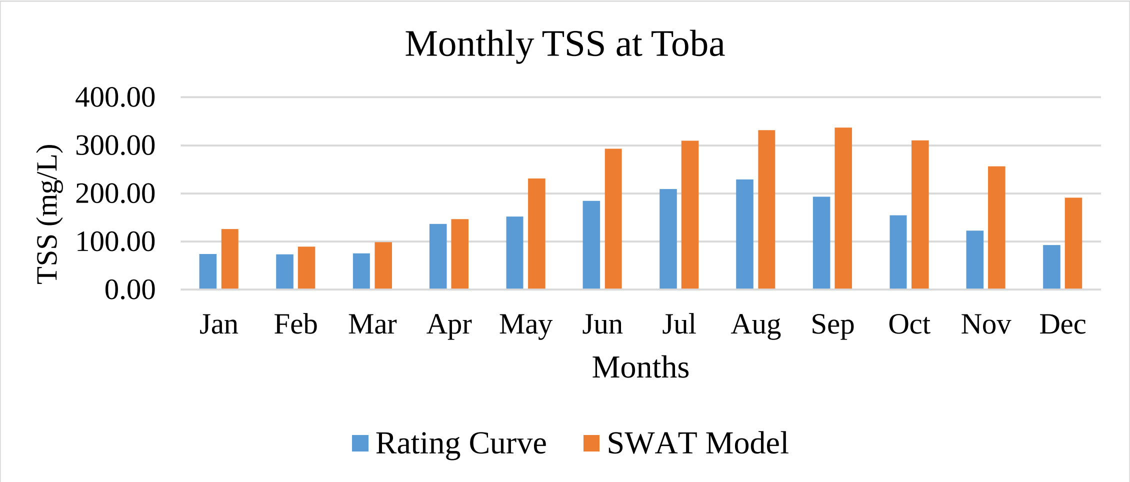

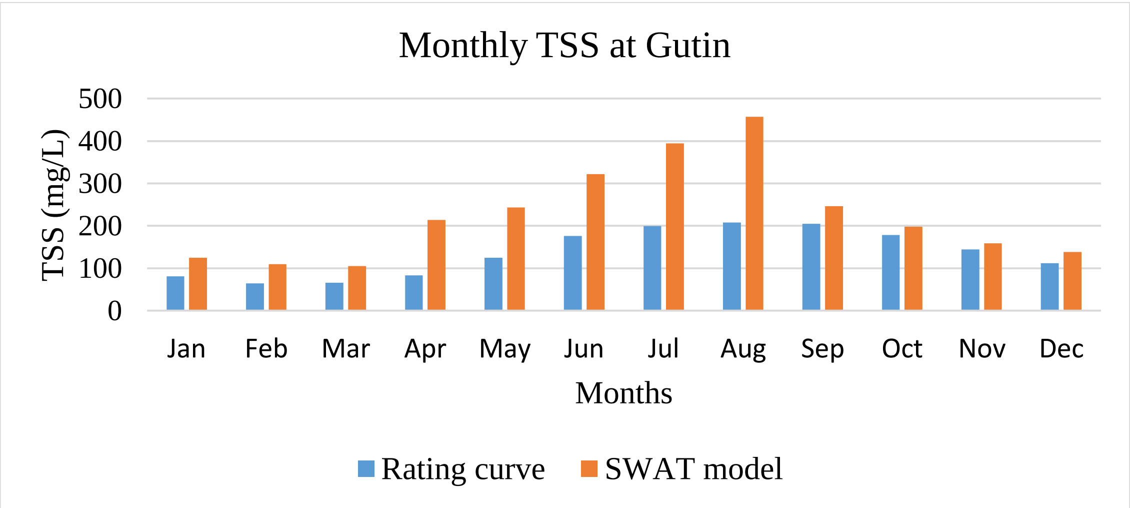

Appendix B: SWAT Model Out

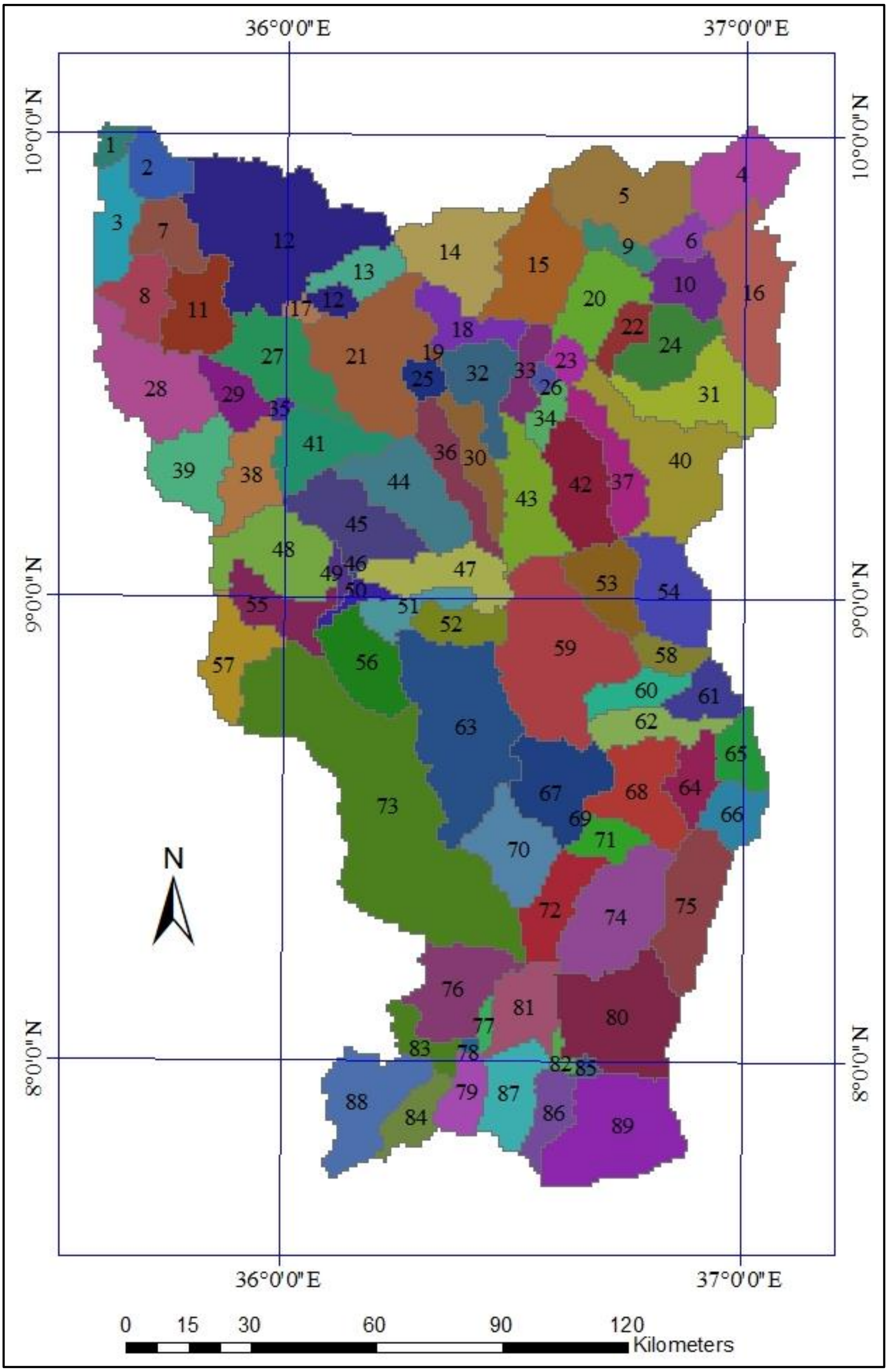

Figure: Location of delineated sub-basins in the watershed

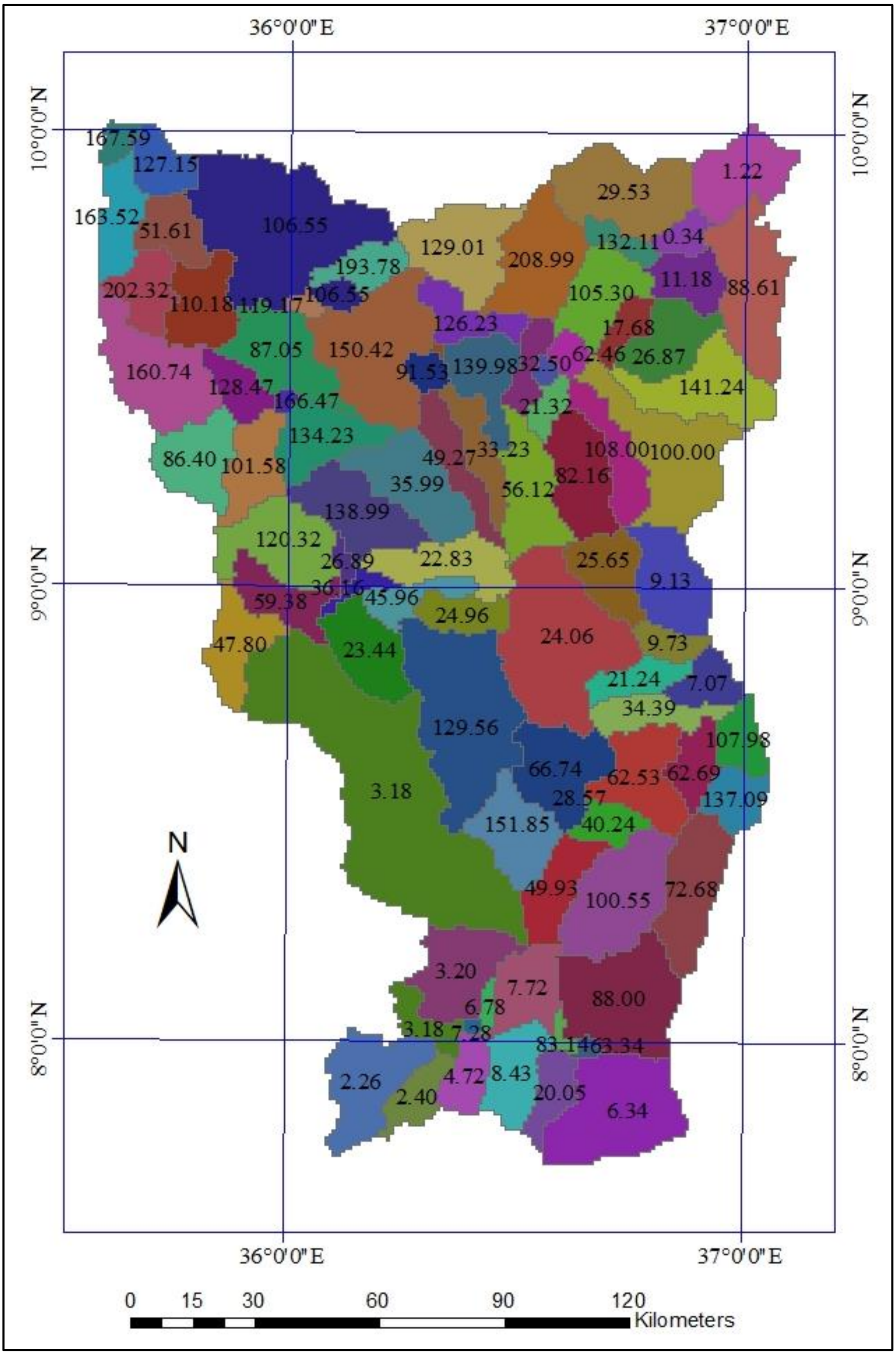

Figure: soil erosion in ton/ha/year from each sub-basins